

Wear Behavior Of Polyethylene Against Titanium Nitride Coated Alloy Surfaces For Joint Replacement

BY

FILIPPO CINOTTI

BSc., Politecnico di Milano, Milano, Italy, 2018

THESIS

Submitted as partial fulfillment of the requirements
for the degree of Master of Science in Bioengineering
in the Graduate College of the
University of Illinois at Chicago, 2020

Chicago, Illinois

Defense Committee:

Markus Wimmer, Chair and Advisor

Mathew Mathew

Roberto Chiesa, Politecnico di Milano

DEDICATION

This thesis is dedicated to all the people that have supported me during the last few years. Your help has been really precious and without You I would not be here today and, above all, I would not be the person I am today. Thanks to my parents, their sacrifice, their strength, their infinite number of wise advice and their unconditioned love. You have made my dreams becoming reality and I will be always thankful to You, Ma & Pa. Thanks to Ricky, my major source of inspiration. Your force, your ability to outweigh every problem with a smile and your bravery has taught me a lot about life and its value. Thanks also to the rest of my family, to my two beautiful cousins, my uncle and aunt and all my grandparents, you have grown me up, and I will never thank you enough for everything you have done for me.

Thank You, Bea, You have done a lot for me during these years and no words can correctly describe how much I have appreciated all this. You are a precious smile for me.

Thank You also to all the old and new friends I have made during this journey, thank You Accia and Gre, thanks to my incredible housemates Cate, Ludo and Nillolo that have made my American days truly unforgettable. Thanks to Chia, Giro, Luke, Matti, and all the Italian crew, to the Rush Lab guys, the Sweden friends, Rita and the neighbors, the soccer team and the two “Augmedted” friends Bek and Pouyan.

You all are a part of this history and You will always be in my thoughts and my heart.

I hope I have not forgotten anyone; You are the best guys!

Filippo

ACKNOWLEDGEMENTS

First of all, I would like to thank prof. Wimmer, Rush University, the University of Illinois at Chicago and Oerlikon Group that have made it possible to work on this topic and realize this thesis. Moreover, I would like to personally thank prof. Wimmer, Spencer and all the Rush Lab family for the opportunities they have offered me, for their unconditioned support and for the passion for their work that they have shared with me. They have been a daily source of inspiration for me and I believe that the created personal relationships transcend the merely professional ones.

Thanks to Prof. Chiesa, from Politecnico di Milano, and to Prof. Mathew Mathew, from UIC, to be part of the commission.

A big thanks go also to Jenna and Prof. Caiani, that have always given a kind and timely support for any problem, guiding us in this experience in order to maximize what we can get from it. In addition, I would like to thank the Italian professors, Prof. Rasponi, Prof. Signorini and Prof. Vesentini that have organized the first part of the courses I have followed for this double degree, but also the American ones, Prof. Esmailbeigi, Prof. Khetani and Prof. Klatt. You all have played an essential role in this formative experience.

FC

TABLE OF CONTENTS

<u>CHAPTER</u>	<u>PAGE</u>
INTRODUCTION	1
1.1 Motivations	3
1.1.1 The wear problem	3
1.1.2 Metal allergy	9
1.3 A possible solution: surface coating	10
1.4 Project Aim	11
1.5 Thesis Structure.....	12
STATE OF THE ART	14
2.1 Introduction	14
2.2 Titanium Nitride as coating material.....	15
2.3 Titanium Nitride in medical literature.....	17
2.3.1 Preclinical studies.....	18
2.3.1 Clinical results.....	19
MATERIALS	21
3.1 CoCr coated/uncoated discs	21
3.2 Ti6Al4V coated/uncoated discs	25
3.3 UHMWPE Pins	28
3.4 AMTI® Ortho-POD	30
3.5 Zygo® Newview 6300 3D optical surface profiler.....	32
3.6 HORIBA® LabRAM HR Evolution, Raman spectrometer.....	33
3.7 LABCONCO XPert® Weigh.....	35
3.8 ZEISS Stemi 2000-C.....	36
METHODS	38
4.1 Discs characterization	38
4.1.1 Evaluation of disc surface roughness	38
4.1.2 Raman spectroscopy of disc surface	43
4.1.3 Post-POD test evaluation of discs surface	47
4.2 Pin-on-Disc (POD) test	48
4.2.1 Introduction	48

TABLE OF CONTENTS (continued)

<u>CHAPTER</u>	<u>PAGE</u>
4.2.2 Test preparation.....	49
4.2.2.1 AMTI® Ortho-POD calibration.....	49
4.2.2.2 Discs cleaning	51
4.2.2.3 Pins soaking	55
4.2.2.4 Testing fluid preparation	59
4.2.2.5 Run the test (CoCr)	62
4.2.2.5 Run the test (Ti6Al4V).....	66
4.2.2.6 Ortho-POD settings	70
4.2.2.7 Post running procedures: cleaning and maintenance	72
4.3 Post-POD test pins characterization.....	86
4.3.1 Evaluation of pins surface with stereomicroscope.....	86
4.3.2 Evaluation of pins surface with Zygo	87
RESULTS	91
5.1 Discs characterization	91
5.1.1 Evaluation of disc surface roughness	91
5.1.2 Raman spectroscopy of disc surface	109
5.1.3 Post-POD test evaluation of discs surface	148
5.2 Pin-on-Disc (POD) test	160
5.2.1 Introduction	160
5.2.2 Test setup	160
5.3 Post-POD test pins characterization.....	109
5.3.1 Evaluation of pins surface.....	198
5.3.2 Evaluation of pins surface using Zygo.....	208
DISCUSSION AND CONCLUSION	220
APPENDICES	233
Appendix A	234
Appendix B	236
Appendix C	

Appendix D	241
TABLE OF CONTENTS (continued)	

<u>CHAPTER</u>	<u>PAGE</u>
Appendix E	244
Appendix F	247
Appendix G	250
Appendix H	253
Appendix I	256
CITED LITERATURE	265
VITA	270

LIST OF TABLES

<u>TABLE</u>		<u>PAGE</u>
I	CoCr DISC SUPPLY FROM FACTORY	22
II	Ti6Al4V DISC SUPPLY FROM FACTORY	25
III	CALIBRATION VALUES FOR POD.....	50
IV	DESCRIPTION OF THE DISCS USED FOR ROUND 1, CoCr TEST.	52
V	DESCRIPTION OF THE DISCS USED FOR ROUND 2, CoCr TEST.	53
VI	DESCRIPTION OF THE DISCS USED FOR ROUND 3, CoCr TEST.	53
VII	DESCRIPTION OF THE DISCS USED FOR ROUND 1, Ti6Al4V TEST.	54
VIII	DESCRIPTION OF THE DISCS USED FOR ROUND 2, Ti6Al4V TEST.	54
IX	DESCRIPTION OF THE DISCS USED FOR ROUND 3, Ti6Al4V TEST.	55
X	DESCRIPTION OF PINS USE FOR DIFFERENT ROUNDS IN CoCr TEST.....	58
XI	DESCRIPTION OF PINS USE FOR DIFFERENT ROUNDS IN Ti6Al4V TEST.....	59
XII	RUNNING SCHEME FOR ROUND 1, CoCr TEST.	63
XIII	RUNNING SCHEME FOR ROUND 2, CoCr TEST.	64
XIV	RUNNING SCHEME FOR ROUND 3, CoCr TEST.	65
XV	RUNNING SCHEME FOR ROUND 1, Ti6Al4V TEST.....	67
XVI	RUNNING SCHEME FOR ROUND 2, Ti6Al4V TEST.....	68
XVII	RUNNING SCHEME FOR ROUND 3, Ti6Al4V TEST.....	69
XVIII	SETTINGS DEFINITION FOR THE TESTS. WEARING PATH, AXIAL FORCE, AXIAL PRESSURE, PROCESS FREQUENCY, FLUID TEMPERATURE AND NUMBER OF CYCLES FOR EACH STAGE ARE REPORTED.....	70
XIX	RECAP VERSION OF THE ROUGHNESS TABLE FOR CoCr TEST.	93
XX	SUMMARY OF THE ARITHMETIC ROUGHNESS FOR CoCr TEST....	95
XXI	RECAP VERSION OF THE ROUGHNESS TABLE FOR Ti6Al4V TEST.....	112

LIST OF TABLES (continued)

<u>TABLE</u>	<u>PAGE</u>
XXII SUMMARY OF THE ARITHMETIC ROUGHNESS FOR Ti6Al4V TEST.....	114
XXIII FINAL SUMMARY TABLE CONTAINING ALL THE RESULTS OBTAINED DURING THE EXPERIMENT.	221
XXIV ANOVA TWO-FACTORS WITH REPLICATIONS TEST.....	221
XXV POST HOC ANALYSES ADJUSTED FOR MULTIPLE COMPARISON.	221
XXVI INTEGRAL VERSION OF ROUGHNESS MEASUREMENT TABLE, CoCr TEST	235
XXVII INTEGRAL VERSION OF ROUGHNESS MEASUREMENT TABLE, Ti6Al4V TEST	237
XXVIII AVERAGE WEIGHT AND STANDARD DEVIATION OF THE WEIGHT EVALUATED FOR EACH STAGE OF THE TEST.	239
XXIX AVERAGE WEIGHT AND STANDARD DEVIATION OF THE WEIGHT EVALUATED FOR THE SOAK PIN.	2400
XXX AVERAGE WEIGHT AND STANDARD DEVIATION OF THE WEIGHT EVALUATED FOR EACH STAGE OF THE TEST.	242
XXXI AVERAGE WEIGHT AND STANDARD DEVIATION OF THE WEIGHT EVALUATED FOR THE SOAK PIN.	243
XXXII AVERAGE WEIGHT AND STANDARD DEVIATION OF THE WEIGHT EVALUATED FOR EACH STAGE OF THE TEST.	245
XXXIII AVERAGE WEIGHT AND STANDARD DEVIATION OF THE WEIGHT EVALUATED FOR THE SOAK PIN.	246
XXXIV AVERAGE WEIGHT AND STANDARD DEVIATION OF THE WEIGHT EVALUATED FOR EACH STAGE OF THE TEST.	248
XXXV AVERAGE WEIGHT AND STANDARD DEVIATION OF THE WEIGHT EVALUATED FOR THE SOAK PIN.	249
XXXVI AVERAGE WEIGHT AND STANDARD DEVIATION OF THE WEIGHT EVALUATED FOR EACH STAGE OF THE TEST.	251

LIST OF TABLES (continued)

<u>TABLE</u>		<u>PAGE</u>
XXXVII	AVERAGE WEIGHT AND STANDARD DEVIATION OF THE WEIGHT EVALUATED FOR THE SOAK PIN.	252
XXXVIII	AVERAGE WEIGHT AND STANDARD DEVIATION OF THE WEIGHT EVALUATED FOR EACH STAGE OF THE TEST.	254
XXXIX	AVERAGE WEIGHT AND STANDARD DEVIATION OF THE WEIGHT EVALUATED FOR THE SOAK PIN.	255

LIST OF FIGURES

<u>FIGURE</u>		<u>PAGE</u>
1	Relationship between cause of failure and time to failure in THA implants	2
2	Cellular and molecular pathways of the osteoclast genesis and influence of wear debris particles in bone resorption process	5
3	Schematic of the adverse reaction caused by the release of metal ions.	7
4	Disc 2D geometry of frontal and top plane.	23
5	Discs 3D geometry.	23
6	Different discs type. From left to right it is possible to see Uncoated CoCr disc, TiN coating, tech #1 disc, TiN coating, tech #2, TiN coating, tech #3 disc, Ag-doped TiN coating disc, Uncoated CoCr disc from the LAB.	24
7	Details of final surface polishing.	24
8	Discs 2D geometry of frontal plane and top plane.	26
9	Discs 3D geometry.	26
10	Different discs type. From left to right it is possible to see Uncoated Ti6Al4V disc, TiN coating, tech #1 disc, TiN coating, tech #2, TiN coating, tech #3 disc and Ag-doped TiN coating disc.....	27
11	Details of final surface polishing.	27
12	Pins 2D geometry of frontal plane and top plane.	28
13	Pins 3D geometry.	29
14	AMTI Ortho-POD device.....	30
15	Zygo Newview 6300	32
16	HORIBA LabRAM HR Evolution.....	33
17	LABCONCO XPert weigh.....	35
18	ZEISS 2000-C stereomicroscope	36
19	Micro2.app interface.	39

LIST OF FIGURES (continued)

<u>FIGURE</u>		<u>PAGE</u>
20	Zygo Measurement settings.	40
21	Roughness measurement mask.....	41
22	“LabSpec6” software interface. In the image the location of the focusing button, in the upper bar, has been highlighted with a red circle.	44
23	Settings interface of “LabSpec6” software interface.	45
24	“LabSpec6” software interface. In the image the location of the capture button, on the left of the upper bar, has been highlighted with a red circle.	46
25	3D description of the path followed by the pin.	71
26	2D description of the path followed by the pin. Top view.....	71
27	Stitch.app interface.....	88
28	Zygo Measurement settings.	89
29	Summary of the arithmetic roughness for CoCr test. All the value of Ra, collected “Before” and “After” the pin on disc (POD) test, are subdivided into disc type groups and shown in nm.	95
30	Model of the mask that has been used to collect measurements using Zygo.	96
31	Intensity map collected from CoCr disc number 2 “Before” and “After” the pin on disc test. These maps have been collected in position 3 on the disc and so, on the wearing path.	97
32	Intensity map collected from CoCr disc number 2 “Before” and “After” the pin on disc test. These maps have been collected in position 5 on the disc and so, on the unworn zone.	99
33	Intensity map collected from Tech #1 disc number 7 “Before” and “After” the pin on disc test. These maps have been collected in position 3 on the disc and so, on the wearing path.....	100
34	Surface profile collected from Tech #1 disc number 7 “Before” and “After” the pin on disc test. These maps have been collected in position 3 on the disc and so, on the wearing path.....	101

LIST OF FIGURES (continued)

<u>FIGURE</u>		<u>PAGE</u>
35	Intensity map collected from Tech #1 disc number 7 “Before” and “After” the pin on disc test. These maps have been collected in position 5 on the disc and so, on the unworn zone.....	102
36	Intensity map collected from Tech #2 disc number 10 “Before” and “After” the pin on disc test. These maps have been collected in position 3 on the disc and so, on the wearing path.....	103
37	Intensity map collected from Tech #2 disc number 10 “Before” and “After” the pin on disc test. These maps have been collected in position 5 on the disc and so, on the unworn zone.....	104
38	Intensity map collected from Tech #3 disc number 13 “Before” and “After” the pin on disc test. These maps have been collected in position 3 on the disc and so, on the wearing path.....	105
39	Intensity map collected from Tech #3 disc number 14 “Before” and “After” the pin on disc test. These maps have been collected in position 5 on the disc and so, on the unworn zone.....	106
40	Intensity map collected from AgTiN coated disc number 18 “Before” and “After” the pin on disc test. These maps have been collected in position 1 on the wearing path.	107
41	Intensity map collected from AgTiN coated disc number 18 “Before” and “After” the pin on disc test. These maps have been collected in position 5 on the disc and so, on the unworn zone.....	109
42	Intensity map collected from CoCr disc from the LAB number 23 “Before” and “After” the pin on disc test. These maps have been collected in position 2 on the disc and so, on the wearing path.	110
43	Intensity map collected from CoCr disc from the LAB number 23 “Before” and “After” the pin on disc test. These maps have been collected in position 5 on the disc and so, on the unworn zone.	111

LIST OF FIGURES (continued)

<u>FIGURE</u>		<u>PAGE</u>
44	Summary of the arithmetic roughness for Ti6Al4V test. All the value of Ra, collected “Before” and “After” the pin on disc (POD) test, are subdivided into disc type groups and shown in nm.	114
45	Intensity map collected from Ti6Al4V disc number 25 “Before” and “After” the pin on disc test. These maps have been collected in position 3 on the disc and so, on the wearing path.....	116
46	Intensity map collected from Ti6Al4V disc number 25 “Before” and “After” the pin on disc test. These maps have been collected in position 5 on the disc and so, on the unworn zone.....	117
47	Intensity map collected from Tech #1 disc number 29 “Before” and “After” the pin on disc test. These maps have been collected in position 3 on the disc and so, on the wearing path.....	118
48	Intensity map collected from Tech #1 disc number 29 “Before” and “After” the pin on disc test. These maps have been collected in position 5 on the disc and so, on the unworn zone.....	119
49	Intensity map collected from Tech #2 disc number 33 “Before” and “After” the pin on disc test. These maps have been collected in position 3 on the disc and so, on the wearing path.....	120
50	Intensity map collected from Tech #2 disc number 33 “Before” and “After” the pin on disc test. These maps have been collected in position 5 on the disc and so, on the unworn zone.....	121
51	Intensity map collected from Tech #3 disc number 37 “Before” and “After” the pin on disc test. These maps have been collected in position 3 on the disc and so, on the wearing path.....	122
52	Intensity map collected from Tech #3 disc number 37 “Before” and “After” the pin on disc test. These maps have been collected in position 5 on the disc and so, on the unworn zone.....	124

LIST OF FIGURES (continued)

<u>FIGURE</u>		<u>PAGE</u>
53	Intensity map collected from AgTiN coated disc number 41 “Before” and “After” the pin on disc test. These maps have been collected in position 1 on the wearing path.	125
54	Intensity map collected from AgTiN coated disc number 41 “Before” and “After” the pin on disc test. These maps have been collected in position 5 on the unworn zone.	126
55	Raman spectroscopy for CoCr uncoated disc number 1.	128
56	Raman spectra of ortho-xylene: comparison between pure experimental (grey) and resolved (black) spectra	129
57	Raman spectroscopy for tech #1 coated disc number 5	131
58	Raman spectroscopy for Tech #2 coated disc number 9	133
59	Raman spectroscopy for Tech #3 coated disc number 13	134
60	Raman spectroscopy for AgTiN coated disc number 17	136
61	Raman spectroscopy for CoCr uncoated disc from the lab number 21.....	138
62	Raman spectroscopy for Ti6Al4V uncoated disc number 24	140
63	Raman spectroscopy for Tech #1 coated disc number 28	142
64	Raman spectroscopy for Tech #2 coated disc number 32	143
65	Raman spectroscopy for Tech #3 coated disc number 36	145
66	Raman spectroscopy for AgTiN coated disc number 40	147
67	Picture of the surface of the disc number 1.	149
68	Picture of the surface of the disc number 4.	150
69	Picture of the surface of the disc number 8.	151
70	Picture of the surface of the disc number 12.	152
71	Picture of the surface of the disc number 16.	153
72	Picture of the surface of the disc number 21.	154
73	Picture of the surface of the disc number 24.	155
74	Picture of the surface of the disc number 28.	156
75	Picture of the surface of the disc number 32.	157

LIST OF FIGURES (continued)

<u>FIGURE</u>		<u>PAGE</u>
76	Picture of the surface of the disc number 36.	158
77	Picture of the surface of the disc number 40.	158
78	Setup for the pin on disc (POD) test.	160
79	Total weight loss for Round 1 of CoCr test	162
80	weight loss measured week by week for Round 1 of CoCr test	163
81	Pin weight “Before test” and “After 1M cycles” for Round 1, CoCr test..	164
82	Final difference of weight for each pin for Round 1, CoCr test.....	165
83	Total weight loss for Round 2 of CoCr test	166
84	weight loss measured stage by stage for Round 2 of CoCr test	167
85	Pin weight at “0.25M” cycles and “After 1M cycles” for Round 2, CoCr test.	168
86	Final difference of weight for each pin for Round 2, CoCr test.....	168
87	Total weight loss for Round 3 of CoCr test	169
88	weight loss measured stage by stage for Round 3 of CoCr test	170
89	Pin weight “Before test” and “After 1M cycles” for Round 3, CoCr test..	171
90	Final difference of weight for each pin for Round 3, CoCr test.....	171
91	Interpolation curve of the debris production data from POD test on CoCr disc.	172
92	Interpolation curve of the debris production data from POD test on Tech #1 disc.	173
93	Interpolation curve of the debris production data from POD test on Tech #2 disc..	175
94	Interpolation curve of the debris production data from POD test on Tech #3 disc.	176
95	Interpolation curve of the debris production data from POD test on AgTiN disc.	177
96	Interpolation curve of the debris production data from POD test on Lab disc.	178

LIST OF FIGURES (continued)

<u>FIGURE</u>		<u>PAGE</u>
97	Roughness-Wearing rate relationship graph.	179
98	Total weight loss for Round 1 of Ti6Al4V test.....	182
99	weight loss measured week by week for Round 1 of Ti6Al4V test.....	182
100	Pin weight “Before test” and “After 1M cycles” for Round 1, Ti6Al4V test.	183
101	Final difference of weight for each pin for Round 1, Ti6Al4V test.....	183
102	Total weight loss for Round 2 of Ti6Al4V test	185
103	weight loss measured stage by stage for Round 2 of Ti6Al4V test	185
104	Pin weight at “Before test” cycles and “After 1M cycles” for Round 2, Ti6Al4V test.....	187
105	Final difference of weight for each pin for Round 2, Ti6Al4Vtest.....	187
106	Total weight loss for Round 3 of Ti6Al4V test	188
107	weight loss measured stage by stage for Round 3 of Ti6Al4V test	189
108	Pin weight “Before test” and “After 1M cycles” for Round 3, Ti6Al4V test.	190
109	Final difference of weight for each pin for Round 3, Ti6Al4Vtest.....	190
110	Interpolation curve of the debris production data from POD test on Ti6Al4V disc.....	191
111	Interpolation curve of the debris production data from POD test on Tech #1 disc.	192
112	Interpolation curve of the debris production data from POD test on Tech #2 disc.	194
113	Interpolation curve of the debris production data from POD test on Tech #3 disc.	195
114	Interpolation curve of the debris production data from POD test on AgTiN disc.	196
115	Roughness-wearing rate dependency.	197
116	Picture of the contact surface of the pin OE1.....	199

LIST OF FIGURES (continued)

<u>FIGURE</u>		<u>PAGE</u>
117	Picture of the contact surface of the pin OE2.....	200
118	Picture of the contact surface of the pin OE3.....	200
119	Picture of the contact surface of the pin OE4.....	201
120	Picture of the contact surface of the pin OE5.....	202
121	Picture of the contact surface of the pin OE6.....	203
122	Picture of the contact surface of the pin OE22.....	203
123	Picture of the contact surface of the pin OE23.....	204
124	Picture of the contact surface of the pin OE24.....	205
125	Picture of the contact surface of the pin OE25.....	206
126	Picture of the contact surface of the pin OE26.....	206
127	Picture of the contact surface of the pin OE6, used as reference.	207
128	Picture that grouped the 3D model and the Surface map of the contact surface of the pin OE10.....	209
129	Picture that grouped the 3D model and the Surface map of the contact surface of the pin OE11.....	209
130	Picture that grouped the 3D model and the Surface map of the contact surface of the pin OE12.....	210
131	Picture that grouped the 3D model and the Surface map of the contact surface of the pin OE13.....	211
132	Picture that grouped the 3D model and the Surface map of the contact surface of the pin OE8.....	212
133	Picture that grouped the 3D model and the Surface map of the contact surface of the pin OE9.....	213
134	Picture that grouped the 3D model and the Surface map of the contact surface of the pin OE22.....	213
135	Picture that grouped the 3D model and the Surface map of the contact surface of the pin OE23.....	214

LIST OF FIGURES (continued)

<u>FIGURE</u>		<u>PAGE</u>
136	Picture that grouped the 3D model and the Surface map of the contact surface of the pin OE24.....	215
137	Picture that grouped the 3D model and the Surface map of the contact surface of the pin OE25.....	216
138	Picture that grouped the 3D model and the Surface map of the contact surface of the pin OE26.....	217
139	Picture that grouped the 3D model and the Surface map of the contact surface of the pin OE27.....	218
140	Picture that grouped the 3D model and the Surface map of the contact surface of the pin OE28, used as a reference.	218
141	SEM image from Tech #1 coated disc surface.....	218
142	SEM image from Tech #2 coated disc surface.....	218
143	SEM image from Tech #3 coated disc surface.....	218
144	SEM image from AgTiN coated disc surface.	218
145	Complete version of the "Total weight loss" graph.	239
146	Complete version of the "Weight loss week by week" graph.	2399
147	Soak pin weight variation.....	240
148	Soak pin weight “before” and “after” the pin on disc test.	240
149	Complete version of the "Total weight loss" graph.	242
150	Complete version of the "Weight loss week by week" graph.	242
151	Soak pin weight variation.....	243
152	Soak pin weight “before” and “after” the pin on disc test.	243
153	Complete version of the "Total weight loss" graph.	245
154	Complete version of the "Weight loss week by week" graph.	245
155	Soak pin weight variation.....	246
156	Soak pin weight “before” and “after” the pin on disc test.	246
157	Complete version of the "Total weight loss" graph.	248

LIST OF FIGURES (continued)

<u>FIGURE</u>		<u>PAGE</u>
158	Complete version of the "Weight loss stage by stage" graph.....	248
159	Soak pin weight variation.....	249
160	Soak pin weight “before” and “after” the pin on disc test.	249
161	Complete version of the "Total weight loss" graph.	251
162	Complete version of the "Weight loss stage by stage" graph.....	251
163	Soak pin weight variation.....	252
164	Soak pin weight “before” and “after” the pin on disc test.	252
165	Complete version of the "Total weight loss" graph.	254
166	Complete version of the "Weight loss stage by stage" graph.....	254
167	Soak pin weight variation.....	255
168	Soak pin weight “before” and “after” the pin on disc test.	255
169	Permission to reprint Figure 1 from (4)	257
170	Permission to reprint Figure 2 from (11)	258
171	Permission to reprint Figure 3 from (13)	259
172	Permission to reprint Figure 14	260
173	Permission to reprint Figure 15	261
174	Permission to reprint Figure 16	262
175	Permission to reprint Figure 17	263
176	Permission to reprint Figure 56 from (37)	264

LIST OF ABBREVIATIONS

POD	Pin-On-Disc
THA	Total Hip Arthroplasty
TKA	Total Knee Arthroplasty
TJA	Total Joint Arthroplasty
OCP	Osteoclast Precursor Cells
IL-6	Interleukin-6
IL-1 β	Interleukin-1 β
UHMWPE	Ultra High Molecular Weight Polyethylene
FDA	Food and Drug Administration
COF	Coefficient Of Friction
RA	Arithmetic Roughness
TA	Transverse Acoustic
LA	Longitudinal Acoustic
2A	second-order Acoustic
TO	Transverse Optical
Mcycles	Million Cycles
SD	Standard Deviation

LIST OF ABBREVIATIONS (continued)

WR	Wear Rate
----	-----------

SUMMARY

The introduction of joint arthroplasty has revolutionized orthopedic surgery. For decades, clinicians and engineers have worked together to design and realized some durable and efficient implants able to reproduce the functional goal of biological structures while reducing the adverse reactions induced by their introduction inside the human body.

However, despite the great reached results, not a single material has been identified as perfect when performing in vivo and the production of wear debris is still considered one of the main drawbacks of this kind of implants.

In order to outweigh these issues, modern researches have found in surface coatings the opportunity to functionally tune the external properties of the implant while maintaining the original mechanical properties of the substrate material. In particular, one material has revealed to be particularly promising due to its characteristics: Titanium Nitride.

This work is entirely dedicated to the exploration of the properties of Titanium Nitride (TiN) as a coating material, with a particular focus on their dependency on the coating process and on the working conditions.

The performances of this material have been tested and compared to the ones of the uncoated substrates and the obtained results have been critically analyzed paying the way for further interesting developments that are presented in the conclusive chapter of this document.

CHAPTER 1

INTRODUCTION

The introduction of joint arthroplasty has been one of the most important steps in the genesis of modern orthopedic surgery as it has had a great influence on the increased efficiency and efficacy of prosthetic implants.

However, almost everything has changed from the total ivory knee prosthesis that has been implanted by Themistocles Gluck in 1890 in Berlin on the tuberculous knee of a young lady, known as the first implanted total joint prosthesis (1).

For more than a century, surgeons and engineers have worked hard together in order to design and realized some durable and efficient implants in order to reproduce the functional goal of biological structures while reducing the adverse reaction that naturally shows up when introducing foreign materials in the human body.

Today, as a result of this continuous and extended progress tens of thousands of hip or knee replacements are successfully implanted every year in the United States and Europe. Accordingly to recent research, published on *The Journal of Bone and Joint Surgery* in 2015, the prevalence of arthroplasty replacements in 2010 was 0.83% for total hip replacements (THA) and 1.52% for total knee replacements (TKA). Thus, a total of around 7 million Americans having an orthopedic prosthesis (2).

A similar development is happening in Europe where, according to the *National Joint Registry (NJR)*, about 160'000 TKA or THA are executed every year in the UK causing the United kingdom to be the fourth European state in term of THAs performed per 100'000 inhabitants with 194 THAs. Germany, with 296 THAs/100'000 residents, Switzerland, with 287 THAs, and Belgium, with 240 THAs, lead this special ranking in the old continent (3). Despite great developments in prosthetic design and an increasing number of annually performed implants, not a single material has been found that does not require revision when inserted into the human body.

Table 1 Relationship between cause of failure^a and time to failure (time interval to revision)

Time interval to revision	Number of hips requiring revision	Aseptic loosening (%)	Infection (%)	Instability (%)	Component failure (%)	Periprosthetic fracture (%)	Pain (%)
<2 years	79	17.70	24	33	3.80	6.30	15.20
2–5 years	39	46.20	10.30	25.60	0.00	5.10	12.80
5–10 years	49	67.30	14.30	10.30	0.00	2	6.10
>10 years	70	90	5.80	0.00	0.00	2.80	1.40
<5 years	118	27.10	19.60	30.5	2.50	5.90	14.40
>5 years	119	80.70	9.20	4.20	0.00	2.50	3.40
Total	237	51.90	15.60	16.90	2.10	5.50	8

^a Cause of failure is given in the table as the percentage of the group

Figure 1: Relationship between cause of failure and time to failure in THA implants – [4].

In particular, as infection and instability can be considered as the main cause of the loss of primary stability in an implanted device (4–9), accounting for the 57% of the failure events registered within the first two years from the implant, osteolysis and the subsequent aseptic loosening are responsible for almost 90% of the revision events after the first two years, as shown in the table shown in the previous page.

Despite the great developments and the continuous research that has characterized this field, the creation of wear debris from any part of the prosthesis, which has been identified as the main process that led to the loss of secondary stability (10), is still considered as unavoidable.

This is the main reason why the elimination or, more realistically, the reduction of “the wear problem” is considered as one of the most important challenges to solve for modern joint arthroplasty.

1.1 Motivations

1.1.1 The wear problem

As just introduced in the previous paragraph, aseptic loosening has been demonstrated to be mainly associated with a chronic process of bone resorption and damage called osteolysis associated with both osteolytic and inflammatory processes that mainly occur because of the release of metallic and polymeric particles at the implant site (10).

Osteolysis is the result of both the induced weakness of bone tissue caused by the wear debris produced by the interaction of the artificial surfaces of the prosthesis that is released in the implant site and the mechanical instability of the prosthetic components under external forces that may generate micro-movements in the prosthesis that led to bone damage (3).

In particular, when these foreign bodies' particles are generated, they tend to accumulate in the joint synovial fluid and they may eventually be incorporated into the surrounding tissues after the stimulation of the local inflammatory response.

As shown in the image that has been reported on the following page, when entering the human tissues, the most important cell type that is activated by the wear debris are the macrophages, that may respond in two different ways, both contributing to the periprosthetic resorption of bone tissue. First of all, they contribute to the activation of the inflammatory cascade that ends with osteoclast recruitment and activation(11), but recent studies (12) have also demonstrated that wear products also inhibit the protective effect of antiosteoclastogenic cytokines like interferon-gamma, increasing differentiation of macrophages into osteoclasts.

In particular, when the inflammatory process starts osteoclast precursor cells (OCP) differentiate into functional osteoclasts that are responsible for the bone resorption process. This activation is mediated by a wide range of different factors such as *chemokines* or *pro-inflammatory cytokines* that are released by macrophages and other cells that are responsible for the positive (+) or negative (-) modulation of the process.

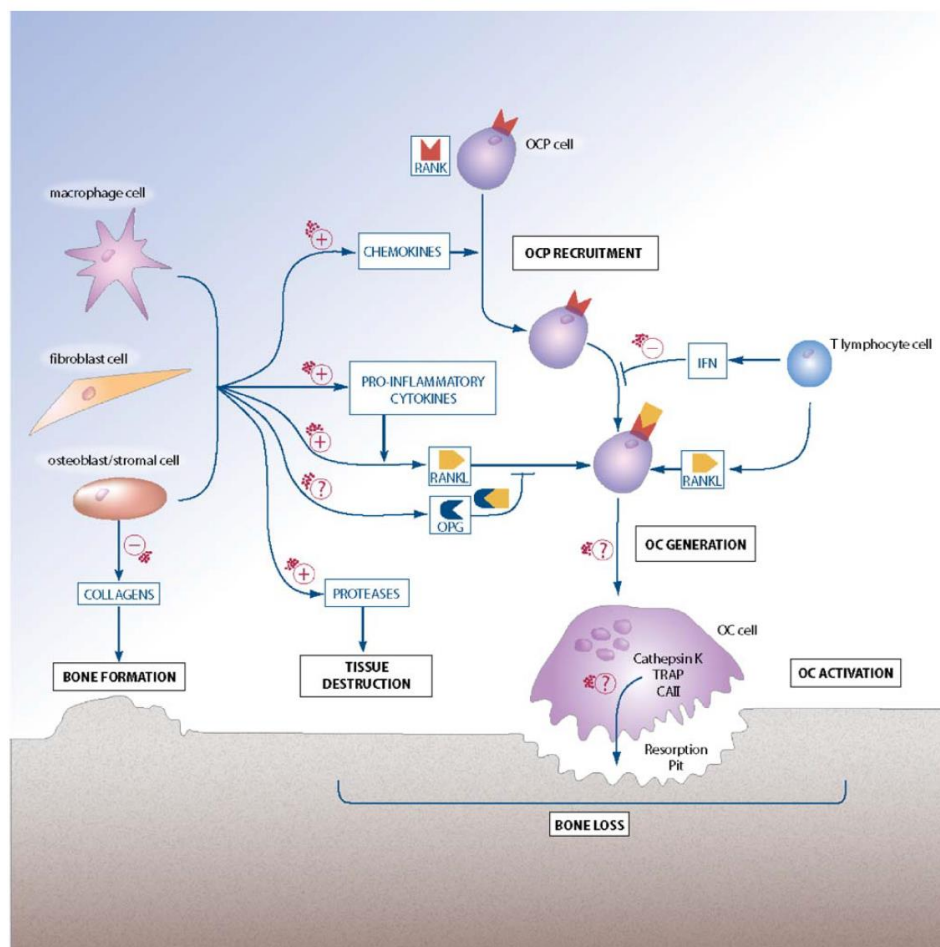


Figure 2: Cellular and molecular pathways of the osteoclast genesis and influence of wear debris particles in bone resorption process – [11].

Moreover, adherent endotoxin on the wear debris particles have been revealed to be the cause of the activation of *interleukin-6 (IL-6)*, *interleukin-1 β (IL-1 β)* and *tumor necrosis factor α (TNF- α)* that contributes to making the activation of osteoclast even more effective (12).

Osteoblasts, fibroblasts and lymphocytes are also involved in the adverse reaction, but they have a minor relevance with respect to macrophages.

If this cascade of events may be considered characteristic of the interaction between biological tissues and any type of wear debris, it is also true that polymer particles and metal ones do not induce the exact same processes when released in the human body. In fact, while Ultra High Molecular Weight Polyethylene (UHMWPE) particles tend to remain close to the implant site, metal ions are more subjected to migration and they tend to accumulate into target organs such as liver, kidneys, heart and even brain causing even more severe problems (13,14).

In addition, the release of these types of materials has been demonstrated to be the main cause of metallosis episodes, associated to the formation of pseudotumors in the tissues that surround the implant site, metal allergies, that will be the main focus of next section, and a contributory cause of osteolysis itself (13,14).

To sum up, the pathogenic mechanisms of implant-associated osteolysis include a wide variety of different mechanisms initiated by the release of wear debris in the living tissues, that manifest themselves in the recruitment of a wide array of cells type as macrophages, fibroblast,

neutrophils, giant cells, but also osteoblast cells that are the main responsible for the processes of bone resorption.

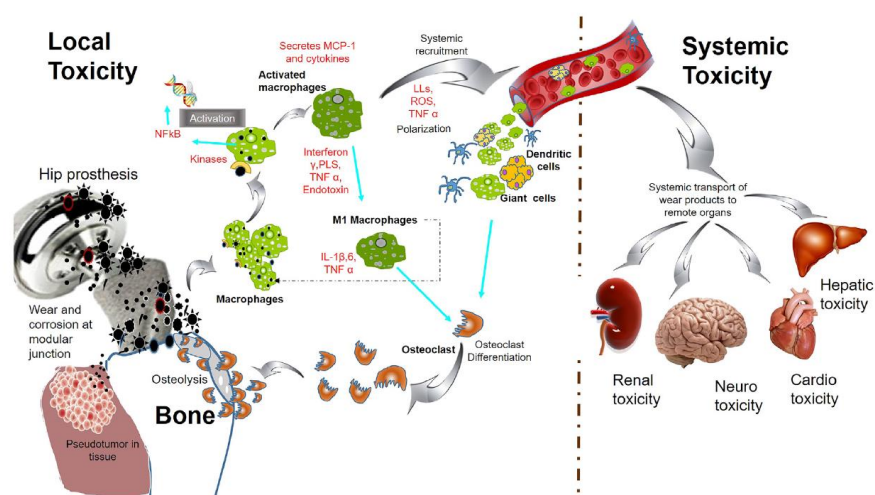


Figure 3: Schematic of the adverse reaction caused by the release of metal ions - [13].

Thus, in order to reduce the risk to induce aseptic loosening one of the most simple solution is to reduce the number of released particles. However, wear products may be produced in a variety of different ways including debris particles from all the main materials of the implant, like

polyethylene, ceramic and metal, but also from the bone cement itself and their bio-reactivity has been demonstrated to depend mainly on two elements: particle characteristics, such as size, concentration in the tissues and composition, and patient biological characteristics (3).

Anyhow, even if any particle may increase the adverse cellular reaction induced by the production of wear debris, cytological examination demonstrated that more than 70% of the overall amount of wear debris produced by a Metal-on-polyethylene prosthesis is constituted of polyethylene particles (3).

All these elements explained the long series of changes that have characterized the history of joint arthroplasty and in particular of the materials used to design the different prostheses and why biotribology will be the main field directly involved in the future development of this sector.

From *Metal-on-metal* prosthesis, quite diffuse in the '70s and then disappeared till today because of metallosis issue and potential carcinogenic effects caused by the release of metal ions, to *Ceramic-on-ceramic* prosthesis, with their low friction coefficient, low debris production and inert behavior, but also their high costs and risk of early damage, and *Metal-on-polyethylene* ones, characterized by a good cost-efficiency ratio, a predictable lifespan, but also a lot more polymeric debris, joint arthroplasty has been always oriented toward the identification of innovative solutions to limit the occurrence of this problem, while maintaining optimal mechanical characteristics for the prosthesis itself (1,15).

Looking at the future, the most interesting solution may be represented by the coating materials that may enhance the surface properties of the material, that are one of the most important factor that influence the wear production of an orthopedic implant, while maintaining the mechanical properties of the substrate material, that has great relevance in the determination of the ability of the prosthesis itself to substitute the function of the lost biological structure.

1.1.2 Metal allergy

As just introduced in the previous section, one of the main problems associated with the release of metal ions inside the human body is metal hypersensitivity, caused by the adverse immune reaction of metal particles.

In fact, when coupled with particular proteins, these particles may act as antigens for circulating lymphocytes activating an immediate humoral response (7,16). The specific processes involved in the genesis of this hypersensitivity to metal ions are still under analysis and a detailed description of this phenomenon has still to be defined.

However, despite its rare occurrence, <1% of total joint replacements (TJAs) (17), this event may be the cause of chronic debilitating pain and swelling in the implant site that may deeply affect the final result of the operation causing severe impairments in the daily life of the patient. This may even lead to the failure of the implant, forcing the clinician to revise the implant itself.

Thus, when designing a prosthetic implant it is important also to consider the overall amount of metal ions that are released in the tissues by the bearing surfaces and it may be necessary to find some ways to reduce this quantity.

One of the possible solutions may be to use a coating material that will work like a "shield" preventing metal ions from the substrate to be released in the implant site reducing their potential adverse effects. This is particularly true when talking about CoCr substrates that have been demonstrated to be much more subjected to allergic reactions with respect to Ti alloys (14).

1.3 A possible solution: surface coating

As introduced, modern researches in joint arthroplasty, and in particular for THA and TKA, mainly focus on how surface properties of metallic materials may be tuned in order to guarantee optimal performances of the prosthesis, while reducing the wide range of adverse effects that derive from the insertion of an external material into a biological environment.

In order to pursue this challenge, one type of process has gained more and more importance: surface coating. The application of coating material on the surface of a bulk structure, called substrate, essentially consists of the application, toward a wide variety of different techniques, of a small layer of protective material on the zone of the substrate that is subjected to harsh or corrosive environment (18).

In particular, this process has the great advantage of preserving the mechanical properties (e.g. yield modulus, fatigue resistance, bending and creep properties), thermal properties (e.g. thermal expansion and conductivity to transfer heat flux), dynamic load behavior and all the other parameters for which the bulk substrate material has been chosen for when designing the prosthesis while mixing them with upgraded properties in term of corrosion resistance, functional surface properties (e.g. wettability, hardness and coefficient of friction) and also wear resistance in the zone where the coating layer is applied.

Recent studies have a particularly focus on a particular type of coating material: the Titanium Nitride (TiN). This bright gold ceramic material is characterized by a series of particularly interesting properties, detailed in the following chapter, that contribute to theoretically make it one of the best candidates for this kind of process.

1.4 Project Aim

This project has been entirely dedicated to the exploration and the study of the properties of Titanium Nitride with the final aim to investigate the real effectiveness of TiN coating of a metallic surface in reducing the production of wear debris.

In particular, this experiment has been mainly focused on the role of the deposition technique and substrate characteristics in the determination of the final wear resistance properties of the analyzed materials.

To do that, the wear behavior of differently processed TiN coated discs on different substrates, CoCr and Ti6Al4V, have been tested and the results have been compared to reference characteristics obtained for uncoated CoCr and Ti6Al4V discs in the same tests. All the tests have been executed using a defined set of parameters that simulate the condition that the material may experience when implanted into biological living tissue.

To conclude the work, possible further developments and main defects of the used approach have been highlighted.

1.5 Thesis Structure

If Chapter 1 has been mainly dedicated to the introduction of the problems and the possible solutions of them, Chapter 2 will be entirely dedicated to the description of the main characteristics of Titanium nitride and the literature state of the art about this material.

Chapter 3 will contain a brief overview of the main experimental materials used during the test.

Chapter 4 shows the main procedure, or methods, that have been used to perform the analysis. All the procedures have been described in detail in order to allow anyone to replicate these analyses.

Chapter 5 contains a collection of the most interesting results that have been obtained from the performed tests. Only the main results have been reported here, while a bigger collection of data,

containing also some raw information, may be found in the appendices that are contained in Chapter 7.

Chapter 6 will conclude the thesis with a summary of the main outcomes of this work, but also a definition of the main limits of this work and some purposes for further developments of the analysis.

CHAPTER 2

STATE OF THE ART

This chapter has been entirely dedicated to the definition of what is known about Titanium nitride (TiN). Hereunder, the main characteristics of the material will be defined concluding the analysis with a brief review of the literature citation of the use of TiN for the coating of orthopedic implants.

2.1 Introduction

Titanium Nitride (TiN) is an extremely hard ceramic material with reduced density (5.22g/cm^3) and a high melting point (2930°C) that has been used as a coating for mechanical, aerospace and even medical tool steels since the second half of the sixties (19). This success is mainly due to its properties that are strongly dependent on its chemical structure that has been revealed to be quite similar to the one of sodium chloride.

However, it has been in 1972 only when Steinemenan firstly patented the use of titanium implants or titanium derivate for the treatment of biological bone tissue (20). Steinemenan was also the first person to project about the possibility to use a surface layer of coating material to prevent surface corrosion and abrasion in joint arthroplasty implants.

After that moment, a lot of researchers, surgeons and engineers have followed Steinemenan idea and due to its peculiar properties, TiN has been always considered as one of the best types of material to pursue this aim.

2.2 **Titanium Nitride as coating material**

As said, TiN is a gold ceramic layer that may be effectively applied on the joint surface of the metallic prosthesis using different processing techniques because it can guarantee the following interesting properties (21–24):

- *Increased hardness (2400-2600 Hv):* As all the ceramic materials, this material has shown a great surface hardness, about four times greater than the one of CoCr (650 Hv) that makes it being the perfect candidate to constitute a bearing surface.
- *Inert and stable material:* Because of its ceramic soul, TiN does not react with most materials. Moreover, it is oxidation resistant and it is resistant to thermal-induced changes at in-vivo conditions.
- *Biocompatible:* TiN coating has been approved by the FDA as a coating material for arthroplasty implants because it does not react with blood, bones and other biological tissues making it a perfect choice for medical applications.
- *Low friction coefficient (COF):* It depends on the other surface of interaction, but it is extremely low (0.6 for steel alloys)

- *Low surface roughness:* Its surface roughness is really low and the evaluated arithmetic roughness can easily reach values smaller than $0.05\mu\text{m}$.
- *Enhanced wettability characteristics:* They contribute to improve the interaction with the synovial fluid helping to lubricate the joint.
- *Resistance to third body wear:* TiN is also resistant to third body wear that is caused by polymeric or cement particles that may remain blocked in the joint site causing damages on the bearing surfaces. Its high resistance to scratches may prevent this event to cause big damages.
- *Metal allergy risk minimization:* The presence of TiN coating may help to minimize the risk of metal allergy. In fact, the presence of this ceramic layer may help to reduce the number of metal ions that are released in the implant site.
- *Reduced bacterial adhesion:* TiN smooth surface makes it less simple for the microorganisms to attach on the surface. Moreover, TiN may also be doped with other materials, such as Ag particles, to dramatically decrease the occurrence of this phenomenon.
- *Adhesion:* When properly deposited on adequately treated and polished substrates, this material may guarantee high adhesion properties (25).

All these properties, and in particular its low friction coefficient, high wear resistance and chemical inactivity make TiN one of the most interesting materials that may be used as a coating.

However, all these properties are highly dependent on the way the TiN layer is deposited on the surface and so, the processing technique followed to perform the coating has strong relevance in the determination of the effectiveness of the material itself.

2.3 Titanium Nitride in medical literature

As introduced in the previous paragraphs, Titanium Nitride (TiN) properties make this material to be a good candidate to be used as coating material for implantable devices, at least on the theoretical point of view.

However, even if preclinical studies have demonstrated the biocompatibility and tribological properties of this ceramic surface, literature about the application of this material to implant surfaces is much more contradictory and some of the obtained results have been revealed to be different from the expected ones.

This literature analysis is particularly significant in this work as it allows to have a larger understanding of the real properties of this material and the variability of its behavior depending on the imposed boundary conditions and the characteristics the test is focusing on. As known, all these aspects have a strong influence on the final working condition of the material and may have a strong impact on the final obtained results.

A comparison between the experimental results and the clinical outcomes will be introduced in the next two sections in order to identify which are the elements that may weigh the most in the determination of the material results

2.3.1 Preclinical studies

Preclinical studies have been really important for the assessment of some of the properties of the material.

High *resistance to corrosion* (26) has been proven, but also *biocompatibility* has been assessed using different cells type (human bone marrow stem cells and osteoblasts, human fibroblasts, human fetal osteoblasts) and studying their behavior in term of proliferation and differentiation on TiN-coated materials (27). Moreover, in vivo studies has been done also on dogs, rats and rabbits, where TiN coated materials have demonstrated their affinity with the biological environment showing similar or better properties with respect to the uncoated substrates (27,28).

In addition, also the *bacterial adhesion* on the material has been assessed showing a reduced adhesion and proliferation of bacteria on this kind of coating with respect to the control substrate material (29).

To conclude the preclinical studies, great relevance may be attributed to *wear behavior*: experimental researches have shown contradictory results about this property and a strong dependency of performances on the coated material. In particular, when applied to the Ti6Al4V substrate it has been registered improved scratch resistance, reduced amount of abrasive particles formed and also a reduction of the polyethylene debris produced in a Metal-on-polyethylene pin on disc test (27).

However, some cases of adhesion failure of the coating have been identified with the TiN particularly prone to pitting and delamination when articulating against a polymeric pin, but also when TiN has been used as coating of a CoCrMo substrate, showing a fourfold increased wear rate in respect to the control (27).

Anyway, all these properties have revealed to be strongly dependent on substrate characteristics, and in particular, on its Young modulus, on the coating techniques, that determine the adhesion of the TiN coating on the substrate, and on the testing fluid that has been used as the presence of protein has been demonstrated to reduce the wear rate.

2.3.1 Clinical results

The same variability seen for the preclinical tests has been common also to the clinical analysis. If reduced *bacterial adhesion* has been verified also in clinical practice (25), the same positive results have not been obtained by the analysis of TiN coated total knee implants, here no major changes in the clinical outcome has been identified in respect to the control (30), but also of the in-vivo wear properties of TiN coated femoral that has shown an increased fragility in respect to third body wear when implanted (31).

Also in these cases, the boundary conditions have been demonstrated to have an incredibly important role in the determination of the final performances of the prosthesis. In particular, one

element has been identified as the most important aspect in the definition of the properties of the TiN: the coating process.

Third bodywear, cohesive failure and delamination process have been led back to the techniques that are used to deposit this thin layer.

Thus, in order to optimize the performance of the TiN coating, it will be necessary to optimize and standardize the technique that is used to deposit it. In the following chapters, different coating techniques will be studied and tested to verify which condition may help this material to perform at its best.

CHAPTER 3

MATERIALS

The materials used during the experiment will be presented first and, after these ones, the chapter will focus on the description of the procedure that has been performed to characterize and analyze the differences in the behavior of the samples.

3.1 CoCr coated/uncoated discs

Pin on disc (POD) tests have been conducted on CoCr discs, both coated and uncoated. The coated ones have a TiN layer on the surface, applied with different techniques. Ag-doped TiN coating has been used for one set of discs.

Information about the coating processes will not be provided as they are protected by an industrial secret.

All the discs have been cleaned before the coating procedure, polished after the coating application to eliminate eventual defect (this procedure has not been followed for Tech #1 disc) and cleaned again before starting the test.

All the samples have been labeled with a progressive code in order to keep them tracked during the entire experiment. On the next page, a brief summary of the provided sample has been reported.

TABLE I: CoCr DISC SUPPLY FROM FACTORY

Disc type	Number of samples	Code
<i>Uncoated CoCr</i>	4	#1, #2, #3, #4
<i>TiN coating, tech #1</i>	4	#5, #6, #7, #8
<i>TiN coating, tech #2</i>	4	#9, #10, #11, #12
<i>TiN coating, tech #3</i>	4	#13, #14, #15, #16
<i>Ag-doped TiN coating</i>	4	#17, #18, #19, #20

In addition, three more CoCr discs from the laboratory were introduced in order to have a second reference value for the final discussion of results. These additional discs have been labeled with codes #21, #22, #23.

A complete characterization of the 2-Dimensional and 3-Dimensional geometry of the discs has been defined and shown on the following page.

2D geometry of the discs:

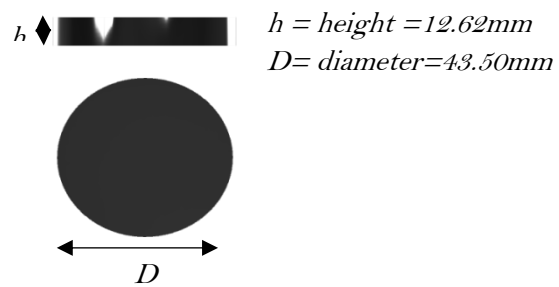


Figure 4: Disc 2D geometry of frontal and top plane.

3D geometry of the discs:

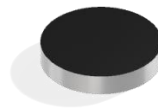


Figure 5: Discs 3D geometry.

Picture of the different discs type:



Figure 6: Different discs type. From left to right it is possible to see Uncoated CoCr disc, TiN coating, tech #1 disc, TiN coating, tech #2, TiN coating, tech #3 disc, Ag-doped TiN coating disc, Uncoated CoCr disc from the LAB.

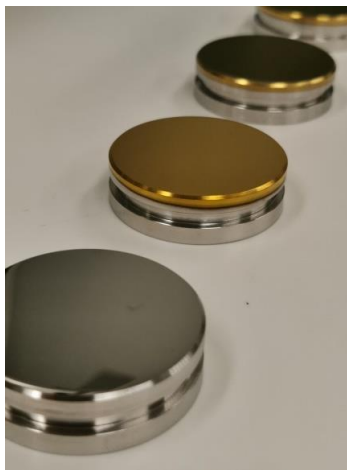


Figure 7: Details of final surface polishing.

3.2 Ti6Al4V coated/uncoated discs

Pin on disc (POD) tests have been conducted also on Ti6Al4V discs, both coated and uncoated. The coated ones have a TiN layer on the surface, applied with different techniques. Ag-doped TiN coating has been used as a coating material for one set of discs.

Information about the coating processes will not be provided as they are protected by an industrial secret. The coating techniques and the procedure that has been followed to process the disc have been equal to the ones explained in the previous section.

All the samples have been labeled with a progressive code in order to keep them tracked during the entire experiment.

Here is a summary of the samples provided by the factory:

TABLE II: Ti6Al4V DISC SUPPLY FROM FACTORY

Disc type	Number of samples	Code
<i>Uncoated Ti6Al4V</i>	4	#24, #25, #26, #27
<i>TiN coating, tech #1</i>	4	#28, #29, #30, #31
<i>TiN coating, tech #2</i>	4	#32, #33, #34, #35
<i>TiN coating, tech #3</i>	4	#36, #37, #38, #39
<i>Ag-doped TiN coating</i>	4	#40, #41, #42, #43

2D geometry of the disc:

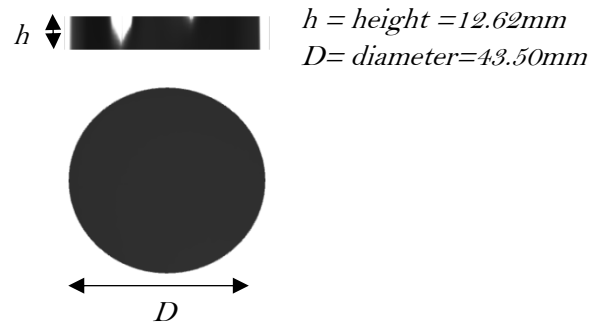


Figure 8: Discs 2D geometry of frontal plane and top plane.

3D geometry of the disc:

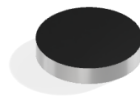


Figure 9, Discs 3D geometry.

Picture of the different discs type:



Figure 10, Different discs type. From left to right it is possible to see Uncoated Ti6Al4V disc, TiN coating, tech #1 disc, TiN coating, tech #2, TiN coating, tech #3 disc and Ag-doped TiN coating disc.



Figure 11: Details of final surface polishing.

3.3 UHMWPE Pins

Pin on disc (POD) test requires polymeric pins in order to test the wear production of different materials. In this test, it has been used 61 cylindrical UHMWPE identical pins, all labeled and separately packaged.

Pins are made of GUR1050 UHMWPE and they have been treated with 30 ± 5 kGy radiation in order to induce crosslinking in the material. Pins have been stored at -80°C before using them. This operation prevents them from the oxidation process.

Hereunder, it has been reported the bi-dimensional and tridimensional geometry of the pins.

2D geometry of the pins:

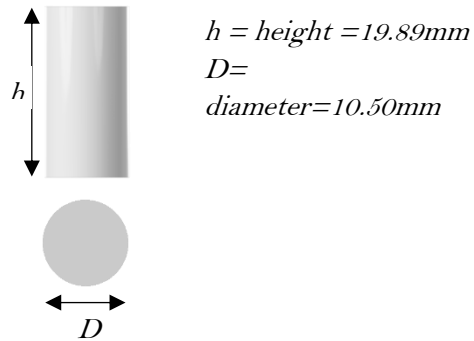


Figure 12: Pins 2D geometry of frontal plane and top plane.

3D geometry of the pins:



Figure 13, Pins 3D geometry.

3.4 AMTI® Ortho-POD

All the pin-on-disc tests have been performed on the Ortho-POD device by AMTI® shown below. Before starting the experiment, we have completed a full calibration of the Ortho-POD.



Figure 14: AMTI Ortho-POD device

Description (32)

The AMTI Ortho-POD is a multidirectional pin-on-disc (POD) machine that is able to replicate all the different motion types that are essential to replicate with the best accuracy the in vivo wear of Ultra High Molecular Weight Polyethylene (UHMWPE) joint implants. This machine is capable of simulating both unidirectional and bidirectional movement, allowing it to reproduce in an easy way the cross-shear motions that may be experienced by a real prosthesis when implanted into an in vivo environment. All the six pin holders provided by the machine have three degrees of freedom that may be controlled separately and all the machine's motions, loads and programs are fully tunable via the included software. Custom wear programs and pin path may be defined in order to simulate specific behaviors of the prosthesis.

All the six testing stations of the Ortho-POD are temperature-controlled in order to simulate the condition that might be experienced by the material into a biological environment. Even the load of each pin-on-disc station is fully programmable up to 445N.

3.5 Zygo® Newview 6300 3D optical surface profiler

In order to perform a full characterization of the discs, a measure of the surface roughness has been performed. Zygo Newview 6300 has been used to achieve these results.

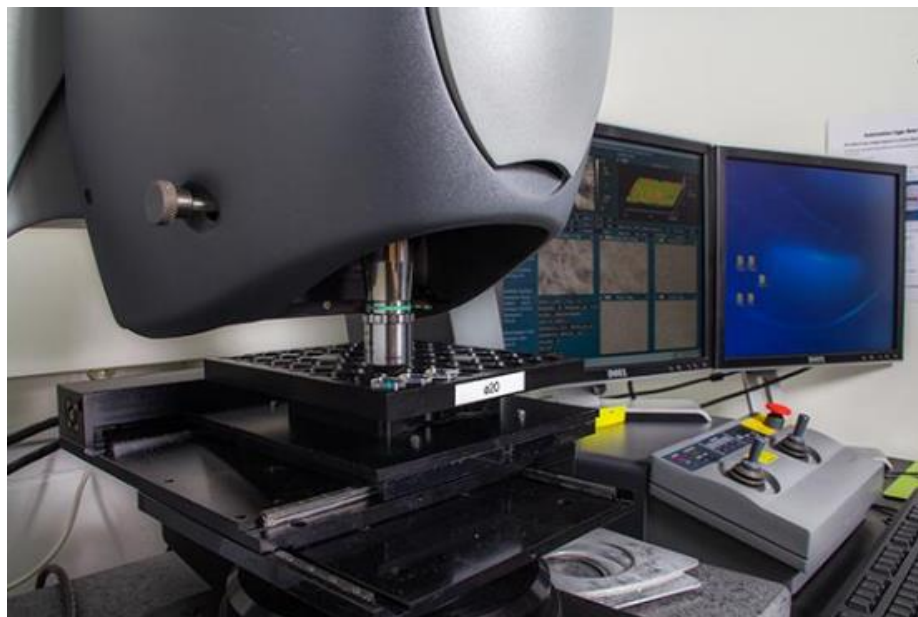


Figure 15: Zygo Newview 6300

Description (33)

The Zygo optical Profiler has been designed for the characterization of the surface characteristics of materials. It is able to collect information about surface roughness, surface

profile, intensity maps and other topographical information in a non-destructive, contactless and quick way. In addition, it is a precise tool that may guarantee surface measurements in the order of nanometers to micrometers. A software, called MetroPro[®] has been used to obtain and process all the data.

3.6 **HORIBA[®] LabRAM HR Evolution, Raman spectrometer**

In order to perform a complete characterization of the discs before and after the wear test, it has also been performed Raman spectroscopy on the surface of all the samples. HORIBA LabRAM HR Evolution has been used to complete this analysis.



Figure 16: HORIBA LabRAM HR Evolution – [34]

Description (34)

The LabRAM HR Evolution Raman microscope has been projected to perform Raman spectroscopy for micro and macro samples.

This instrument has several interesting properties that make it the ideal candidate to perform this type of measurement. First of all, it is compatible with a wide range of laser wavelengths (200-2100nm) allowing a full characterization of the analyzed material. Secondly it is controlled by the “LabSpec 6” software that may be used to control measurement settings, data collection and data elaboration constituting a complete, easy to use and direct tool to perform the tests. In conclusion, it also has the DuoScan™ fast Raman function that may be helpful to capture high precision, ultra-quick Raman maps performing a collection of a high number of data over the defined area in an incredibly low amount of time.

3.7 **LABCONCO XPert® Weigh**

All the weight evaluation has been performed using LABCONCO XPert weigh as it guarantees the 0.01mg sensibility needed for this type of experiment.



Figure 17: LABCONCO XPert weigh

Description (35)

XPert Weigh Boxes has been designed to meet the request of pharmaceutical research, nanotechnology, biochemistry, but it is daily used in many applications around different

researching themes. It has been furnished with inlet and outlet HEPA filters that guarantee a resistant leak-tight physical barrier to protect the operator. Humidity and temperature are controlled inside the weighing chamber. In addition, an anti-static ionizer fan and a balance vibration isolator have been introduced in order to guarantee the higher performance possible during the weighting procedure. The scale has a sensibility of 0.01mg.

3.8 ZEISS Stemi 2000-C

In order to evaluate possible alteration in the surface of pins and/or metal discs, it has been collected qualitative data about changes in morphology. This process has been completed using the following ZEISS 2000-C stereomicroscope coupled with a camera.

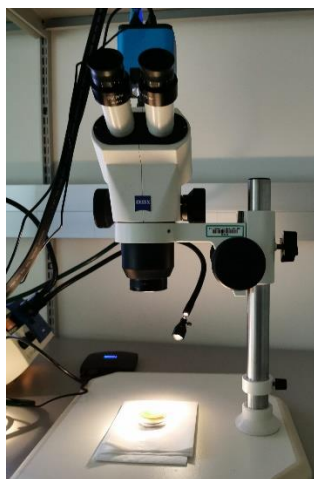


Figure 18: ZEISS 2000-C stereomicroscope

Description (36)

Stemi 2000 stereomicroscope from ZEISS is able to guarantee sharp, free of distortions images. This instrument allows to have big spaces for illumination and sample manipulation, and interchangeable optics ensure functional applications at varying distances. In particular, in this application it has been used 0.4x and neutral lenses with single illumination from above, or coupled lateral illumination sources.

CHAPTER 4

METHODS

4.1 Discs characterization

4.1.1 Evaluation of disc surface roughness

All the roughness evaluations for the surface characterization of the pins have been realized using the Zygo® Newview 6300. In order to complete this aim the following steps have been performed:

Zygo® setup

1. In order to stabilize the machine, the Nitrogen source that supplies the stabilized table, has been opened following standard procedures.
2. A 20x lens has been mounted on the Zygo to perform the measurements.
3. “MetroPro” app has been launched on the computer and “Micro2.app” has been chosen to perform the analysis.

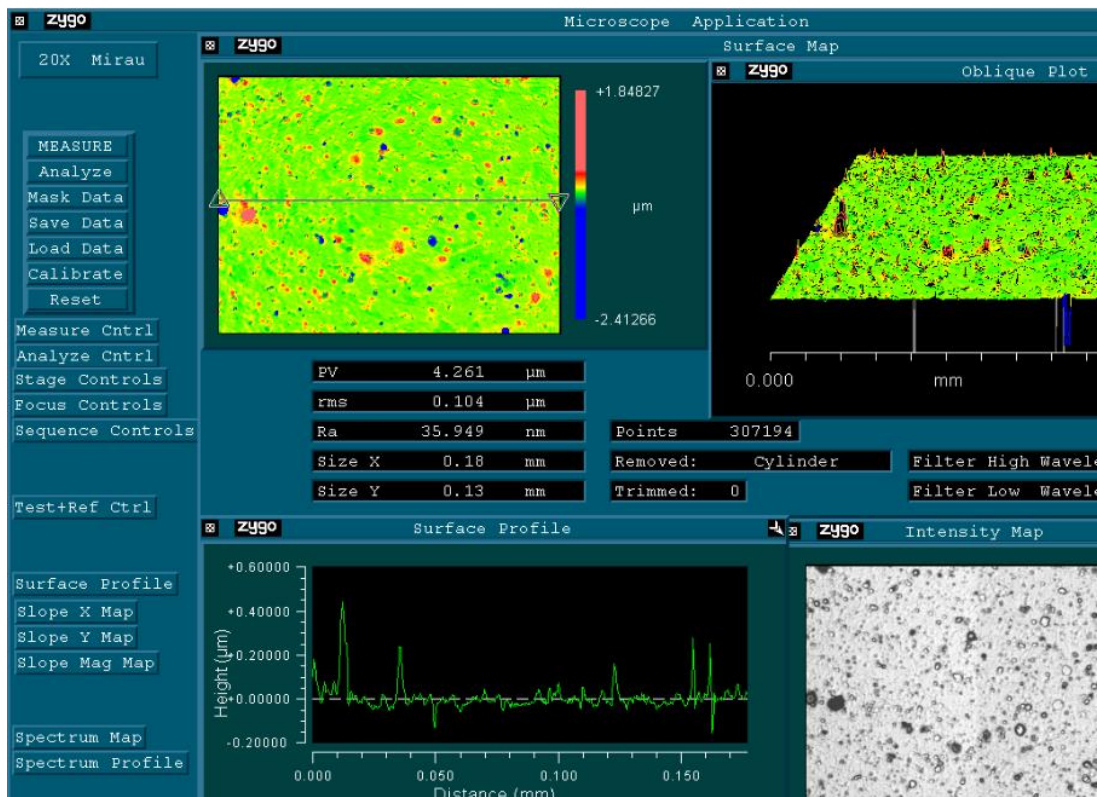
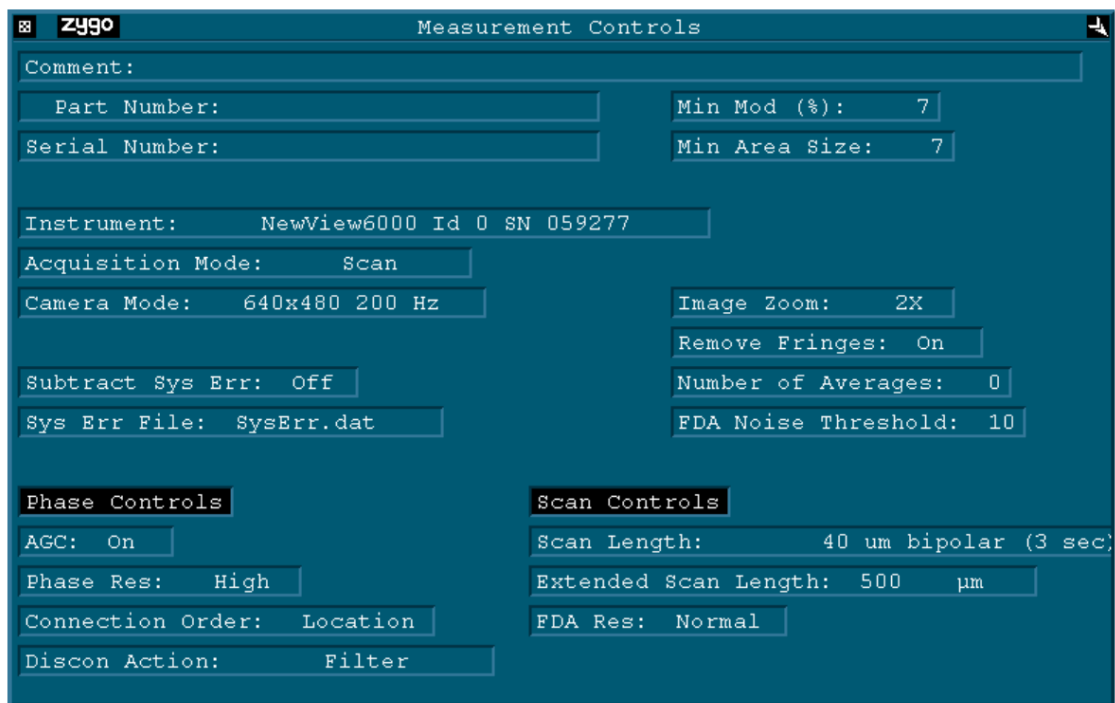


Figure 19: Micro2.app interface¹.

¹ On the left, it is possible to see all the main commands of this software. In the central part of the screen all the most relevant data are shown. In the top-left corner it is possible to see a surface profile heat map, on its right a 3D oblique plot of the surface profile. On the bottom-left corner a linear surface profile is visualized whereas on its right an intensity map of the surface is shown. In addition, the central numbers give you the Pick-Valley maximum distance (PV), the root-mean square error (rms), the arithmetic roughness (Ra), the x-length of the sample (Size X) and the y-length of the sample (Size Y).

4. In “Micro2.app” the following settings have been applied in order to perform the measurements.



The screenshot displays the 'Zygo Measurement Controls' window. It features a dark blue background with white text and input fields. The window is organized into several sections: a top section for general settings, a middle section for instrument and acquisition parameters, and two bottom sections for phase and scan controls. The settings are as follows:

General Settings	
Comment:	
Part Number:	
Serial Number:	
Min Mod (%):	7
Min Area Size:	7

Instrument and Acquisition	
Instrument:	NewView6000 Id 0 SN 059277
Acquisition Mode:	Scan
Camera Mode:	640x480 200 Hz
Image Zoom:	2X
Remove Fringes:	On
Subtract Sys Err:	Off
Number of Averages:	0
Sys Err File:	SysErr.dat
FDA Noise Threshold:	10

Phase Controls	Scan Controls
AGC: On	Scan Length: 40 um bipolar (3 sec)
Phase Res: High	Extended Scan Length: 500 um
Connection Order: Location	FDA Res: Normal
Discon Action: Filter	

Figure 20: Zygo Measurement settings.

Roughness measurement

The next step of the analysis has been to perform the actual surface roughness measurement. In order to quantify the surface roughness of the samples, five measurements have been taken and the average and the standard deviation have been calculated.

1. Discs have been placed on the Zygo plate with the number on their back on the left-hand side.
2. A mask has been applied to them in order to perform the roughness measurements always in the same points. Five measurements are performed on the five points defined by the mask. Points number 1, 2, 3, 4 are on the wearing path, whereas number 5 is in an unworn part.

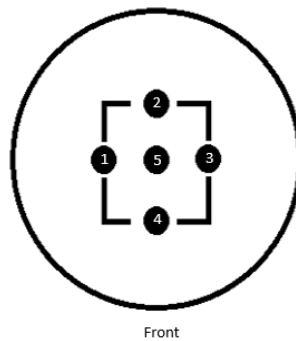


Figure 21: Roughness measurement mask.

3. Locate the Zygo over point number one and try to focus the image. Use the F5 button to adjust the light.
4. As you see interference fringes and you are able to position them parallel to the bottom border of the screen.
5. You can adjust the interference fringes orientation using the two big screws located in the bottom part of the Zygo.
6. Hit “Measurement” to perform the measurement.
7. Take care that "Points" value is above 30700 which means you have a good signal and the sample is focused.
8. To save the data, press “Save Data”.
9. Write the Ra measurement for the surface roughness.
10. To save the images click on the Zygo logo on the top-left corner of them and save them as .tiff files.
11. Repeat the operations from 1 to 7 for all the five points.
12. Repeat the operation from 1 to 8 for all the six discs.

This operation has been performed before and after each round in order to detect and characterize any kind of change in the surface characteristics. At the end of each round an overall number of 10 measurements for each disc, 5 pre-test measurements and 5 post-test

measurements, have been performed. By comparing the average value of the surface roughness before and after the test a quantitative description of the surface changes has been obtained.

4.1.2 Raman spectroscopy of disc surface

In order to evaluate eventual changes in the surface characteristics of the discs a Raman spectroscopy has been performed for a selected set of 7 discs coming from the first round of each test.

In particular, for the selected set of discs the following operations have been repeated twice, one time before the POD test and the second time after the end of the POD test. This process has been followed in order to have comparable results for each disc.

Raman spectroscopy

After the calibration phase that is necessary to correctly set the position of the mirrors, the evaluation of the Raman spectroscopy has been performed following the steps below:

1. Place the Xylene sample in the reference box. This will be helpful to get some references about the position of the peaks of the Raman shift as the ones of the xylene are just defined and evident.
2. Fix the Disc on glass support that will be hosted under the lenses.
3. Launch the desktop app called “LabSpec 6”.All the processes will be done thanks to this app.

4. Click on the camera icon located on the top right corner in the software main page to enter the focusing mode.



Figure 22: “LabSpec6” software interface. In the image the location of the focusing button, in the upper bar, has been highlighted with a red circle.

5. Use a 5x lens to focus on the sample.
6. As you get the focus on the sample change the lens to 50x and get the focus again.

7. Now, it is possible to define the settings of the measurement. For the performed measurements, the following settings have been used:

The image displays two side-by-side screenshots of the LabSpec6 software interface, specifically the 'Parameters' and 'Data range' sections. Both screenshots show the 'Info' tab selected in the top navigation bar.

Left Screenshot (Acq Tab):

- Parameters:**
 - Readout mode: Signal
 - DeNoise: Off
 - ICS correction: On
 - Dark correction: Off
 - Inst. Process: Off
 - Detector temp...: -75.22
 - Instrument: LabRAM HR Evol
 - Detector: Synapse QXTRA
 - Objective: x100_VIS
 - Grating: 1800 (450-850nm)
 - ND Filter: 50%
 - Laser: 532nm_Edge
 - Hole: 150.001
 - Range: Visible
 - Collection: Microscope
 - StageXY: 75x50mm Scan+
 - StageZ: Z motor
 - X (μm): -44810.2
 - Y (μm): 17745.7
 - Z (μm): 763.9
 - Full time(mm...): 18:04
 - Show: ☒ Name ☐ Value
- Data range:**

	Size	Step	From	To
S	2104	0.47528	200.404	1199.92
I			1060.82	2928.33

Right Screenshot (Custom Tab):

- Parameters:**
 - Acq. time (s): 24
 - Accumulations: 7
 - Range (cm⁻¹): 200...1200
 - Windows: 21
 - Auto scanning: On
 - Autofocus: Off
 - Macrospot: Square
 - Spot size (μm): 1.5 x 0.6
 - AutoExposure: Off
 - Spike filter: Multiple accum.
 - Delay time (s): 0
 - Binning: 1
 - Readout mode: Signal
 - DeNoise: Off
 - ICS correction: On
 - Dark correction: Off
 - Inst. Process: Off
 - Detector temp...: -75.22
 - Instrument: LabRAM HR Evol
 - Detector: Synapse QXTRA
 - Objective: x100_VIS
 - Show: ☒ Name ☐ Value
- Data range:**

	Size	Step	From	To
S	2104	0.47528	200.404	1199.92
I			1060.82	2928.33

Figure 23: Settings interface of “LabSpec6” software interface².

² These values are the ones used for the measurements and are directly derivate from a series of several tries. Energy, time of measurement and wavelength have been set to reduce the risk to burn the sample while getting the best results possible from the measurement.

8. Now, it is possible to start the measurement.
9. Hit the measurement button, located right close to the camera one to start the measurement.

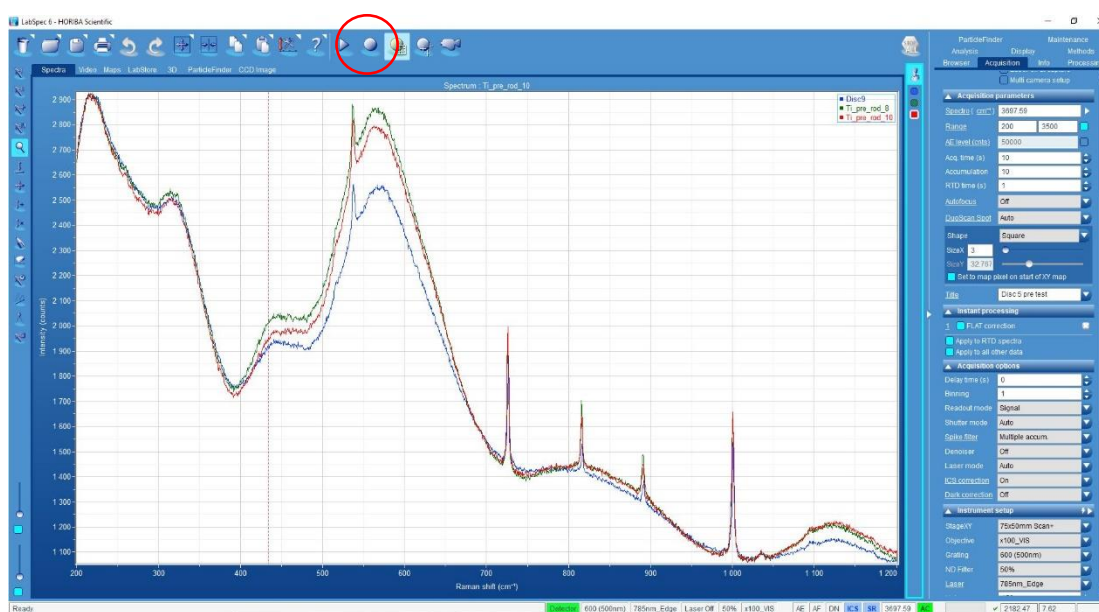


Figure 24: “LabSpec6” software interface. In the image the location of the capture button, on the left of the upper bar, has been highlighted with a red circle.

10. The measurement will take about 20 minutes to be completed.

11. As it is finished save two files, one with .l6s extension will contain all the info about the parameters used in the evaluation. The second one with the .txt extension will contain only the raw data that will be used for further studies.
12. Repeat these operations for all the discs.

When working on the “after” discs these operations have been repeated twice on every single disc. One data set has been taken from the wearing region and another one has been taken from the unworn one.

All the data have been subsequently processed using Origin® 2019 software. Data intensity has been normalized and Raman spectroscopy curves have been compared. The shifts have been calculated using Excel.

4.1.3 Post-POD test evaluation of discs surface

After the end of the test, some shots of the disc surface have been collected using ZEISS 2000-C stereomicroscope. In particular it has been taken shots of the worn zone with both 0.4x and neutral lens and also some shot of the undamaged zone using both 0.4x and neutral lens, too.

In order to acquire different images, light sources have been moved to find the configuration that gives the most interesting and meaningful overview of the differences between undamaged and damaged areas.

This procedure has been repeated for each disc for each round in order to detect macro pieces of evidence of wear on the disc surface and, eventually, material embedded on the worn surface.

4.2 Pin-on-Disc (POD) test

4.2.1 Introduction

In order to evaluate the overall amount of wear produced by the interaction of the metal surface with the UHMWPE counterpart, the Pin-on-Disc (POD) test is the best way to simulate what happens in a biological environment. The Pin-on-Disc setting essentially consists of a cylindrical UHMWPE pin which is attached to a stiff metallic arm that is loaded down onto the test sample, the disc being tested, with a precisely known force. As shown below pin and sample have relative movement that is useful to simulate what happens in real application of the material, like in a hip prosthesis. The elastic arm holding the pin ensures a stable contact point and a controlled position along the wearing track characterizing pin movements on the sample. The kinetic friction coefficient might be determined by evaluating the deflection of the arm, or by the direct evaluation of the change in torque, measured by a sensor positioned in the upper part of the Ortho-POD device. Wear rates for the pin is, then, calculated from the weight of material removed during the test and its relationship with the duration of the wearing test is taken into account. In order to try to fully replicate the condition a material could experience in vivo, a protein solution has been added to the wearing chamber and the temperature has been kept at 37°C.

4.2.2 Test preparation

In order to get all the materials ready for the test, it has been performed a preparation session in which the Ortho-POD machine has been calibrated and both pins and discs have been prepared for further steps.

4.2.2.1 AMTI® Ortho-POD calibration

Before starting the POD test the AMTI® Ortho-POD machine has been disassembled and the force sensor has been calibrated. This process is essential as it allows having the machine ready for the new starting round.

The Ortho-POD calibration reports the temperature, force, angular displacements of the pin and disk motion, and vertical displacement of the pin.

The specifications of each function of the machine relate to what the user can expect from a thermally stable, recently balanced Ortho-POD device. A summary of the specifications is down reported. Calibration values used for the pin on disc machine have been reported on the following page: (*) values are purely representative, whereas the other values have been determined using the "PODCal" function on the given software.

In order to perform the calibration, instructions given by the factory have been followed.

TABLE III: CALIBRATION VALUES FOR POD.

CHANNEL	SENSITIVITY	UNITS	OFFSET	UNCERTAINTY
POST1 FX	.0453*	N/bits	Auto zero	+/-1 N
POST1 FY	.0456*	N/bits	Auto zero	+/-1 N
POST1 FZ	.4835*	N/bits	Auto zero	+/-4 N
POST2 FX	.0471*	N/bits	Auto zero	+/-1 N
POST2 FY	.0478*	N/bits	Auto zero	+/-1 N
POST2 FZ	.4861*	N/bits	Auto zero	+/-4 N
POST3 FX	.0473*	N/bits	Auto zero	+/-1 N
POST3 FY	.0468*	N/bits	Auto zero	+/-1 N
POST3 FZ	.4838*	N/bits	Auto zero	+/-4 N
PIN FB	.0879	Degrees/bit	0.0	+/- 1.5 °
DISC FB	.0879	Degrees/bit	0.0	+/- 1.5 °
VLOAD FB	.2173	N/bit	0.0	+/- 4 N
PIN CMD	.0879	Degrees/bit	0.0	N/A
DISC CMD	.0879	Degrees/bit	0.0	N/A
VLOAD CMD	.2173	N/bit	0.0	N/A
VPS 0	.0049	mm/bit	0.0	.04 mm
VPS 1	.0049	mm/bit	0.0	.04 mm
VPS 2	.0049	mm/bit	0.0	.04 mm
VPS 3	.0049	mm/bit	0.0	.04 mm
VPS 4	.0049	mm/bit	0.0	.04 mm
VPS 5	.0049	mm/bit	0.0	.04 mm
VPS 6	.0049	mm/bit	0.0	.04 mm
SERUM TEMP	.0272	°C/bit	-368	+/-1 °C
PLATE TEMP	.0272	°C/bit	-368	+/-1 °C

4.2.2.2 Discs cleaning

Before starting the POD test each one of the discs involved in the experiment has been cleaned.

- **Motivation**

In order to avoid any kind of contamination from oil, dust or machining residual that may have remained embedded on the surface, each disc has been cleaned before use. General precautions have been applied when working with detergents and contaminated objects: wear chemical resistant gloves, lab coat, and goggles.

- **Materials**

- 70% propanol
- Kimwipes
- Bottled N₂

- **Procedure**

Disc cleaning

1. Put each disc in a separate plastic bag and label all the bags with the code associated with the disc.
2. Fill the bag with a 70% propanol solution.

3. Leave them rest for 10 minutes.
4. Dry them gently with kimwipes.
5. Use N_2 gas to remove any residual water trace.

Hereunder, the discs used for each round are reported.

CoCr Test

Round 1

TABLE IV: DESCRIPTION OF THE DISCS USED FOR ROUND 1, COCr TEST.

Disc type	Disc number
<i>Uncoated CoCr</i>	1
<i>TiN coating, tech #1</i>	5
<i>TiN coating, tech #2</i>	9
<i>TiN coating, tech #3</i>	13
<i>Ag-doped TiN coating</i>	17
<i>Uncoated CoCr (LAB)</i>	21

Round 2

TABLE V: DESCRIPTION OF THE DISCS USED FOR ROUND 2, COCr TEST.

Disc type	Disc number
<i>Uncoated CoCr</i>	2
<i>TiN coating, tech #1</i>	6
<i>TiN coating, tech #2</i>	10
<i>TiN coating, tech #3</i>	14
<i>Ag-doped TiN coating</i>	18
<i>Uncoated CoCr (LAB)</i>	22

Round 3

TABLE VI: DESCRIPTION OF THE DISCS USED FOR ROUND 3, COCr TEST.

Disc type	Disc number
<i>Uncoated CoCr</i>	3
<i>TiN coating, tech #1</i>	7
<i>TiN coating, tech #2</i>	11
<i>TiN coating, tech #3</i>	15
<i>Ag-doped TiN coating</i>	19
<i>Uncoated CoCr (LAB)</i>	23

Ti6Al4V Test

Round 1

TABLE VII: DESCRIPTION OF THE DISCS USED FOR ROUND 1, Ti6Al4V TEST.

Disc type	Disc number
<i>Uncoated Ti6Al4V</i>	24
<i>TiN coating, tech #1</i>	28
<i>TiN coating, tech #2</i>	32
<i>TiN coating, tech #3</i>	36
<i>Ag-doped TiN coating</i>	40
<i>Uncoated CoCr (LAB)</i>	21

Round 2

TABLE VIII: DESCRIPTION OF THE DISCS USED FOR ROUND 2, Ti6Al4V TEST.

Disc type	Disc number
<i>Uncoated Ti6Al4V</i>	25
<i>TiN coating, tech #1</i>	29
<i>TiN coating, tech #2</i>	33
<i>TiN coating, tech #3</i>	37
<i>Ag-doped TiN coating</i>	41
<i>Uncoated CoCr (LAB)</i>	22

Round 3

TABLE IX: DESCRIPTION OF THE DISCS USED FOR ROUND 3, Ti6Al4V TEST.

Disc type	Disc number
<i>Uncoated Ti6Al4V</i>	26
<i>TiN coating, tech #1</i>	30
<i>TiN coating, tech #2</i>	34
<i>TiN coating, tech #3</i>	38
<i>Ag-doped TiN coating</i>	42
<i>Uncoated CoCr (LAB)</i>	23

4.2.2.3 Pins soaking

As done for the discs also the pins have been prepared for the test before starting it.

- **Motivation**

During their shelf life, pins have been conserved at -80°C , in order to limit the possibility of oxidation to occur. As a POD test is ready to start, it is first necessary to prepare seven pins for the experiment. The preparation phase requires two weeks and it is performed in order to stabilize the weight of pins before starting the experiment. In fact, the experiment is performed in an aqueous environment and UHMWPE samples tend to acquire weight when submerged in a water

solution, especially if a force is applied to them. Also in this case, general precautions do apply when working with detergents and contaminated objects: wear chemical resistant gloves, lab coat, and goggles.

- **Materials**

- Deionized water
- Heating bath (37°C)
- Kimwipes
- Bottled N₂
- Vacuum desiccator
- LABCONCO XPert weigh

- **Procedure**

Pin drying

1. Take the pins out from the heating bath.
2. Gently dry them with kimwipes.
3. Use N₂ to remove any residual water trace.
4. Put that the pins in the Vacuum desiccator on labeled plates, so that they can not be mixed.

5. Activate the vacuum creator for 45s and then close the valve. Pins should stay in the desiccator for 30 min.
6. Remove the pins from the desiccator and place them in the LABCONCO XPert® Weigh.
7. Wait for 10 min to stabilize humidity and temperature in the weighing chamber.
8. Weigh the pins.

Pin weighing

1. Turn on LABCONCO XPert® Weigh
2. Calibrate scale (button on the lower left of the screen)
3. Record date, time of measurements.
4. Turn on thermo/hygrometer and barometer, take readings once stabilized
5. Weigh a reference weight in order to verify the accuracy of the measurement
6. Weigh each component three times; move the sample through the ionizer as putting it onto the scale
7. Use tweezers when for sample handling

Pin soaking

After the weighing phase, pins are placed in labeled plastic bags, with the code associated with the pin itself, and submerged in the heating bath at 37°C.

This procedure has been repeated twice a week for two weeks until the pins reach a stable weight. The last pin of the group has been left soaking during the entire round so that it is possible to evaluate which percentage of weight difference is due to the wear and which one is due to the water absorbed by the pin.

Pin soaking phase has been organized in three parts, one for each of the round that has been performed.

TABLE X: DESCRIPTION OF PINS USE FOR DIFFERENT ROUNDS IN CoCr TEST.

Round	Pins number
<i>Round 1</i>	OE1, OE2, OE3, OE4, OE5, OE6, OE7
<i>Round 2</i>	OE8, OE9, OE10, OE11, OE12, OE13, OE14
<i>Round 3</i>	OE15, OE16, OE17, OE18, OE19, OE20, OE21

TABLE XI: DESCRIPTION OF PINS USE FOR DIFFERENT ROUNDS IN Ti6Al4V TEST.

Round	Pins number
<i>Round 1</i>	OE22, OE23, OE24, OE25, OE26, OE27, OE28
<i>Round 2</i>	OE29, OE30, OE31, OE32, OE33, OE34, OE35
<i>Round 3</i>	OE36, OE37, OE38, OE39, OE40, OE41, OE42

4.2.2.4 Testing fluid preparation

- **Motivation**

The consistency of lubricants plays a fundamental role in the tribological behavior of material pairings of endoprosthetic implants. These fluids shall be of organic properties to create an environment as found in vivo, and shall also be validated through comparison with *in-vivo* wear findings. Since the impact of fluid characteristics on test outcome is not fully understood today, special diligence is to be spent in its preparation to create reproducible data. As just said, general precautions do apply when working with detergents and contaminated objects: wear chemical resistant gloves, lab coat, and goggles.

- **Material**

- Deionized water
- Newborn Bovine Calf Serum
- EDTA
- Tris(hydroxymethyl)aminomethane
- NaCl
- Beaker, >2l (for Basic Solution)
- Beaker, size based on the final amount of test fluid
- Scale (mg unit), scale dish
- Heating bath (37°C)
- Magnetic stirrer
- pH-Meter
- Squeeze bottle

- **Procedure**

Basic Solution (Total Amount: 2l)

1. Check all needed equipment and ingredients, verify availability
2. Dilution of 18g NaCl (9g/l) in ca. 1300ml deionized water (on stirrer for ~5min.)
3. Add 54g Tris (27g/l)

4. Add 400mg EDTA (200mg/l)
5. Stir solution with a magnetic stirrer (~15min)
6. Calibration of pH-Electrode
7. Set solution to a pH value of 7.6, carefully adding Hydrochloric Acid (5N)

(Note: The pH-scale is logarithmic, the closer 7.6 is reached, the more impact small amounts of Acid will have)
8. Fill up the beaker with deionized water to 2000ml
9. The storage lifetime of the solution without bovine-serum is 1-2 month (refrigerator)

Final Testing Fluid

1. Defrost and pre-heat the frozen calf serum in water bath at 37-39°C (takes ~1h for 500ml bottle)
2. Fill mixing cylinder with calf serum
3. Add Basic Solution
4. Stir mixture with a magnetic stirrer (~5min)
5. Fill the fluid in a squeeze bottle for use on simulator chambers
6. Storage lifetime (refrigerator) ca. 10 days

4.2.2.5 Run the test (CoCr)

Once the setting phase has been completed, the test has been run using the following set up. It has been decided to do three rounds, divided into four parts lasting 250'000 cycles.

Running scheme

This is the scheme that has been followed by performing the different rounds of the test. Each step has been reported in order to make the procedure fully replicable.

Round 1

1. Pin-on-disc test assembly.
2. Pin-on-disc test running for 250'000 cycles (0-0.25M).
3. Pieces dismount. Pins are dismounted and weighted. All the components are cleaned in order to prepare the device for the following part.
4. Pin-on-disc test running for 250'000 cycles (0.25-0.5M).
5. Pieces dismount. Pins are dismounted and weighted. All the components are cleaned in order to prepare the device for the following part.
6. Pin-on-disc test running for 250'000 cycles (0.5-0.75M).
7. Pieces dismount. Pins are dismounted and weighted. All the components are cleaned in order to prepare the device for the following part.
8. Pin-on-disc test running for 250'000 cycles (0.75-1M).

9. Pieces dismount. Pins are dismounted and weighted. All the components are cleaned in order to prepare the device for the following part.
10. Collection of one sample of the solution from each wear chamber. These samples have been stored in glass bottles. Bottles have been labeled with the number of the associated disc.
11. Bottles are stored at -79°C

This is the configuration of pins/discs that has been adopted for round 1.

TABLE XII: RUNNING SCHEME FOR ROUND 1, CoCr TEST.

ROUND 1	STATION	DISK NUMBER	DISK TYPE	PIN CODE	SOAK PIN
	1	1	CoCr	OE1	OE7
	2	5	TiN coating, tech #1	OE2	
	3	9	TiN coating, tech #2	OE3	
	4	13	TiN coating, tech #3	OE4	
	5	17	AgTiN	OE5	
	6	21	CoCr(LAB)	OE6	

After each test, the disc has been rotated two positions clockwise in order to avoid any case of dependency between the wearing rate and the station on which the test has been performed.

Round 2

For round number two, it has been followed the same series of operations just seen for Round 1.

This is the configuration of pins/discs that has been adopted for round 2.

TABLE XIII: RUNNING SCHEME FOR ROUND 2, CoCr TEST.

ROUND 2	STATION	DISK NUMBER	DISK TYPE	PIN CODE	SOAK PIN
	1	18	AgTiN	OE8	OE14
	2	22	CoCr(LAB)	OE9	
	3	2	Cocr	OE10	
	4	6	TiN coating, tech #1	OE11	
	5	10	TiN coating, tech #2	OE12	
	6	14	TiN coating, tech #3	OE13	

Round 3

For round number three, it has been followed the same series of operations just seen for Round one.

This is the configuration of pins/discs that has been adopted for round 3.

TABLE XIV: RUNNING SCHEME FOR ROUND 3, CoCr TEST.

ROUND 3	STATION	DISK NUMBER	DISK TYPE	PIN CODE	SOAK PIN
	1	11	TiN coating, tech #2	OE15	OE21
	2	15	TiN coating, tech #3	OE16	
	3	19	AgTiN	OE17	
	4	23	CoCr(LAB)	OE18	
	5	3	Cocr	OE19	
	6	7	TiN coating, tech #1	OE20	

4.2.2.5 Run the test (Ti6Al4V)

Once the setting phase has been completed, the test has been run using the following set up. It has been decided to do three rounds, divided into four parts lasting 250000 cycles.

Running scheme

This is the scheme that has been followed by performing the different rounds of the test. Each step has been reported in order to make the procedure fully replicable.

Round 1

1. Pin-on-disc test assembly.
2. Pin-on-disc test running for 250'000 cycles (0-0.25M).
3. Pieces dismount. Pins are dismounted and weighted. All the components are cleaned in order to prepare the device for the following part.
4. Pin-on-disc test running for 250'000 cycles (0.25-0.5M).
5. Pieces dismount. Pins are dismounted and weighted. All the components are cleaned in order to prepare the device for the following part.
6. Pin-on-disc test running for 250'000 cycles (0.5-0.75M).
7. Pieces dismount. Pins are dismounted and weighted. All the components are cleaned in order to prepare the device for the following part.

8. Pin-on-disc test running for 250'000 cycles (0.75-1M).
9. Pieces dismount. Pins are dismounted and weighted. All the components are cleaned in order to prepare the device for the following part.
10. Collection of one sample of the solution from each wear chamber. These samples have been stored in glass bottles. Bottles have been labeled with the number of the associated disc.
11. Bottles are stored at -79°C

This is the configuration of pins/discs that has been adopted for round 1.

TABLE XV: RUNNING SCHEME FOR ROUND 1, Ti6Al4V TEST.

ROUND 1	STATION	DISK NUMBER	DISK TYPE	PIN CODE	SOAK PIN
	1	24	Ti6Al4V	OE22	OE28
	2	28	TiN coating, tech #1	OE23	
	3	32	TiN coating, tech #2	OE24	
	4	36	TiN coating, tech #3	OE25	
	5	40	AgTiN	OE26	
	6	21	CoCr(LAB)	OE27	

After each test, the disc has been rotated two positions clockwise in order to avoid any case of dependency between the wearing rate and the station on which the test has been performed.

Round 2

For round number two, it has been followed the same series of operations just seen for Round 1.

This is the configuration of pins/discs that has been adopted for round 2.

TABLE XVI: RUNNING SCHEME FOR ROUND 2, Ti6Al4V TEST.

ROUND 2	STATION	DISK NUMBER	DISK TYPE	PIN CODE	SOAK PIN
	1	41	AgTiN	OE29	OE35
	2	22	CoCr(LAB)	OE30	
	3	25	Ti6Al4V	OE31	
	4	27	TiN coating, tech #1	OE32	
	5	33	TiN coating, tech #2	OE33	
	6	37	TiN coating, tech #3	OE34	

Round 3

For round number three, it has been followed the same series of operations just seen for Round 1.

This is the configuration of pins/discs that has been adopted for round 3.

TABLE XVII: RUNNING SCHEME FOR ROUND 3, Ti6Al4V TEST.

ROUND 3	STATION	DISK NUMBER	DISK TYPE	PIN CODE	SOAK PIN
	1	34	TiN coating, tech #2	OE36	OE42
	2	38	TiN coating, tech #3	OE37	
	3	42	AgTiN	OE38	
	4	23	CoCr(LAB)	OE39	
	5	26	Ti6Al4V	OE40	
	6	30	TiN coating, tech #1	OE41	

4.2.2.6 Ortho-POD settings

Pin-on-disc (POD) settings have been manually defined using the factory software. Set values for the main parameters have been reported in order to clarify the boundary conditions of the test.

TABLE XVIII: SETTINGS DEFINITION FOR THE TESTS. WEARING PATH, AXIAL FORCE, AXIAL PRESSURE, PROCESS FREQUENCY, FLUID TEMPERATURE AND NUMBER OF CYCLES FOR EACH STAGE ARE REPORTED.

Parameter	Set value
<i>Wearing path</i>	Square
<i>Applied axial force</i>	10.9N
<i>Applied axial pressure</i>	~395.46kPa
<i>Frequency</i>	1Hz
<i>Temperature</i>	37°C
<i>Number of cycles for each part</i>	250'000

As far as the wearing path is concerned, it has been decided to use a square layout because it allows creating a more realistic simulation of what happens in vivo. In fact, during the application of the prosthesis the UHMWPE experience multidirectional stress. Moreover, unidirectional

stress, like the one experienced by the POD test with circular wearing path makes polyethylene fibers aligning in the direction of stress, making the wearing rate decreasing drastically. Hereunder, it has been reported the geometrical description of the wearing path.

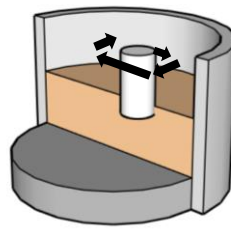
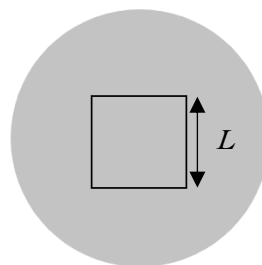


Figure 25: 3D description of the path followed by the pin.



$$L=15mm$$

Figure 26: 2D description of the path followed by the pin. Top view.

4.2.2.7 Post running procedures: cleaning and maintenance

In order to complete the cleaning and maintenance procedures, we follow a standard operating procedure that has been previously approved in the Tribology LAB of Rush University.

- **Motivation**

Cleanliness and precision are important in the setup and maintenance of the AMTI pin on disc (POD) tests as they may directly affect the final results of the experiment. Lab coat and gloves should be worn. Safety glasses are an option, but they are highly recommended. General laboratory safety and good lab practice regulations apply.

- **Materials**

Pipette tips x 16, 10ml pipette, labeled sample tubes, thawed newborn calf serum (based on the experiment)

- **Procedure**

The POD should first be dismantled, then cleaned, and finally weighing of test specimens. Extreme care should be taken to avoid contamination and to maintain proper sample orientations. Time may be managed by performing many tasks during periods of ultrasonic cleaning and drying. Regular cleaning can be accomplished with two people working simultaneously in about three hours. Remember to turn on both scales before starting.

DISASSEMBLY

Dismantle Disc Plate

The POD machine test setup must first be dismantled to clean.

1. Record test finish time and cumulative count on AMTI® software.
2. Open the taped plastic protection layer keeping attention not to damage it.
3. Loosen the three vertical clamps on each post.
4. Rotate lowering crank clockwise until the top head is at its highest level.
5. The disc plate is fixed to the base by magnets. Therefore, the two white thumbscrews may be rotated to detach the disc plate holder from the magnets, although it will be slightly off-balance during this procedure. Care should be taken to ensure the calf serum in each testing chamber does not spill. When the thumbscrews have been fully rotated, the disc plate can be gently lifted off the POD. You can, eventually, help yourself with a flathead screwdriver if necessary.
6. Carry the disc plate carefully to the preparation lab and place gently on paper towels on the countertop.

Detach, Clean, and Weigh Polyethylene Pins

The polyethylene pins need to be detached from the POD for cleaning and weighing. Care should be taken and fresh gloves should be used when handling the pins.

1. Remove the large acrylic boundary by twisting it downward. Carefully slide the chamber out without touching the pins.
2. Remove the arms (holding the pins) from the POD by loosening the nut with an Allen key. Carefully pull off the arm by pulling vertically downward. Extreme care is needed to ensure that the polyethylene pin is not touched.
3. Repeat for all six units and transport them to the lab for disassembly.
4. To dismount the pins, the mounting nuts must be loosened using an adjustable wrench. Clean the wrench with ethanol and kimwipes before use. Carefully, remove each nut without touching the pin surface.
5. Gently wiggle the pinout of the pin holder and slide off the white, plastic ferrule towards the bottom of the pin away from the testing surface.
6. The polyethylene pins (soak control and test pins) should now be cleaned and weighed following the pin cleaning procedure down reported.
7. The pin cleaning procedure should be conducted during serum sample collection. Dismount all pieces of the pin holder and soak in Terg-A-zyne during sample collection.

Serum Sample Collection

Serum samples are collected from each test chamber, but only in the last 250k cycles. Thus, for each wound we will have 6 serum samples collected in the last running test from 750k to 1mln cycles.

1. Dismantle the individual test chambers from the disc plate by setting the plate on the counter with an overhang so that the *bottom fixing screw* from one chamber is exposed. Use a Phillips screwdriver to gently unscrew the bottom fixing screw, and the chamber may be carefully lifted off of the plate. A single white plastic dowel pin will be attached to the chamber and should be gently twisted to remove and set aside. Place the chambers on layered kimwipes to remove excess water from the bottom of the chambers. Repeat this process until all six test chambers are free.
2. Weigh and record the test chambers and then return the test chambers to their original weights (should have been noted in the lab notebook before the start of testing) by adding Millipore water to compensate for evaporation.
3. Using the electric pipette and a 15 ml plastic pipette with a pipette tip placed on the end of it, “bubble” one test chamber to homogenize the solution. Each chamber should be bubbled with a new pipette tip (to prevent cross-contamination).
4. Complete this process for all 6 test chambers.
5. Put the samples in the freezer.

Disassemble Chambers and disc plate

The chambers must be disassembled for cleaning.

1. Push the discs out of acrylic encasing. Try to make sure that contact with the disc is as close to the edges as possible. Removing the discs is often difficult.
2. The o-ring seal should be removed from the disc by pinching it around to a bulge.
3. Remove the *outer chamber boundary* of the disc plate by pulling it vertically.
4. Remove the large o-ring seal of the disc plate for cleaning.

CLEANING PROCEDURES

- **Materials**

- Kimwipes
- Terg-A-Zyme® detergent (Alconox, Inc., USA)
- Distilled water
- Ultrasonic cleaner
- Bottled N₂
- Vacuum desiccator
- 70% Propanol, optima grade
- LABCONCO XPert weigh
- Digital Thermo/hygrometer (Amprobe, Inc., USA)

UHMWPE Pins cleaning

The polyethylene pins must be cleaned and then weighed every 250k cycles. Weighing of the components quantifies the amount of wear that the components experience during the simulated motion of the human joint.

Components cleaning will follow this procedure:

1. Clean the components manually first by rinsing in distilled water and wiping with Kimwipes. Visually check the surface to ensure that no residual "film" or particles remain on the implants
2. Place components in Ziploc bag and fill halfway with distilled water. Seal bag ensuring while pushing out any air so that components are completely submerged in water
3. Place bag in the ultrasonic cleaner for 10 minutes
4. Remove components from the bag and rinse both components and bag with distilled water
5. Place components back in bag filling halfway with Terg-A-Zyme® soap mixture. Seal bag ensuring while pushing out any air so that components are completely submersed in the soap mixture
6. Place bag in the ultrasonic cleaner for 10 minutes
7. Remove components from the bag and rinse both components and bag with distilled water
8. Repeat rinsing, ultrasonic cleaning procedure with distilled water (10 minutes)

9. Repeat rinsing, ultrasonic cleaning procedure one last time using distilled water (5 minutes)
10. At this point put on clean and dry gloves
11. Remove components from the bag and rinse them with distilled water
12. Dry components with Kimwipes
13. Blow components dry using N₂
14. Place components in a small beaker under a fume hood and fill the beaker with 70% Propanol until components are submerged. Let sit for 5 minutes.
15. Remove components from 70% Propanol and dry with Kimwipes
16. Blow components dry using N₂ and place them in the vacuum chamber for 30 minutes
17. Remove components from the vacuum chamber, place on Kimwipes on a tray
18. Let components acclimatize in the area next to scale for 10 minutes.

Metal parts cleaning

All removed metal parts (testing discs, arms, pin holders, mounting nuts, excluding the bottom fixing screws) of the POD should be cleaned as follows:

1. Using the scrub brush, gently scrub all metal parts (excluding the testing discs) using Terg-A-zyne. Terg-A-zyne should be poured onto each testing disc and rubbed lightly with a rubber glove.

2. Rinse again with distilled water.
3. Place the arms in one small, labeled, Ziploc bag.
4. Each disc should be placed in its small Ziploc bag to ensure that the surfaces will not be scratched.
5. The pin holders and mounting nuts should be in their Ziploc bag.
6. Fill each bag with Terg-A-zyne.
7. Put all 6 disc bags in the ultrasonic cleaner for 10 minutes.
8. Remove and rinse with distilled water.
9. Fill the bags with distilled water.
10. Ultrasonically clean for 10 minutes.
11. Remove and rinse with distilled water.
12. Fill the bags of all the metal components with 70% Propanol, ensuring full submergence of the components.
13. When the discs are done their last ultrasonic cleaning, remove metal parts from propanol bath and place on laid-out absorbance sheets for drying.
14. Dry all the metal discs one by one using N₂.
15. The large disc plate should be cleaned by rinsing with distilled water, scrubbing with Terg-A-zyne, rinsing again with distilled water, and sprayed with ethanol to ensure the entire surface is covered. Let air dry on sheet.

Non-metal parts cleaning

All removed non-metal parts (o-rings, plastic ferrules, dowel pins, acrylic encasings, including the bottom fixing screws) of the POD should be cleaned as follows:

1. Using the scrub brush, gently scrub all parts (especially the acrylic encasings) using Terg-A-zyne.
2. Rinse again with distilled water.
3. Place the o-rings, plastic ferrules, dowel pins, bottom fixing screws and acrylic encasing in one labeled small Ziploc bag.
4. Each acrylic encasing should be carefully and thoroughly scrubbed with Terg-A-zyne and rinsed with distilled water.
5. Fill each bag with distilled water, and push any air out before sealing the bag.
6. The one bag of non-metal parts should be placed in the ultrasonic cleaner with the 2 bags of pin holders and mounting nuts. The same ultrasonic cleaning procedure applies for this bag of non-metal parts (10 minutes with distilled water, 10 minutes with Terg-A-zyne and 10 minutes with distilled water again).
7. All parts should be placed on a sheet with metal parts for air drying.
8. Both large outer acrylic boundaries should be rinsed with distilled water, scrubbed with Terg-A-zyne, rinsed again with distilled water and placed on the sheet to air dry.

Ortho-POD device cleaning

1. Wipe down the POD with Kimwipes and ethanol, ensuring any remaining adhesive tape is removed.
2. Wipe the area where the pins are placed with propanol and Kimwipes.
3. Gently pull down each pin station and wipe away any leaking grease.

WEIGHING OF COMPONENTS

General advice: take measurements with all doors shut to avoid any draft. Do not have people walk in and out.

1. Turn on LABCONCO XPert® Weigh
2. Calibrate scale (button on the lower left of the screen)
3. Record date, time of measurements.
4. Turn on thermo/hygrometer and barometer, take readings once stabilized
5. Weigh a reference weight in order to verify the accuracy of the measurement
6. Weigh each component three times; move the sample through the ionizer as putting it onto the scale
7. Use tweezers when for sample handling
8. Record date and time of measurements.

RE-ASSEMBLY

Reassemble Test Chambers (While Pins are being weighed)

Nitrogen gas should be used to blow dry test parts that are not completely dry, especially in screw holes of the test discs and disc plate and the pin holders and mounting nuts. Take note that the chamber numbers and disc plate numbers correspond and are paired (refer to lab book for disc plate numbers).

1. After cleaning, the o-ring seals can be replaced on the clean and dry disc plates (fit from the bottom of the disc, avoiding contact with the testing surface).
2. A drop or two of distilled water should be used to moisten the o-ring seal to facilitate the sliding of the acrylic encasing. Dry the assembled chamber with nitrogen gas to remove any remaining water.
3. Fill each chamber with 15 mL of testing serum.
4. Place the large o-ring back onto the clean and dry disc plate.
5. Then, the test chambers can be screwed into the disc plate using the bottom fixing screws and plastic dowel pins (the dowel pins go into the holes of the disc plate that are closest to the center). Proper orientation of the test chambers should be maintained (the inscription on the bottom of each disc is placed on the left side when mounting onto the disc plate).

Reassemble Pins

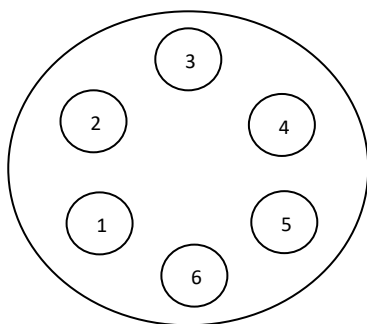
After the pins have been examined, weighed, and cleaned according to the appropriate procedure, the pins should be mounted for the next test round.

1. Arm screw will be on the internal side.
2. Screw the pin holders into the arms. Using an adjustable wrench that has been cleaned with propanol and kimwipes, tighten the holders in the arms.
3. Place the plastic ferrules in each pin holder with the wedge downwards.
4. Carefully handling each test pin slide the pin through the ferrule into the pin holder avoiding to touch the testing surface. Ensure that the proper pin is in the corresponding arm (refer to lab book).
5. Carefully slide the mounting nut overtop of the pin, ensuring no contact with the testing surface.
6. Screw on the mounting nut and gently tighten with the clean, adjustable wrench. Do not tighten too much or the plastic ferrule will break, but tighten enough to ensure no loosening during testing.

Re-mounting on POD

Once the pins and testing chambers are all reassembled, re-mounting onto the POD can commence.

1. Screw down the white thumbscrews (they are magnets and the bottom disc will not move with them up).
2. Go to "Manual Mode" on the POD program. Hit "Balance" and then "Home position".
3. When it has stabilized hit "rest position" for the disc, pins and Fz.
4. Screw up each white thumbscrew to prepare for placing of the disc plate.
5. Remount the pin units onto the POD in the correct station positioning (stations 1-6) (Ie. Pin unit labeled 1 goes to station 1 etc.) When facing the POD the very back unit is "Station 3". Stations numbers then increase clockwise. Also, the pins should be on the right side and the arm screws should be facing in.



Top View

6. Tighten the screws with the Allen key.
7. Carefully slide the largest acrylic boundary past the pins and twist up to tighten.
8. Carefully carry the disc plate (with all the chambers already affixed) to the POD and very carefully place it on the magnetic disc (if this is done too roughly, the testing solution in each chamber can be spilled). The label “6” on the disc plate is closest to you. The disc plate only fits one way.
9. Lower the disc plate using the white thumb screws.
10. Back in the preparation lab, fill a large beaker with distilled water.
11. Carefully fill the water bath. This requires extreme care that water is not sprayed into the testing chambers. Pour remaining water in the beaker into the temperature sustaining water bath on the floor.

TEST COMMENCEMENT

1. In manual mode on the POD software, press “Balance” button.
2. In manual mode on the POD software, press the “Home position” button for the pins and disc again. This will ensure the pins and discs are in the testing position.
3. Lower the pins into the testing position by turning the *lowering crank* clockwise. Extreme care should be taken to lower the pins to a point where the lower acrylic boundary will have a ~3mm gap with the upper fixture.

Warning! Do not click on home position for it will crash all parts.

4. Tighten the 3 vertical clamps, when the desired position has been achieved.
5. Tape down the surrounding plastic bag covering, ensuring no air holes (this prevents evaporation).
6. Exit Manual Mode and open Monitor Mode.
7. Assuming all the correct test details (ie. waveform, loop count, repetitions etc.) are on the Monitor Mode, the test may be started by pressing “Start”.

TEST MAINTENANCE

The water bath should be filled so the water level sits just below the upper horizontal slit. Failure to do this will result in temperature inconsistency.

4.3 Post-POD test pins characterization

4.3.1 Evaluation of pins surface with stereomicroscope

After the end of the test, some shots of the pin's surface have been collected using ZEISS 2000-C stereomicroscope. In particular it has been taken shots of the worn zone with both 0.4x and neutral lens.

In order to acquire different images, light sources have been moved to find the configuration that gives the most interesting and meaningful overview of the differences between undamaged

and damaged areas. This procedure has been repeated for each pin for each round in order to detect macro pieces of evidence of the type of scratches on the surface of the pins and, eventually, material embedded on the worn surface.

4.3.2 Evaluation of pins surface with Zygo

All the quantitative surface evaluations for the after test characterization of the pins have been realized using the Zygo® Newview 6300. In order to complete this aim the following steps have been performed:

Zygo® setup

1. In order to stabilize the machine, the Nitrogen source that supplies the stabilized table, has been opened following standard procedures.
2. A 20x lens has been mounted on the Zygo to perform the measurements.
3. “MetroPro” app has been launched on the computer and “Stitch.app” has been chosen to perform the analysis. In the following page, the main characteristics of the app have been reported.

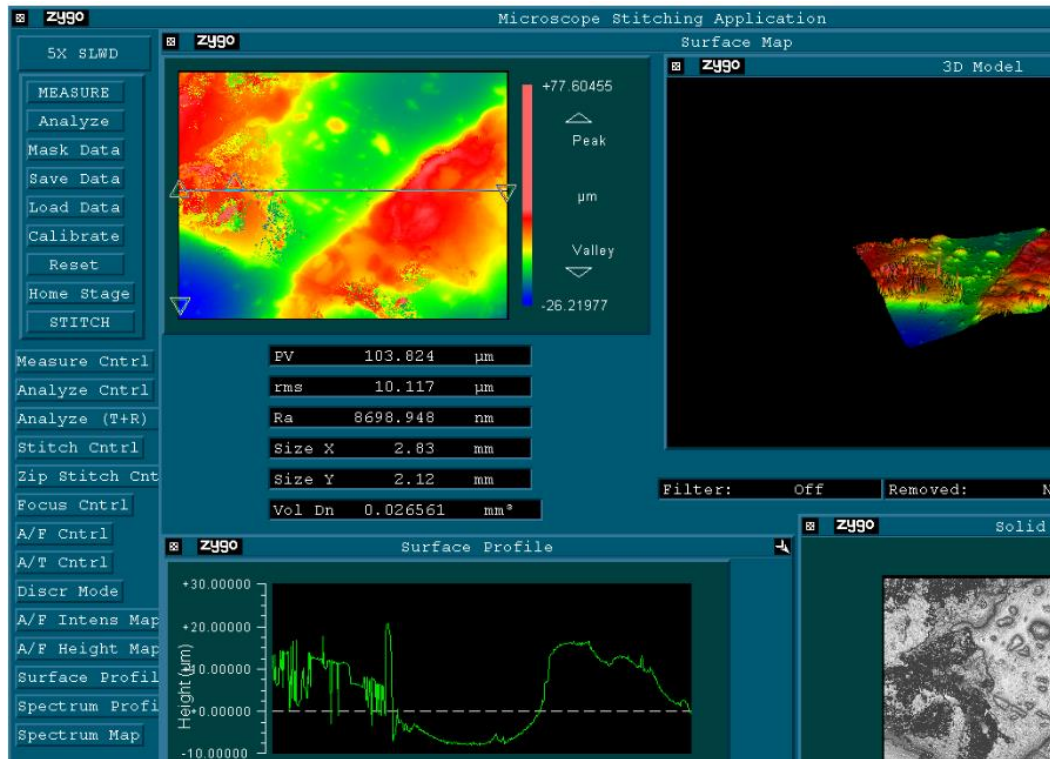
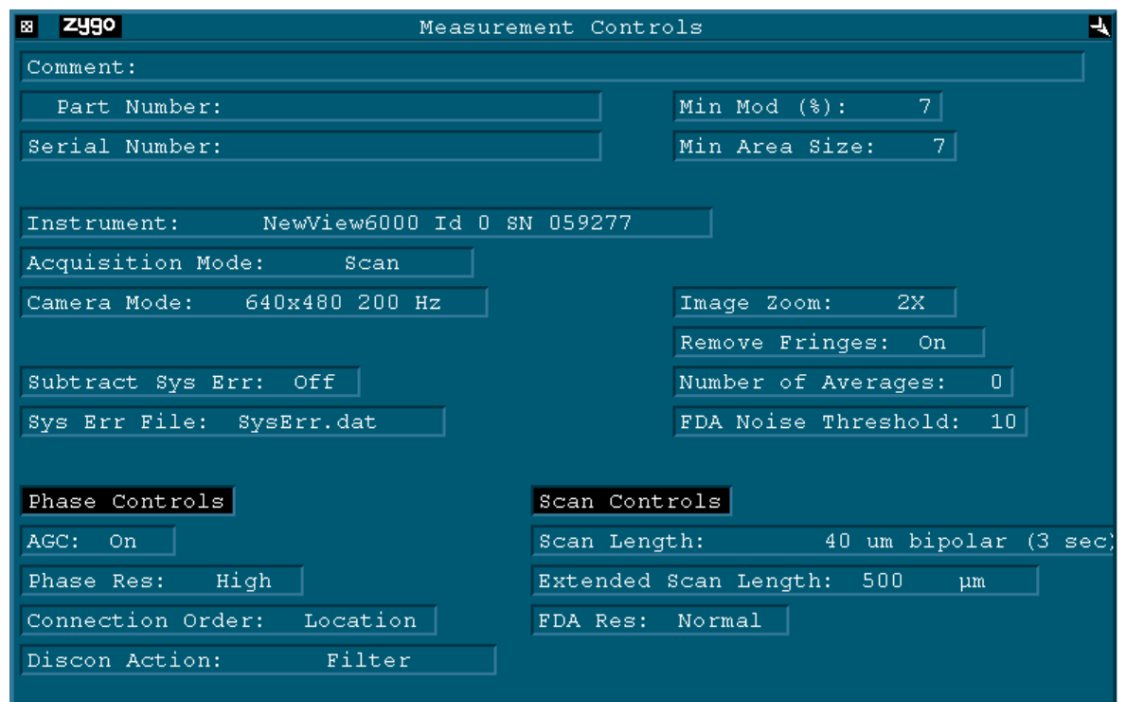


Figure 27: Stitch.app interface³.

³ On the left, it is possible to see all the main commands of this software. In the central part of the screen all the most relevant data are shown. In the top-left corner it is possible to see a surface profile heat map, on its right a 3D oblique plot of the surface profile. On the bottom-left corner a linear surface profile is visualized whereas on its right an intensity map of the surface is shown. In addition, the central numbers give you the Pick-Valley maximum distance (PV), the root-mean square error (rms), the arithmetic roughness (Ra), the x-length of the sample (Size X) and the y-length of the sample (Size Y).

4. In “Stitch.app” the following settings have been applied in order to perform the measurements.



The screenshot shows the 'zygo Measurement Controls' window. It contains several input fields and buttons for configuring measurement parameters. The settings are organized into sections: General, Instrument, Acquisition, Camera, Image, Subtract, Sys Err, Phase Controls, and Scan Controls.

Section	Parameter	Value
General	Comment:	
	Part Number:	
	Serial Number:	
	Min Mod (%):	7
General	Min Area Size:	7
	Instrument:	NewView6000 Id 0 SN 059277
Acquisition	Acquisition Mode:	Scan
Camera	Camera Mode:	640x480 200 Hz
Image	Image Zoom:	2X
Image	Remove Fringes:	On
Subtract	Subtract Sys Err:	Off
Subtract	Sys Err File:	SysErr.dat
Image	Number of Averages:	0
Image	FDA Noise Threshold:	10
Phase Controls	AGC:	On
	Phase Res:	High
	Connection Order:	Location
	Discon Action:	Filter
Scan Controls	Scan Length:	40 um bipolar (3 sec)
	Extended Scan Length:	500 μm
	FDA Res:	Normal

Figure 28: Zygo Measurement settings.

Surface profile evaluation

The next step of the analysis has been to evaluate the actual surface profile. In order to do that the following steps have been followed:

1. Pins have been placed on the Zygo plate.
2. Locate the Zygo over the pin and try to focus the image. Use F5 button to adjust the light.
3. Look for interference fringes and position them parallel to the bottom border of the screen.
4. It is possible to adjust the interference fringes orientation using the two big screws located in the bottom part of the Zygo.
5. Hit “Measurement” to perform the measurement.
6. Take care that "Points" value is above 30700 which means you have a good signal and the sample is focused.
7. To save the data, press “Save Data”.
8. To save the images click on Zygo logo on the top-left corner of them and save them as .tiff files.
9. Repeat the operation from 1 to 8 for all the seven pins.

This operation has been performed after round one of each test in order to detect and characterize any kind of change in the surface characteristics.

CHAPTER 5

RESULTS

This section of the manuscript will be entirely dedicated to the illustration of the result obtained in the different stages of the experiment.

These outcomes will be treated one by one, trying to follow the same order of the experiments presented in the “Methods” part of the document.

In addition, part of the raw data has been reported in the appendix while only the final outcomes have been reported here. The hope is to make the reading simpler for the reader, avoiding to have excessive unneeded information in this paragraph.

All the results, singularly presented in this section will be useful in the conclusive “Discussion” chapter in which the final collective outcomes of the work will be presented to the reader.

5.1 Discs characterization

5.1.1 Evaluation of disc surface roughness

All the roughness evaluations for the surface characterization of the pins have been realized using the Zygo® Newview 6300 as defined in the previous paragraph.

The process has been repeated twice for each disk, collecting five measurements for each attempt and calculating their average and the standard deviation.

The tables that contain all the raw results have been reported in the appendix, whereas the following results have been reported here:

1. Mean value of the surface arithmetic roughness (Ra), expressed in nm, for each disk before the pin on disk (POD) test;
2. Standard deviation of the surface arithmetic roughness (Ra) measurements collected for each disk before the pin on disk (POD) test;
3. Mean value of the surface arithmetic roughness (Ra), expressed in nm, for each disk after the pin on disk (POD) test;
4. Standard deviation of the surface arithmetic roughness (Ra) measurements collected for each disk after the pin on disk (POD) test;
5. One significant Intensity map for each coating technique collected before the pin on disk (POD) test;
6. One significant Intensity map for each coating technique collected after the pin on disk (POD) test;

The outcomes have been reported both for the CoCr experiment and the Ti6Al4V one.

*CoCr test*TABLE XIX: RECAP VERSION OF THE ROUGHNESS TABLE FOR CoCr TEST⁴.**SURFACE ROUGHNESS - RA**

TEST #1												
	#1 (CoCr)		#5 (Tech #1)		#9 (Tech #2)		#13 (Tech #3)		#17 (AgTiN)		#21 (Lab)	
	Before	After	Before	After	Before	After	Before	After	Before	After	Before	After
<u>AVG</u>	4.83	4.65	14.51	18.83	38.07	28.30	13.34	11.88	48.16	59.39	7.05	6.71
<u>STD</u>	0.75	0.41	2.425	4.802	7.919	5.288	0.806	1.063	11.17	14.36	1.32	1.36
TEST #2												
	#2 (CoCr)		#6 (Tech #1)		#10 (Tech #2)		#14 (Tech #3)		#18 (AgTiN)		#22 (Lab)	
	Before	After	Before	After	Before	After	Before	After	Before	After	Before	After
<u>AVG</u>	3.84	4.44	15.48	18.07	27.02	23.90	15.90	13.65	51.14	55.50	7.83	9.01
<u>STD</u>	0.15	0.46	3.694	3.700	2.119	3.294	0.993	0.989	11.67	8.10	0.99	2.69
TEST #3												
	#3 (CoCr)		#7 (Tech #1)		#11 (Tech #2)		#15 (Tech #3)		#19 (AgTiN)		#23 (Lab)	
	Before	After	Before	After	Before	After	Before	After	Before	After	Before	After
<u>AVG</u>	3.80	5.02	16.09	16.92	40.64	31.70	15.52	12.31	46.37	71.59	4.33	6.20
<u>STD</u>	0.15	1.33	5.646	4.31	12.00	3.998	2.034	3.550	10.76	26.47	0.39	0.85

⁴ All the values for the arithmetic roughness are expressed in nm.

The table collects all the final results we have obtained in terms of surface roughness for the CoCr test. The first important thing to notice is that the uncoated discs have a surface roughness that is well below the one shown by the coated discs. Moreover, good variability in terms of Ra may be noticed also in the coated disc. This variability is strongly dependent on the coating procedure.

As shown a general increase of surface arithmetic roughness has been registered after the pin on disc (POD) test for all the disc types with the exception of Tech #2 and Tech #3 discs.

In particular, for TiN coating discs processed with Tech #2 technique a major decrease of Ra has been detected, whereas the reduction for the Tech #3 case is smaller. However, it has been observed a bigger standard deviation for Tech 2 in respect to the technology number 3 and this is mainly due to the coating material intrinsic characteristics.

In conclusion, for bulk CoCr and the CoCr discs from the LAB the roughness slightly increases, whereas for Tech #1 processed discs and Ag-TiN coated ones the growth of Ra is higher.

In the following page, a bar chart that illustrates all the variations in the surface roughness of the different discs has been reported. Moreover, a final summary of the value of the surface roughness Ra, obtained as the average value of the three measurements that have been performed, has been calculated for each disc type.

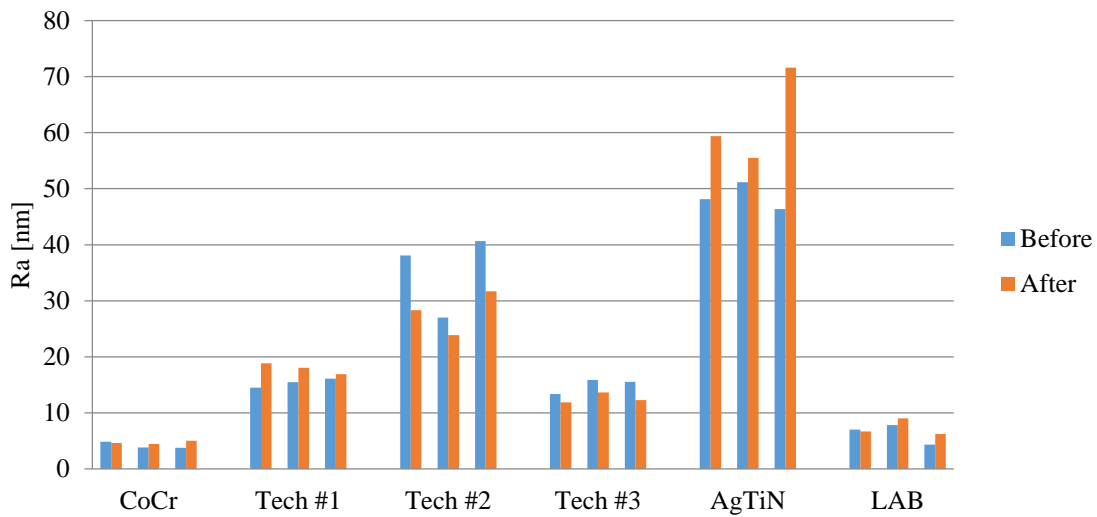


Figure 29: Summary of the arithmetic roughness for CoCr test. All the value of Ra, collected “Before” and “After” the pin on disc (POD) test, are subdivided into disc type groups and shown in nm.

TABLE XX: SUMMARY OF THE ARITHMETIC ROUGHNESS FOR CoCr TEST⁵.

SUMMARY SURFACE ROUGHNESS – RA

	CoCr		Tech #1		Tech #2		Tech #3		AgTiN		Lab	
	Before	After	Before	After	Before	After	Before	After	Before	After	Before	After
<u>AVG</u>	4.160	4.707	15.36	17.94	35.24	27.97	14.92	12.61	48.56	62.16	6.41	7.31
<u>STD</u>	0.45	0.85	4.14	4.29	8.39	4.27	1.38	2.21	11.14	18.00	0.98	1.80

⁵ These values are calculated as the average of the number shown in the previous table and are expressed in nm.

In addition, the surface characteristics of each disc have been studied using the Zygo. In particular, for all the five points of measurement an Intensity map has been collected, both before and after the pin on disc (POD) test.

These images are interesting as they contain visible proof of how the surface characteristics have been modified by the wearing test.

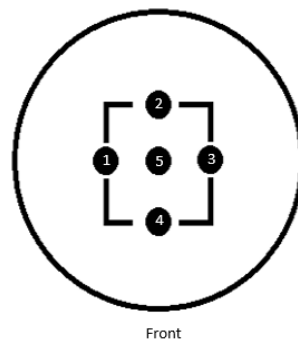


Figure 30: Model of the mask that has been used to collect measurements using Zygo⁶.

⁶ Numbers 1, 2, 3, 4 and 5 represents the points of measurement whereas the square path represents the wearing path. Points 1, 2, 3 and 4 are located on the wearing path, whereas point number 5 is located on an unworn area and it has been used as a reference.

Hereunder, the most significant ones have been reported choosing one from the measurement point number 5 that represent the unworn zone and another one from one of the point 1, 2, 3 or 4 located on the wearing path. These Intensity maps have been reported both in their “before” version and their “after” version in order to better visualize all the differences in their characteristics.

CoCr disc

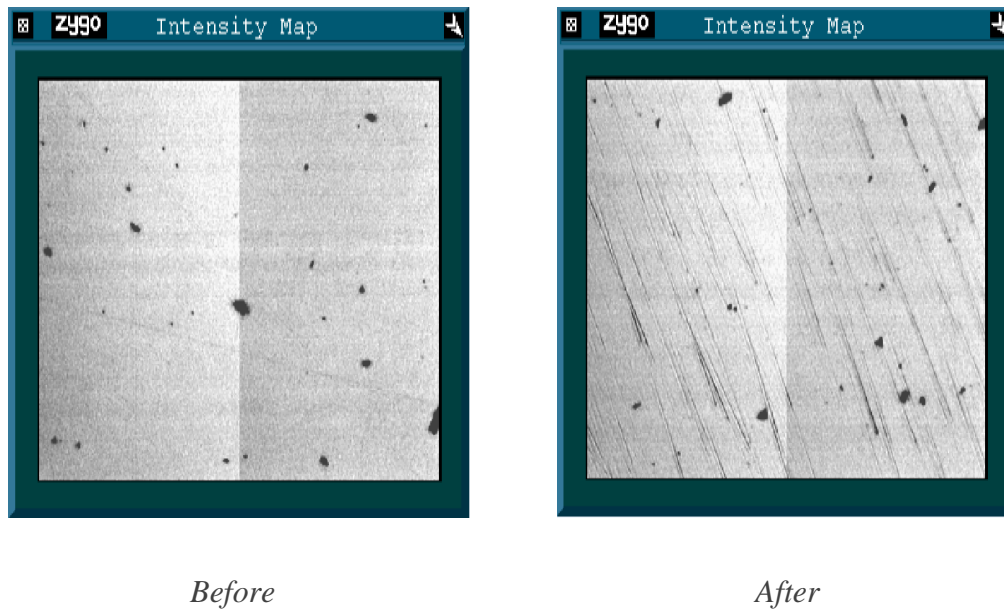


Figure 31: Intensity map collected from CoCr disc number 2 “Before” and “After” the pin on disc test. These maps have been collected in position 3 on the disc and so, on the wearing path.

As far as the CoCr disc concerned, the surface of the uncoated disc appears quite smooth with minor defects on the surface before the pin on disc test. This is demonstrated also by the value of arithmetic roughness showed in TABLE XX that is well below 5 nm.

Moreover, by eye-comparing the “Before” disc with the “After” disc, the pin on disc (POD) test has not caused any major change in the visible characteristics of the surface of the material.

However, when focusing on the microscopic characteristics of the damaged area, here represented in the Intensity maps collected from point number three of the mask, it has been noticed the presence of some scratches oriented as the direction of movement of the pin on the surface itself. In order to assess the dependency between the change in surface characteristics and the performed pin on disc (POD) test, an intensity map image has been collected also from point five of the mask.

This point is not on the wearing path and so the metallic material is not in contact with the polymeric pin in point number five. This is why no major changes or scratches are visible in this area, even when observed at the microscopic level.

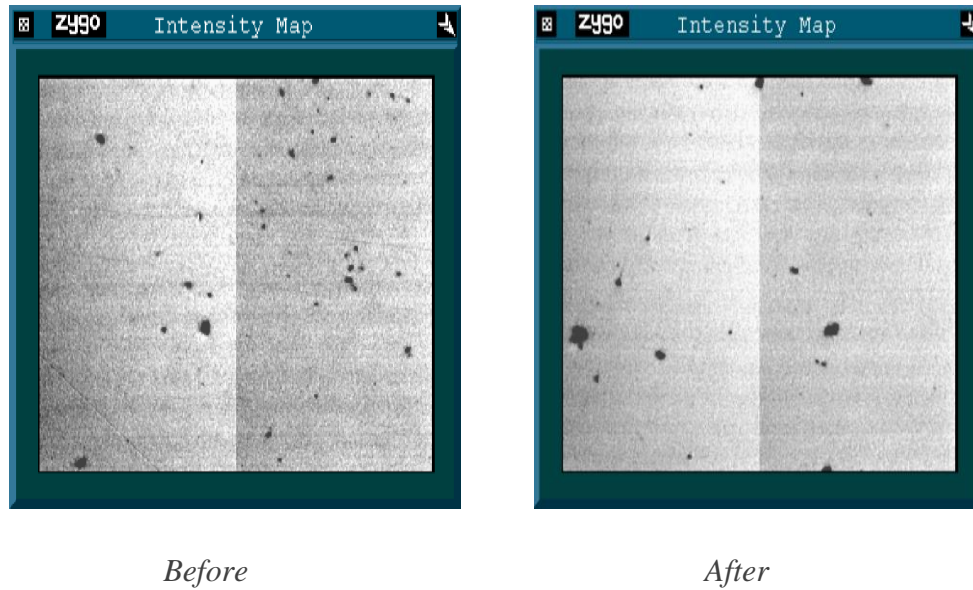


Figure 32: Intensity map collected from CoCr disc number 2 “Before” and “After” the pin on disc test. These maps have been collected in position 5 on the disc and so, on the unworn zone.

Tech #1 disc

Focusing on the disc coated with TiN deposited with Tech #1, it is evident how the layer deposited on the upper side of the disc has affected the surface characteristics. In fact, many more defects may be noticed on the surface that results in more rough. This is demonstrated also by the fact that the evaluated arithmetic surface for this type of discs is around 15-17nm as shown in TABLE XX.

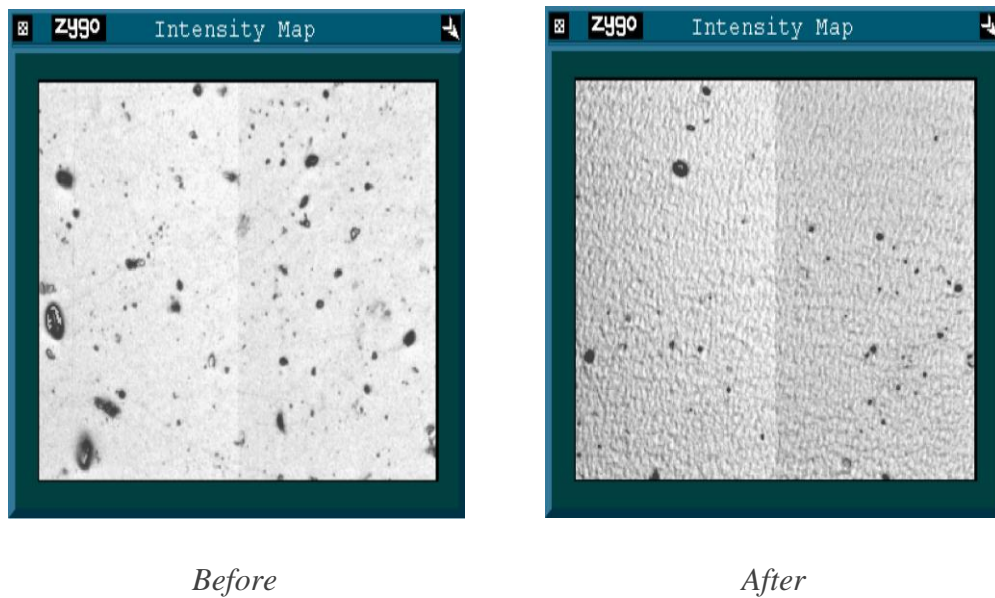


Figure 33: Intensity map collected from Tech #1 disc number 7 “Before” and “After” the pin on disc test. These maps have been collected in position 3 on the disc and so, on the wearing path.

Moreover, when looking at the microscopic characteristics of the damaged area, here represented in the Intensity maps collected from point number three of the mask, it has been noticed the presence of an important area of damage.

As highlighted by the “After” image, the zone in which the pin on disc (POD) test has been performed shows the presence of a new kind of micro-roughness. This is maybe linked with the change in the surface characteristics of the material coating the bulk CoCr disk that has been noticed during the experiment.

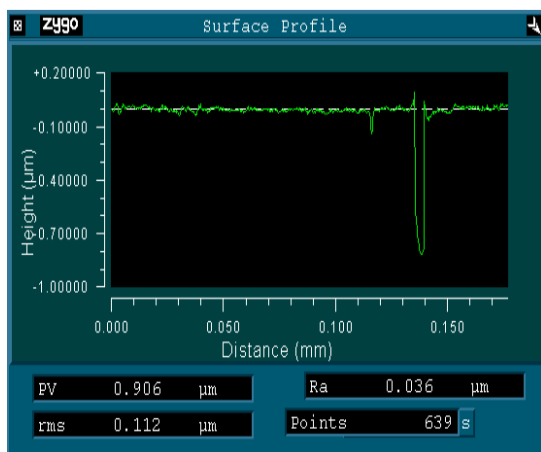
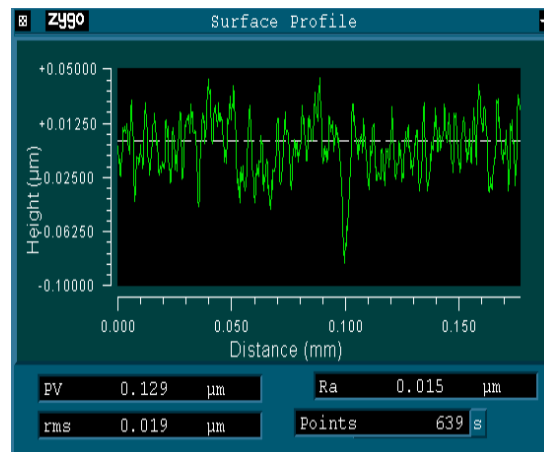
*Before**After*

Figure 34: Surface profile collected from Tech #1 disc number 7 “Before” and “After” the pin on disc test. These maps have been collected in position 3 on the disc and so, on the wearing path.

This change is also well visible when analyzing the differences in surface linear profile measured before and after the pin on disc test. As shown in the images, the profile has been modified by the interaction with the pin and appears to be rougher. The Ra value in the “Before” case account also for the defect on the right part and this is why the evaluated arithmetic roughness is bigger.

In order to assess the dependency between the change in surface characteristics and the performed pin on disc (POD) test, an intensity map image has been collected also from point five of the mask.

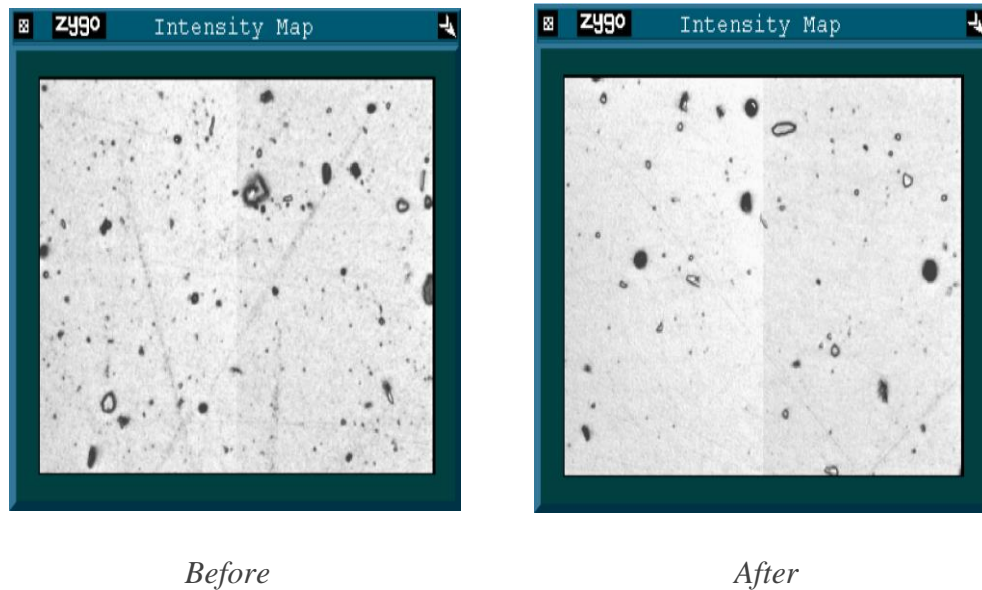


Figure 35: Intensity map collected from Tech #1 disc number 7 “Before” and “After” the pin on disc test. These maps have been collected in position 5 on the disc and so, on the unworn zone.

This point is not on the wearing path and so the metallic material is not in contact with the polymeric in point number five. This is why no major changes are visible in this area, even when observed at the microscopic level. As shown in the image collected from Zygo, the micro-roughness is not present in this case because this part of the disc has not interacted with the moving pin during the POD test. This material showed the highest difference in terms of surface characteristics in the group we have tested during this experiment.

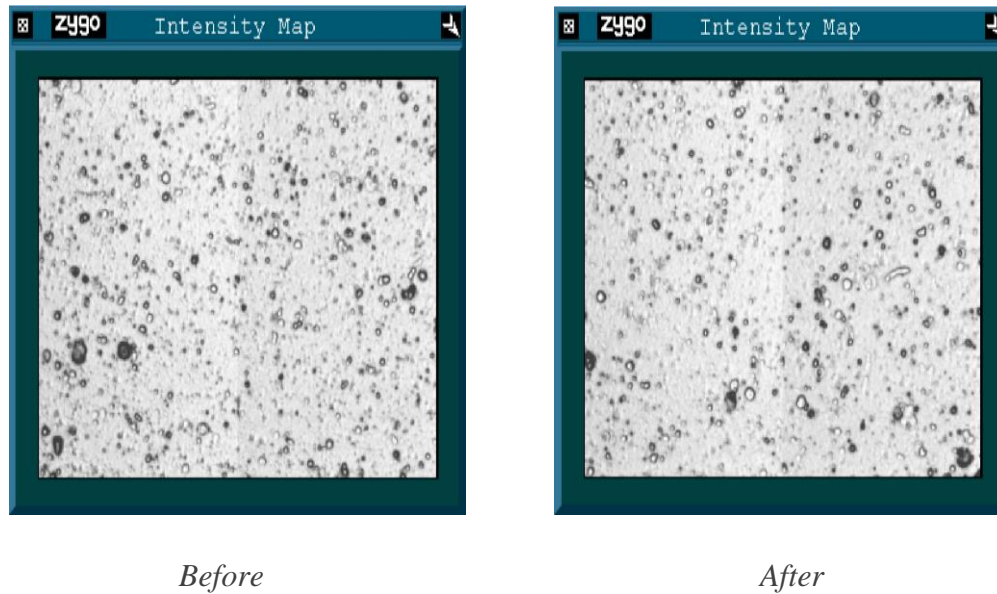
Tech #2 disc

Figure 36: Intensity map collected from Tech #2 disc number 10 “Before” and “After” the pin on disc test. These maps have been collected in position 3 on the disc and so, on the wearing path.

As far as the disc coated with technique #2 concerned, the surface appears rough with a lot of defects even before the pin on disc test. This is confirmed also by the value of arithmetic roughness showed in TABLE XX that is around 30 nm, about 7 times bigger than the Ra of the uncoated CoCr disc.

Moreover, by eye-comparing the “Before” disc with the “After” disc, the pin on disc (POD) test has not caused any major change in the visible characteristics of the surface of the material.

This eye appearance has been confirmed also by the microscopic analysis that has been performed using Zygo microscope. In fact, when focusing the attention on the microscopic characteristics of the damaged area, here represented in the Intensity maps collected from point number three of the mask reported in the previous page, it has been noticed no visible changes in the surface characteristics.

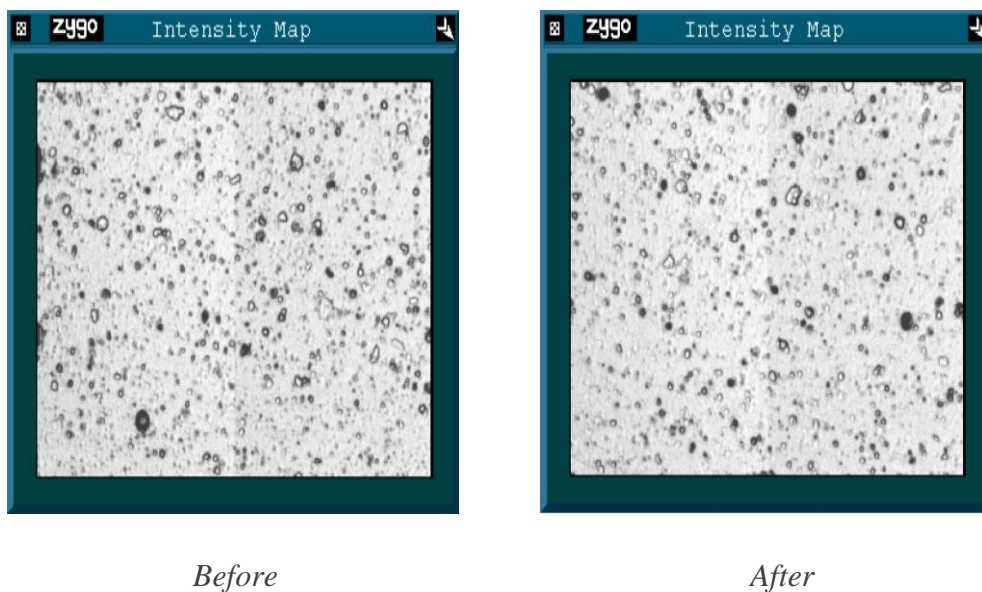


Figure 37: Intensity map collected from Tech #2 disc number 10 “Before” and “After” the pin on disc test. These maps have been collected in position 5 on the disc and so, on the unworn zone.

In order to assess the dependency between the change in surface characteristics and the performed pin on disc (POD) test, an intensity map image has been collected also from point five of the mask.

This point is not on the wearing path and so the metallic material is not in contact with the polymeric pin in point number five. This is why no major changes or scratches are visible in this area, even when observed at the microscopic level.

Tech #3 disc



Figure 38: Intensity map collected from Tech #3 disc number 13 “Before” and “After” the pin on disc test. These maps have been collected in position 3 on the disc and so, on the wearing path.

Considering, now, the discs coated with process number 3, the surface of these materials show a visible difference in respect to the one seen for the other coating processes. Defects are less and a particular pattern is visible on the layer covering the bulk CoCr disc. This is responsible also for the value of arithmetic roughness showed in TABLE XX that is well around 13-14 nm. Moreover, by eye-comparing the “Before” disc with the “After” disc, the pin on disc (POD) test, only minor changes are the visible characteristics of the surface of the material.

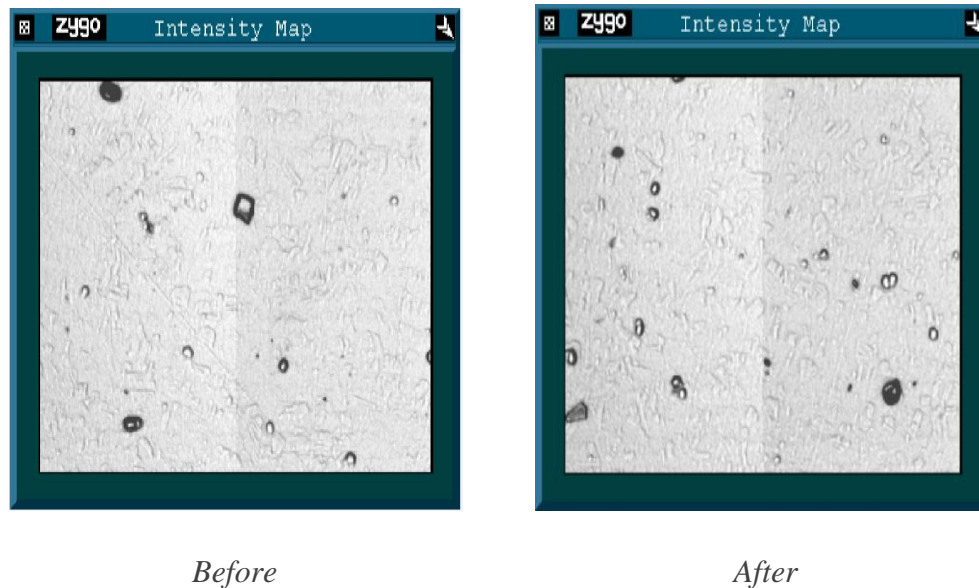


Figure 39: Intensity map collected from Tech #3 disc number 14 “Before” and “After” the pin on disc test. These maps have been collected in position 5 on the disc and so, on the unworn zone.

However, when focusing the attention on the microscopic characteristics of the damaged area, here represented in the Intensity maps collected from point number three of the mask, it has been noticed the presence of some scratches oriented as the direction of movement of the pin on the surface itself. The pattern itself seems to be oriented in the same direction of the external stress.

As seen for the other discs, an intensity map image has been collected also from point five of the mask. This is why no major changes are visible in this area, even when observed at the microscopic level.

AgTiN disc

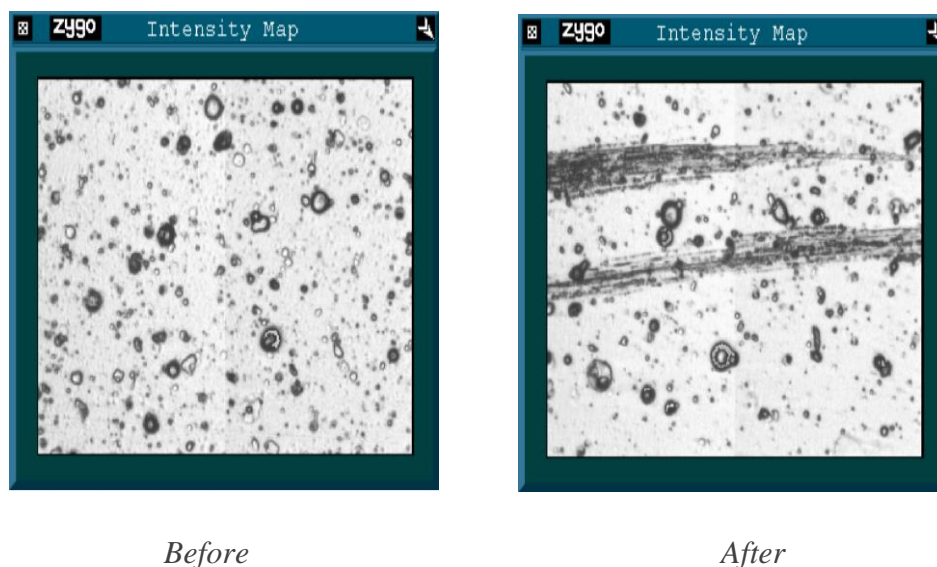


Figure 40: Intensity map collected from AgTiN coated disc number 18 “Before” and “After” the pin on disc test. These maps have been collected in position 1 on the wearing path.

When looking at the AgTiN coated disc, it has been noticed that the surface of this treated disc appears to be rich in defects also before the pin on disc test. This fact is deeply linked with the high value of arithmetic roughness showed in TABLE XX for this material, which is well over 45 nm.

This material shows the highest surface roughness of the entire group of tested discs.

In addition, when eye-comparing the “Before” disc with the “After” disc, the pin on disc (POD) test has caused some big scratches on the material that is well visible even at the macroscopic level.

Focusing on the microscopic characteristics of the damaged area, here represented in the Intensity maps on the right collected from point number one of the mask, it has been noticed the presence of some scratches of big dimension oriented as the direction of movement of the pin on the surface itself.

In order to assess the dependency between the change in surface characteristics and the performed pin on disc (POD) test, an intensity map image has been collected also from point five of the mask.

This point is not on the wearing path and so the metallic material is not in contact with the polymeric in point number five. This is why no major changes or scratches are visible in this area, even when observed at the microscopic level.

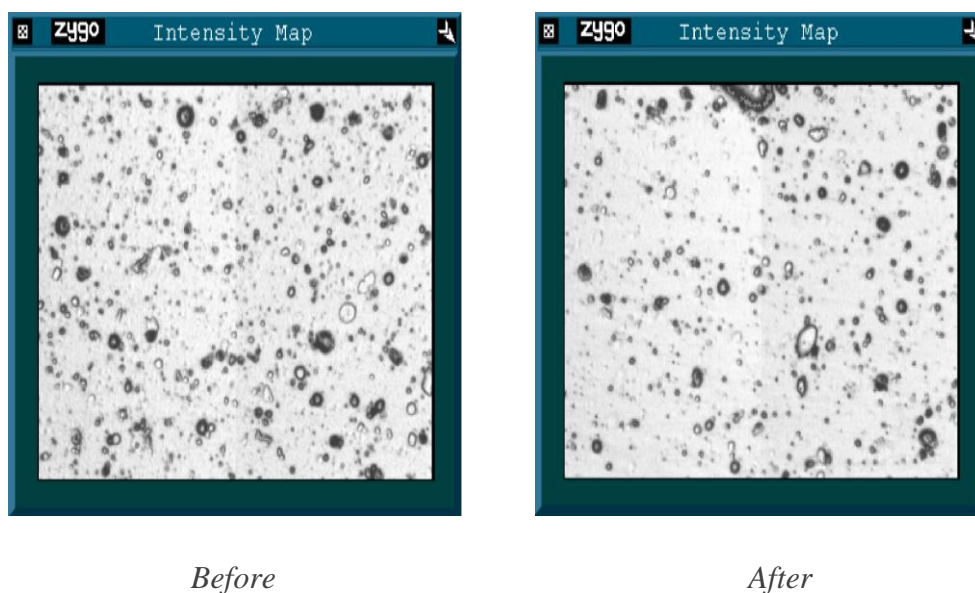


Figure 41: Intensity map collected from AgTiN coated disc number 18 “Before” and “After” the pin on disc test. These maps have been collected in position 5 on the disc and so, on the unworn zone.

Lab disc

As far as the CoCr disc from the LAB concerned, the surface of the uncoated disc appears quite smooth with minor defects on the surface before the pin on disc test. This is demonstrated also by the value of arithmetic roughness showed in TABLE XX that is well below 8 nm.

Moreover, by eye-comparing the “Before” disc with the “After” disc, the pin on disc (POD) test has not caused any major change in the visible characteristics of the surface of the material.

However, when focusing the attention on the microscopic characteristics of the damaged area, here represented in the Intensity maps collected from point number two of the mask, it has been noticed the presence of some long scratches oriented as the direction of movement of the pin on the surface itself.

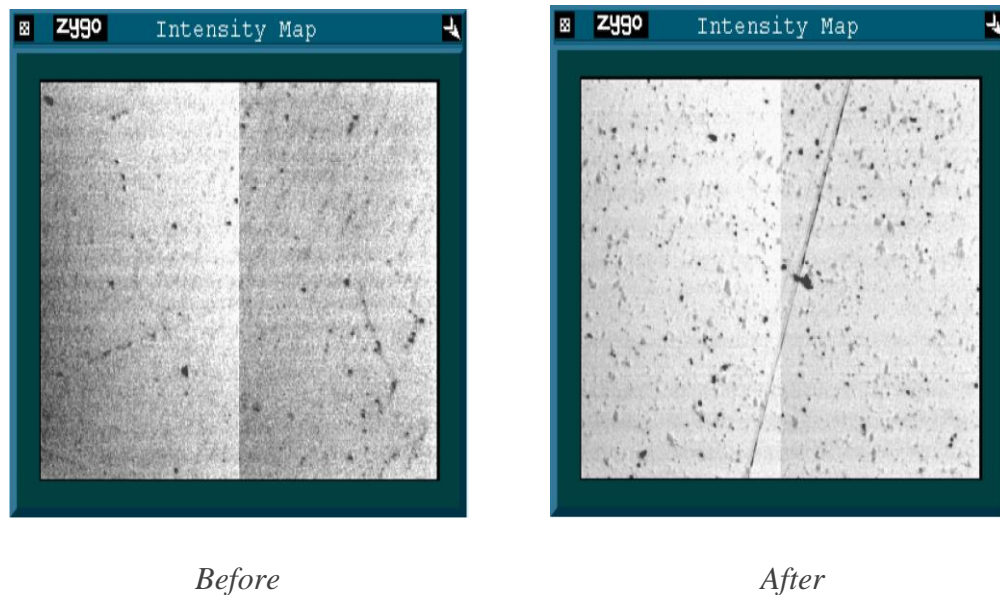


Figure 42: Intensity map collected from CoCr disc from the LAB number 23 “Before” and “After” the pin on disc test. These maps have been collected in position 2 on the disc and so, on the wearing path.

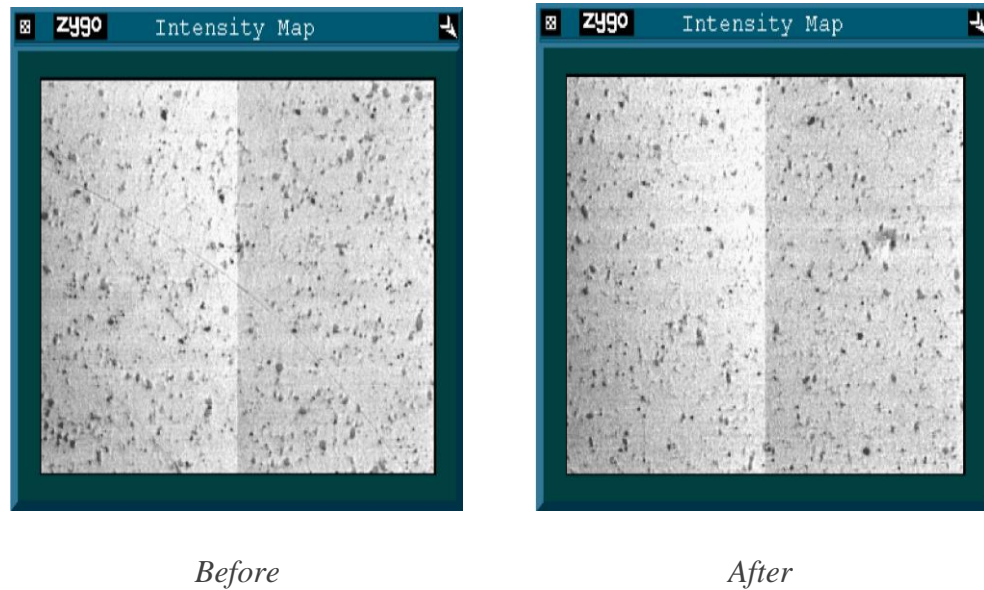


Figure 43: Intensity map collected from CoCr disc from the LAB number 23 “Before” and “After” the pin on disc test. These maps have been collected in position 5 on the disc and so, on the unworn zone.

In order to assess the dependency between the change in surface characteristics and the performed pin on disc (POD) test, an intensity map image has been collected also from point five of the mask.

This point is not on the wearing path and so the metallic material is not in contact with the pin in point number five. This is why no major changes or scratches are visible in this area, even when observed at the microscopic level.

*Ti6Al4V test*TABLE XXI: RECAP VERSION OF THE ROUGHNESS TABLE FOR Ti6Al4V TEST⁷.**SURFACE ROUGHNESS - RA**

TEST #1										
	#24 (Ti6Al4V)		#28 (Tech #1)		#32 (Tech #2)		#36 (Tech #3)		#40 (AgTiN)	
	Before	After	Before	After	Before	After	Before	After	Before	After
<u>AVG</u>	17.342	19.292	30.649	38.649	44.149	46.695	34.154	38.096	66.095	65.033
<u>STD</u>	2.935	4.998	3.432	12.758	3.292	16.636	4.124	11.850	9.564	9.571
TEST #2										
	#25 (Ti6Al4V)		#29 (Tech #1)		#33 (Tech #2)		#37 (Tech #3)		#41 (AgTiN)	
	Before	After	Before	After	Before	After	Before	After	Before	After
<u>AVG</u>	17.353	21.246	29.392	37.368	37.316	34.150	23.667	26.877	62.402	66.446
<u>STD</u>	3.806	7.251	1.849	5.422	3.708	6.979	2.536	10.187	8.425	16.153
TEST #3										
	#26 (Ti6Al4V)		#30 (Tech #1)		#34 (Tech #2)		#38 (Tech #3)		#42 (AgTiN)	
	Before	After	Before	After	Before	After	Before	After	Before	After
<u>AVG</u>	17.000	35,000	31.170	27,200	46.036	50,400	26.031	32,600	67.105	60,200
<u>STD</u>	4.099	20,384	9.193	9,680	5.624	17,387	0.847	3,647	7.490	20,608

⁷ All the values are expressed in nm.

The table collects all the final results of surface roughness for the test performed using the Ti6Al4V coated/uncoated discs. The first important thing to look at is that the uncoated discs have a surface roughness that is well below the one shown by the coated discs. Moreover, good variability in terms of Ra may be noticed also in the coated disc, with the AgTiN coated discs showing the highest arithmetic surface roughness. This variability is strongly dependent on the coating procedure.

As shown a general increase of surface arithmetic roughness has been registered after the pin on disc (POD) test for all the disc types except for AgTiN disc in the first test that has been performed and Tech #2 disc for the second test.

In particular, for TiN coating discs processed with Tech #2 technique a light increase of Ra has been detected, whereas the reduction for the AgTiN case is remarkable.

In conclusion, for bulk Ti6Al4V and also for all the other coated discs the pin on disc test has caused a change in the surface roughness, decreasing the smoothness of the interface.

Hereunder, a bar chart that illustrates all the variations in the surface roughness of the different discs has been reported. Moreover, a final summary of the value of the surface roughness Ra, obtained as the average value of the three measurements that have been performed, has been reported for each disc type.

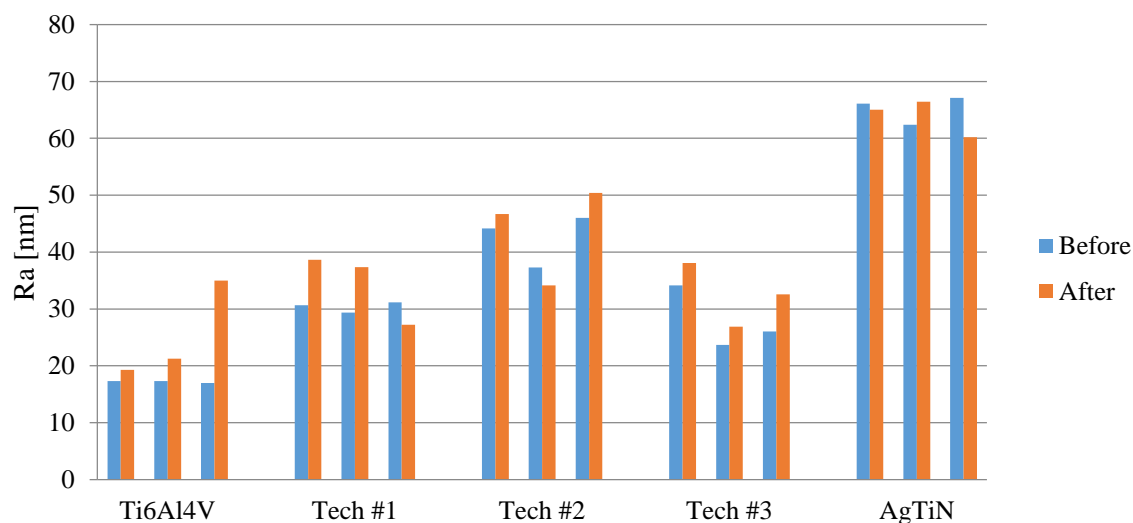


Figure 44: Summary of the arithmetic roughness for Ti6Al4V test. All the values of Ra, collected "Before" and "After" the pin on disc (POD) test, are subdivided into disc type groups and shown in nm.

TABLE XXII: SUMMARY OF THE ARITHMETIC ROUGHNESS FOR Ti6Al4V TEST⁸.

SUMMARY SURFACE ROUGHNESS – RA

	Ti6Al4V		Tech #1		Tech #2		Tech #3		AgTiN	
AVG	Before	After	Before	After	Before	After	Before	After	Before	After
	17,23	25,18	30,40	34,41	42,50	43,75	27,95	32,52	65,20	63,89
STD	3.64	12.82	5.76	9.76	4.33	14.47	2.83	9.26	8.54	16.10

⁸ These values are calculated as the average of the number shown in the previous table and are expressed in nm.

The same analysis seen for the CoCr test has been repeated also for the Ti6Al4V one in order to collect some information about any change in surface characteristics of the discs after the end of the pin on disc (POD) test. Hereunder, all the most important results have been reported, collecting them under the main materials used for the test.

Ti6Al4V disc

As far as the TiAl4V disc concerned, the surface of the uncoated disc appears quite smooth with minor defects on the surface before the pin on disc test. This is demonstrated also by the value of arithmetic roughness showed in TABLE XXII that is about 17 nm. This value is higher than the uncoated CoCr disc and this is probably due to the polishing technique that has been used for this set of discs that was not as precise as the one for the first set.

Moreover, by eye-comparing the “Before” disc with the “After” disc, the pin on disc (POD) test has not caused any major change in the visible characteristics of the surface of the material.

However, when on the microscopic characteristics of the damaged area, here represented in the Intensity maps collected from point number three of the mask, it has been noticed the presence of some oriented pattern on the surface that may derive from the polishing technique that has been used.

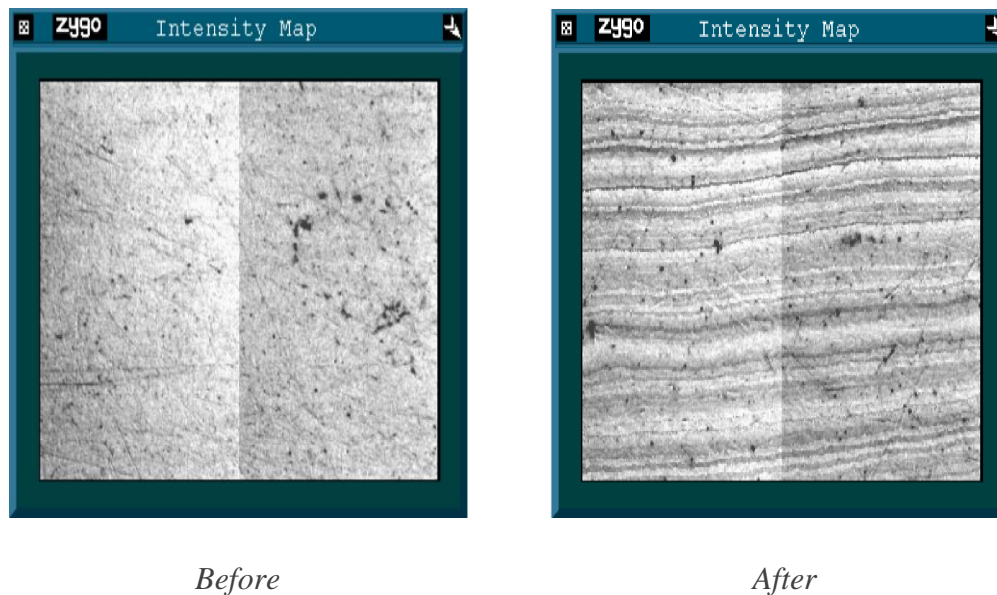


Figure 45: Intensity map collected from Ti6Al4V disc number 25 “Before” and “After” the pin on disc test. These maps have been collected in position 3 on the disc and so, on the wearing path.

In order to assess the dependency between the change in surface characteristics and the performed pin on disc (POD) test, an intensity map image has been collected also from point five of the mask.

This point is not on the wearing path and so the metallic material is not in contact with the polymeric pin in point number five. The same behavior shown for point 3 has been registered also for this point and so it is independent of the pin on disc itself. This behavior will be common to all the discs of this set.

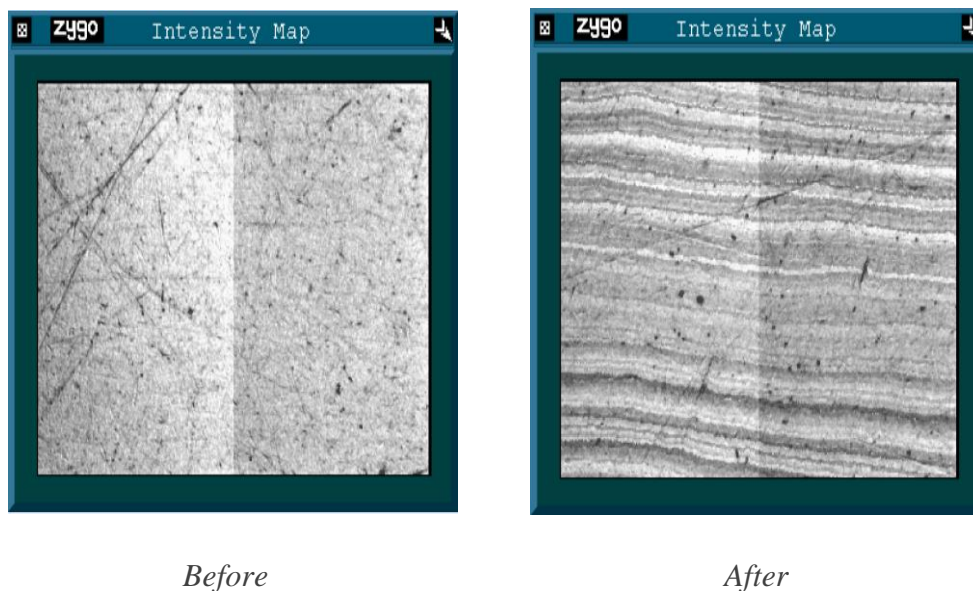


Figure 46: Intensity map collected from Ti6Al4V disc number 25 “Before” and “After” the pin on disc test. These maps have been collected in position 5 on the disc and so, on the unworn zone.

Tech #1 disc

Focusing on the disc coated with TiN deposited with Tech #1, it is evident how the layer deposited on the upper side of the disc has affected the surface characteristics. In fact, many more defects may be noticed on the surface that results in rougher. This is demonstrated also by the fact that the evaluated arithmetic surface for this type of discs is around 30 nm as shown in TABLE XXII.

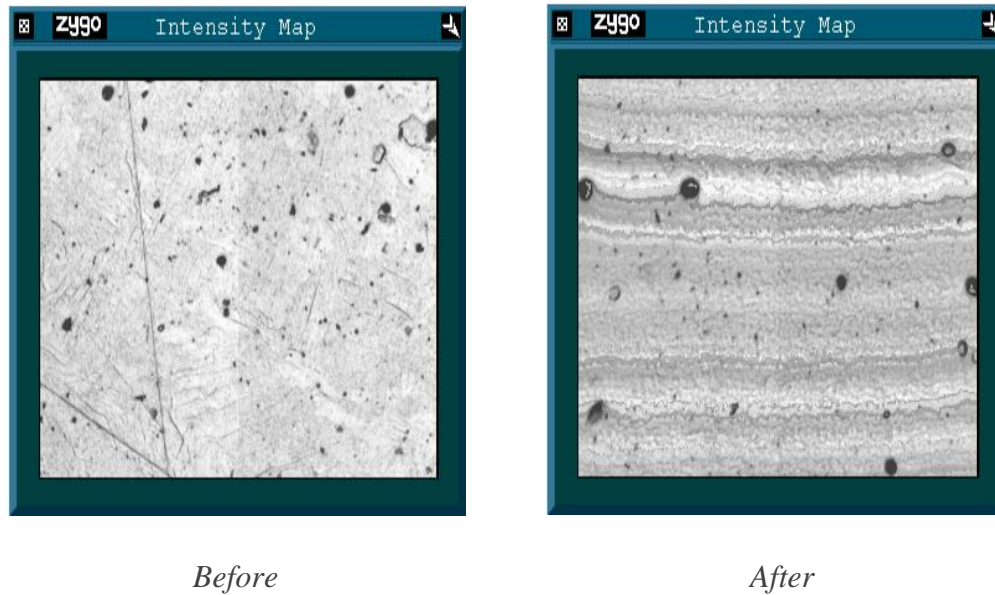


Figure 47: Intensity map collected from Tech #1 disc number 29 “Before” and “After” the pin on disc test. These maps have been collected in position 3 on the disc and so, on the wearing path.

Moreover, when looking at the microscopic characteristics of the damaged area, here represented in the Intensity maps collected from point number three of the mask, it has been noticed the presence of an important area of damage.

As highlighted by the "After" image, the zone in which the pin on disc (POD) test has been performed show the presence of a new kind of micro-roughness. This is because part of the material coating the bulk Ti6Al4V disk has been removed during the experiment. In addition, the same pattern observed for Ti6Al4V disc is present also in this case.

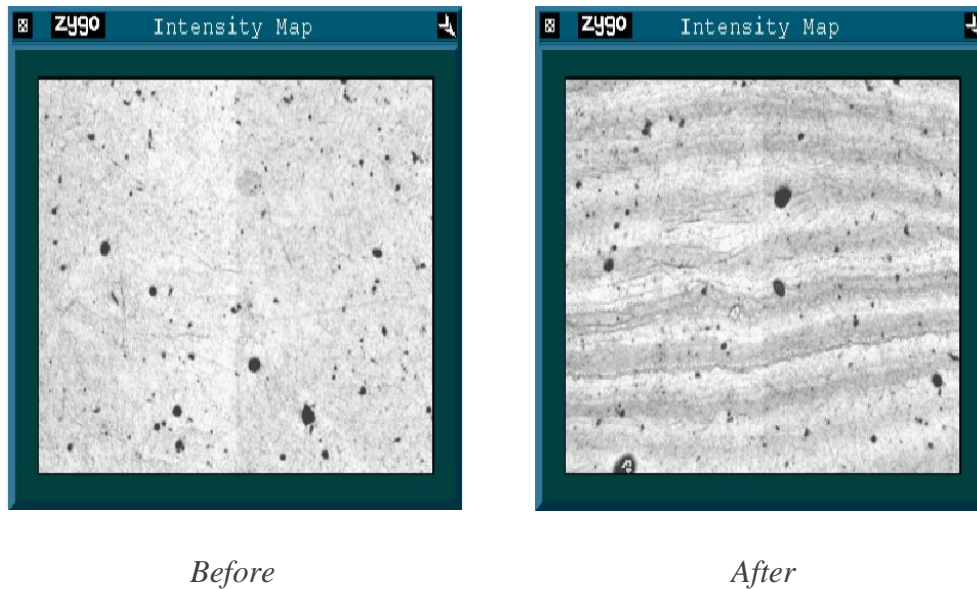


Figure 48: Intensity map collected from Tech #1 disc number 29 “Before” and “After” the pin on disc test. These maps have been collected in position 5 on the disc and so, on the unworn zone.

In order to assess the dependency between the change in surface characteristics and the performed pin on disc (POD) test, an intensity map image has been collected also from point five of the mask.

This point is not on the wearing path and so the metallic material is not in contact with the polymeric in point number five. This is why no major changes are visible in this area, even when observed at the microscopic level. As shown in the image collected from Zygo, the micro-roughness is not present in this case because this part of the disc has not interacted with the

moving pin during the POD test. This material showed the highest difference in terms of surface characteristics in the group we have tested during this experiment.

However, as just said for the bulk Ti6Al4V case, also in this case the pattern is present even in point number 5 because it appears to be independent of the POD test.

Tech #2 disc

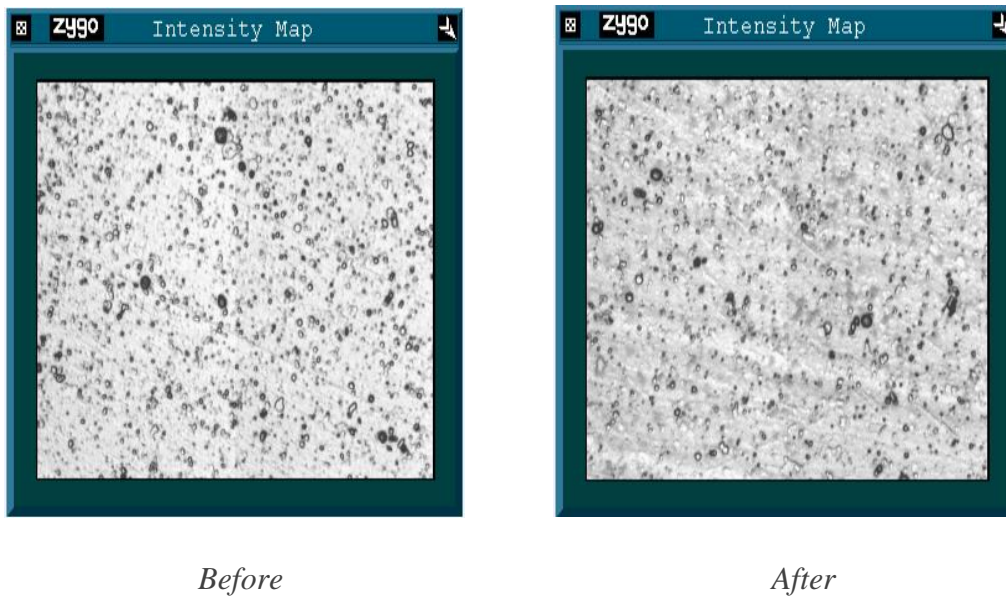


Figure 49: Intensity map collected from Tech #2 disc number 33 “Before” and “After” the pin on disc test. These maps have been collected in position 3 on the disc and so, on the wearing path.

As far as the disc coated with technique #2 concerned, the surface appears rough with a lot of defects on the surface before the pin on disc test. This is confirmed also by the value of arithmetic roughness showed in TABLE XXII that is around 40-45 nm.

This eye appearance has been confirmed also by the microscopic analysis that has been performed using Zygo microscope. In fact, when focusing the attention on the microscopic characteristics of the damaged area, here represented in the Intensity maps collected from point number three of the mask, it has been noticed no visible changes in the surface characteristics apart from the lines that define the common pattern.



Figure 50: Intensity map collected from Tech #2 disc number 33 “Before” and “After” the pin on disc test. These maps have been collected in position 5 on the disc and so, on the unworn zone.

In order to assess the dependency between the change in surface characteristics and the performed pin on disc (POD) test, an intensity map image has been collected also from point five of the mask.

This point is not on the wearing path and so the metallic material is not in contact with the polymeric pin in point number five. This is why no major changes or scratches are visible in this area, even when observed at the microscopic level.

Tech #3 disc

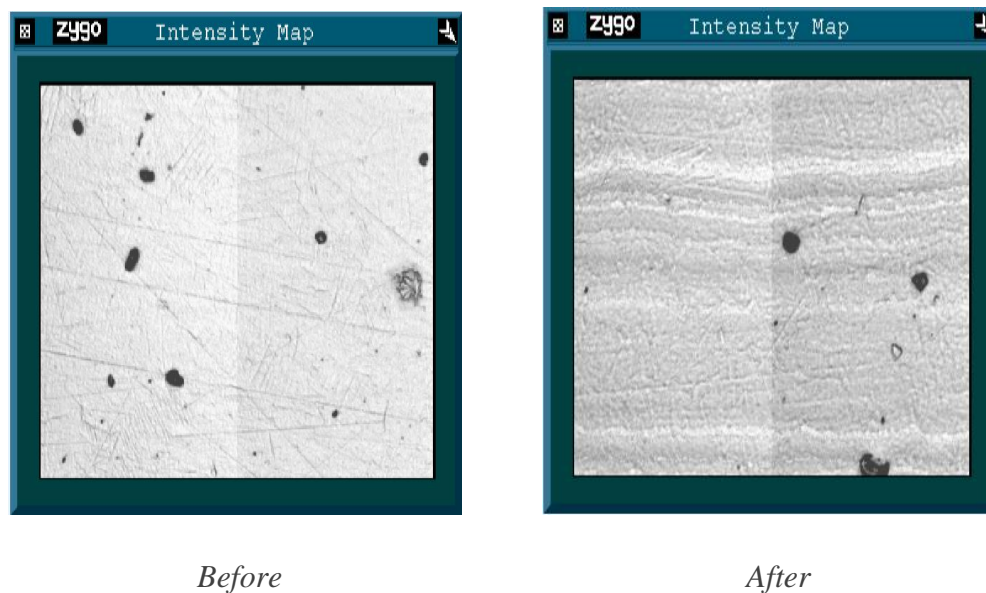


Figure 51: Intensity map collected from Tech #3 disc number 37 “Before” and “After” the pin on disc test. These maps have been collected in position 3 on the disc and so, on the wearing path.

Considering, now, the discs coated with process number 3, the surface of these materials show a visible difference in respect to the one seen for the other coating processes. Defects are less and a particular pattern is visible on the layer covering the bulk CoCr disc. This is responsible also for the value of arithmetic roughness showed in TABLE XXII that is well around 30 nm.

Moreover, by eye-comparing the “Before” disc with the “After” disc, the pin on disc (POD) test, only minor changes are the visible characteristics of the surface of the material.

However, when focusing the attention on the microscopic characteristics of the damaged area, here represented in the Intensity maps collected from point number three of the mask, it has been noticed the presence of a rough zone, not visible "Before" the pin on disc test in the area of interaction with the polymeric pin. This is probably because during the experiment part of the coating material, present on the surface, has been removed.

In addition, it has been noticed, also in this case the pattern derived from the polishing procedure.

As seen for the other discs, in order to assess the dependency between the change in surface characteristics and the performed pin on disc (POD) test, an intensity map image has been collected also from point five of the mask.

This point is not on the wearing path and so the metallic material is not in contact with the pin in point number five. This is why no major changes are visible in this area, even when observed at the microscopic level.

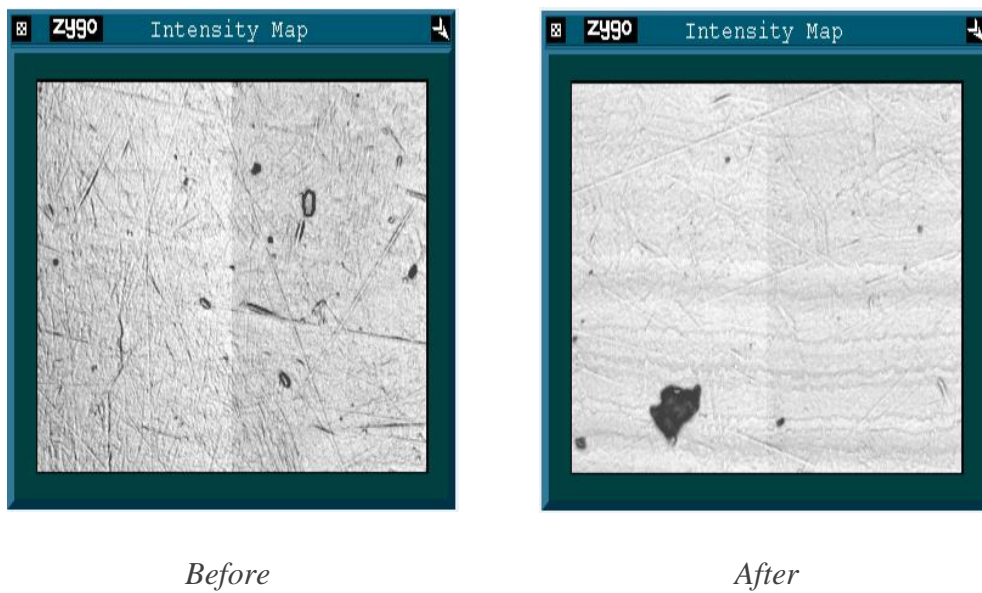


Figure 52: Intensity map collected from Tech #3 disc number 37 “Before” and “After” the pin on disc test. These maps have been collected in position 5 on the disc and so, on the unworn zone.

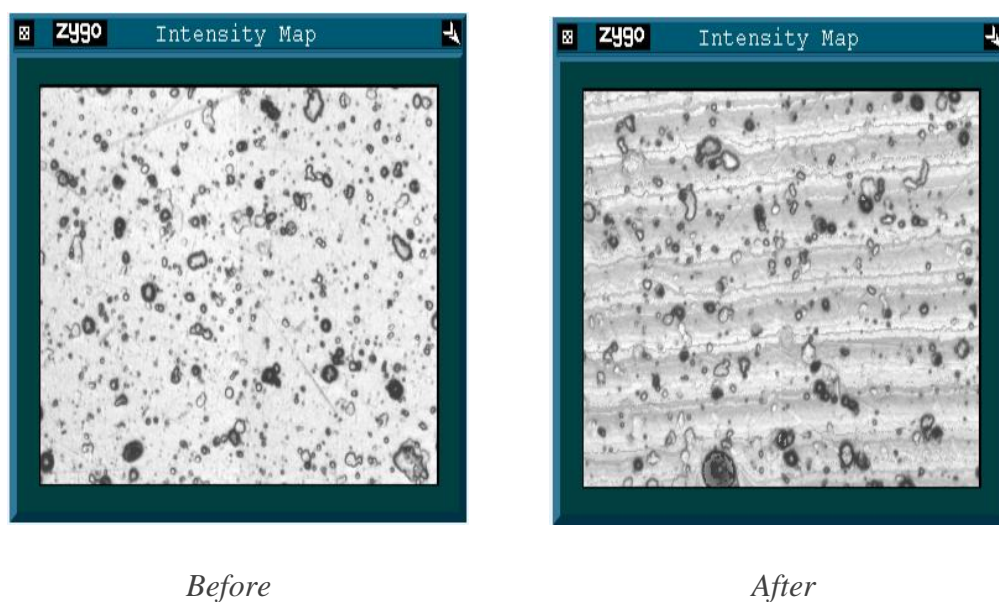
AgTiN disc

Figure 53: Intensity map collected from AgTiN coated disc number 41 “Before” and “After” the pin on disc test. These maps have been collected in position 1 on the wearing path.

When looking at the AgTiN coated disc, it has been noticed that the surface of this treated disc appears to be rich in defects on the surface even before the pin on disc test. This fact is deeply linked with the high value of arithmetic roughness showed in TABLE XXII for this material, which is well over 65 nm.

This is 3-4 times the roughness shown by the uncoated Ti6Al4V disc.

This material shows the highest surface roughness of the entire group of tested discs.

In addition, when eye-comparing the "Before" disc with the "After" disc, the pin on disc (POD) test has caused some big scratches on the material that is well visible even at the macroscopic level.

Focusing the attention on the microscopic characteristics of the damaged area, here represented in the Intensity maps on the right collected from point number one of the masks, it has been noticed only the presence of the pattern derived from a polishing technique that is common to all the disc in this test.

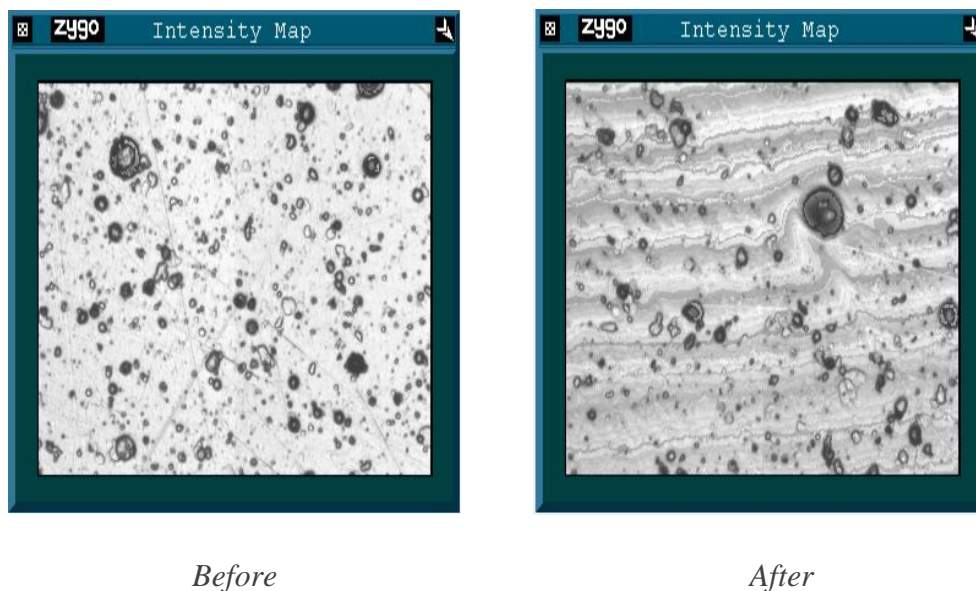


Figure 54: Intensity map collected from AgTiN coated disc number 41 "Before" and "After" the pin on disc test. These maps have been collected in position 5 on the unworn zone.

In order to assess the dependency between the change in surface characteristics and the performed pin on disc (POD) test, an intensity map image has been collected also from point five of the mask.

This point is not on the wearing path and so the metallic material is not in contact with the polymeric in point number five. This is why no major changes, apart from the common pattern, or scratches are visible in this area, even when observed at the microscopic level.

5.1.2 Raman spectroscopy of disc surface

In order to evaluate eventual changes in the surface characteristics of the discs a Raman spectroscopy has been performed for a selected set of 7 discs coming from the first round of each test. In particular, for the selected set of discs the analysis have been repeated twice, one time before the POD test and the second time after the end of the POD test. This process has been followed in order to have comparable results for each disc.

Here, the results of the Raman analysis will be reported subdividing them depending on the test, they are coming from.

CoCr test

CoCr disc

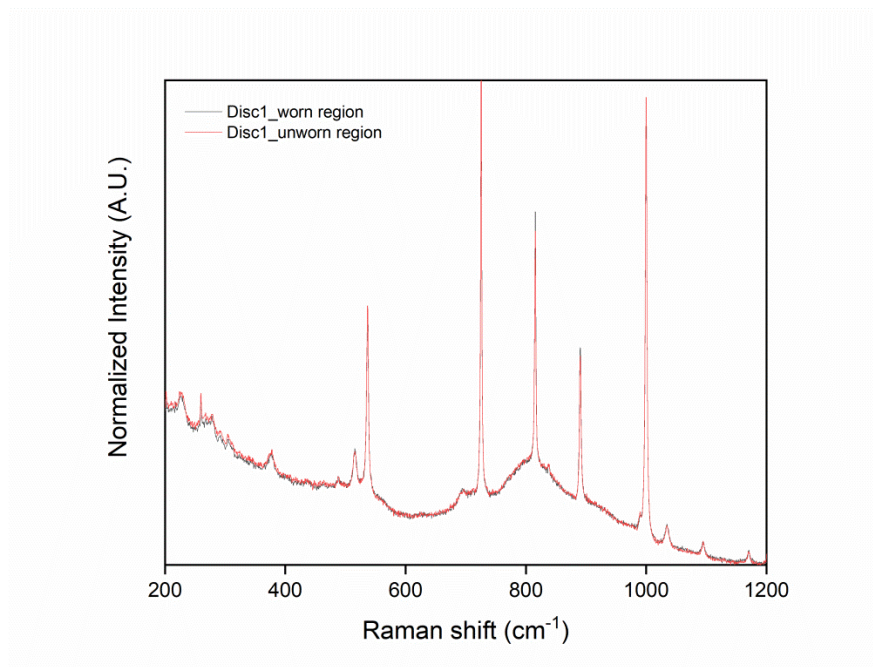


Figure 55: Raman spectroscopy for CoCr uncoated disc number 1⁹.

The first analyzed disc has been the CoCr uncoated disc number 1. The results relative to this disc will be used to introduce some concepts that will be useful also for the other materials.

⁹ The analysis has been performed twice. In red, it is possible to see the graph determined for the undamaged area, whereas the graph from the damaged zone has been colored in black. The intensity has been normalized between 0 and 1.

First of all, the main spikes located at 540, 750, 830, 900 and 1000 cm^{-1} are linked to the presence of ortho-Xylene used as a reference in the machine that performs the Raman spectroscopy. In particular, this material has been chosen as a reference because its spikes are localized at a discrete and fixed point, making its study a good way to determine how good the calibration of the machine was.

This means that the peaks captured by the Raman machine have to exactly correspond to the theoretical ones (37) otherwise the entire Raman graph has to be corrected for the shift. Moreover, these peaks demonstrate how coherent the measurement was between the “worn” and “unworn” region.

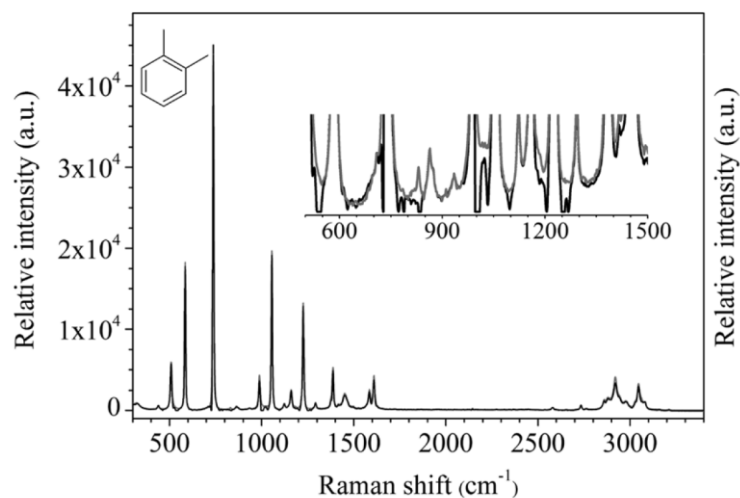


Figure 56: Raman spectra of ortho-xylene: comparison between pure experimental (grey) and resolved (black) spectra. – [37].

The theoretical position of the peaks for ortho-Xylene has been reported above. As noticeable, the real peaks found during the experiment correspond to the bibliographical ones.

If focusing, on the Raman curve now it is possible to notice that there are not major curves or peaks apart from the ones introduced by the xylene. This is because CoCr and, in general, bulk metallic materials are not so sensible to Raman tests and the results that may be reached are not really significant.

However, it has been noticed that no major changes in the graph can be observed meaning that nothing has changed on the surface and no external materials like proteins or polymeric particles have remained embedded on it.

Tech #1 disc

The first TiN coated disc that has been studied was Tech #1 processed disc number 5. As just seen, the main vertical spikes are linked to the presence of the o-xylene used as a reference to evaluate the exact calibration of the machine.

However, the observed curve has shown, in this case, a behavior that has been common to all the Raman curve defined for TiN coated biomaterials. As expected from bibliography (38), the presence of four principal peaks at 235, 320, 440, and 570 cm^{-1} have been highlighted. These peaks correspond to transverse acoustic (TA), longitudinal acoustic (LA), second-order acoustic

(2A), and transverse optical (TO) modes of TiN. In addition, two subsequent peaks have been observed at 800 and 1100 cm^{-1} .

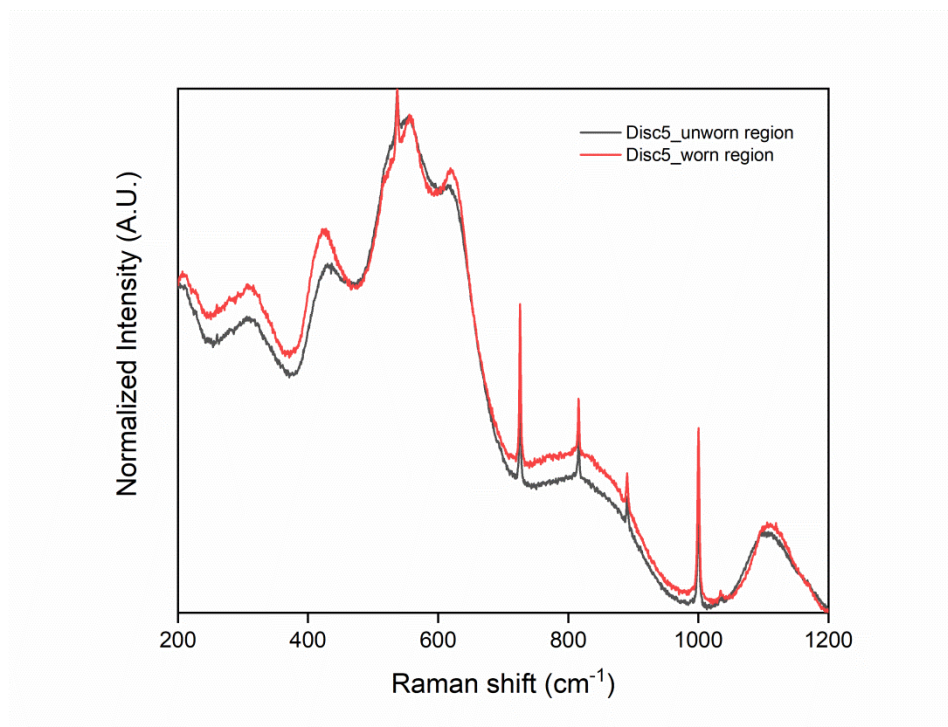


Figure 57: Raman spectroscopy for tech #1 coated disc number 5 ¹⁰.

These peaks are not as sharp as the ones of xylene because the Raman spectroscopy is less efficient on crystalline solids with respect to the fluid.

¹⁰ The analysis has been performed twice. In red, it is possible to see the graph determined for the undamaged area, whereas the graph from the damaged zone has been colored in black. The intensity has been normalized between 0 and 1.

When comparing the two graphs, it has been observed a leftward shift of the second-order acoustic (2A), whereas the other peaks have not changed. Using Microsoft Excel and the dataset collected from the Raman machine, it has been proven a shift equal to:

$$\text{Shift} = - 8.422 \text{ cm}^{-1}$$

Where "-" symbol is used for leftward shift and "+" sign is used for the rightwards shift. This is proof that something has changed in the damaged area affecting also the data collected by the Raman. In conclusion, it is useful to remember that the changes in Intensity are not taken into account when performing a Raman analysis because the intensity is mainly affected by boundary effects and condition like air temperature and humidity, a small variation on the light source power or micro-movements of the machine support (39-41).

Tech #2 disc

The same procedure seen for disc number 5 has been performed also for disc number 9. In this particular case no major shift or changes between the unworn zone and the damaged one have been determined and the resulting graph superimposes almost perfectly. This thing authorizes to suppose that only minor changes have happened on the surface of the disc and nor protein or polymeric debris have remained embedded on it.

However, it is still important to notice that even for the TiN coating processed with tech #2, the same major shift at 235, 320, 440, and 570 cm^{-1} and the two subsequent peaks at 800 and

1100 cm^{-1} have been registered. In particular, for the transverse acoustic (TA) and the longitudinal acoustic (LA), a higher value of intensity has been determined. This fact may be linked to different origins also linked with external environmental factors (39-41).

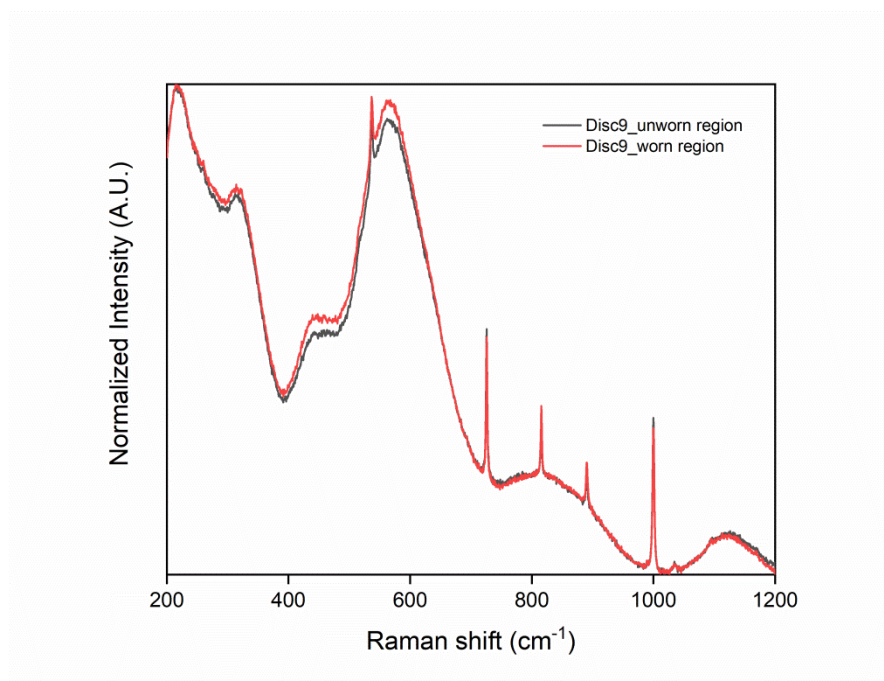


Figure 58: Raman spectroscopy for Tech #2 coated disc number 9 ¹¹.

In conclusion, it is important to remember that the sharp peaks come from the o-xylene used as a reference for the calibration of the machine

¹¹ The analysis has been performed twice. In red, it is possible to see the graph determined for the undamaged area, whereas the graph from the damaged zone has been colored in black. The intensity has been normalized between 0 and 1.

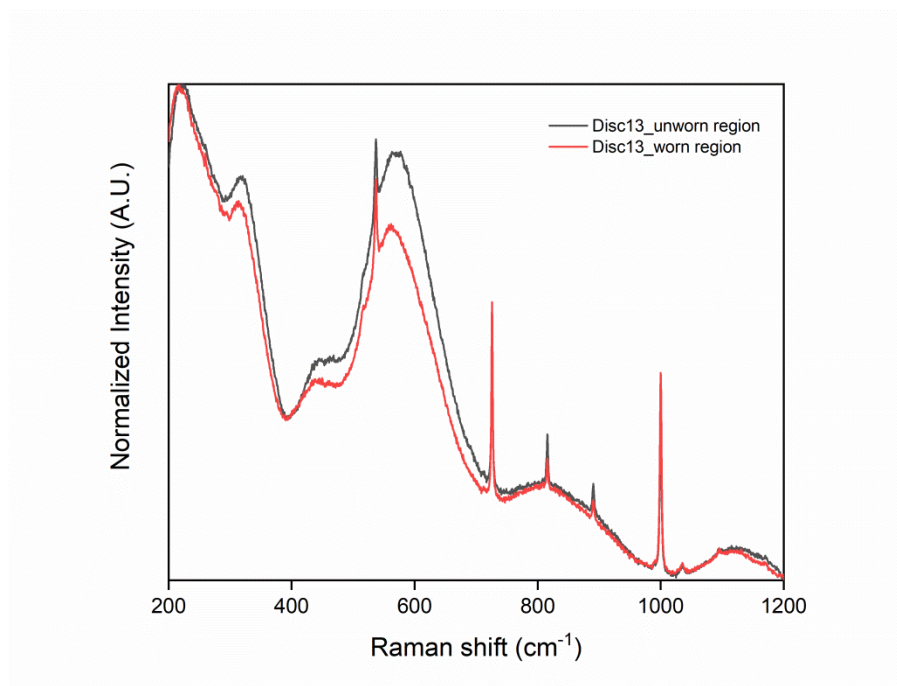
Tech #3 disc

Figure 59, Raman spectroscopy for Tech #3 coated disc number 13 ¹².

As far as tech #3 processed disc concern, it has been analyzed the disc number 13. As just said, also in this test the main sharp spikes are linked to the presence of the o-xylene used for the calibration.

¹² The analysis has been performed twice. In red, it is possible to see the graph determined for the undamaged area, whereas the graph from the damaged zone has been colored in black. The intensity has been normalized between 0 and 1.

However, the observed curve has been characterized by some behavior that is common to almost all the TiN coating. In fact, as expectable from the bibliography(38), the presence of four principal peaks have been highlighted and in particular the first two peaks were more similar to tach #2 processed disc than tech #1 processed disc. In addition, two subsequent peaks have been observed at 800 and 1100 cm^{-1} .

These peaks are not as sharp as the ones of xylene because the Raman spectroscopy is less efficient on crystalline solids with respect to the fluid.

When comparing the two graphs, it has been observed a leftward shift of the second-order acoustic (2A), and also a minor shift of the transverse optical that has not been taken into account because it was a minor shift. Other peaks have not changed. Using the raw data collected from the machine and elaborating them on Microsoft, it has been quantified the leftward shift equal to:

$$\text{Shift} = - 4.943 \text{ cm}^{-1}$$

Where "-" symbol is used for leftward shift and "+" sign is used for the rightwards shift. This is proof that something has changed in the damaged area affecting also the data collected by the Raman.

AgTiN disc

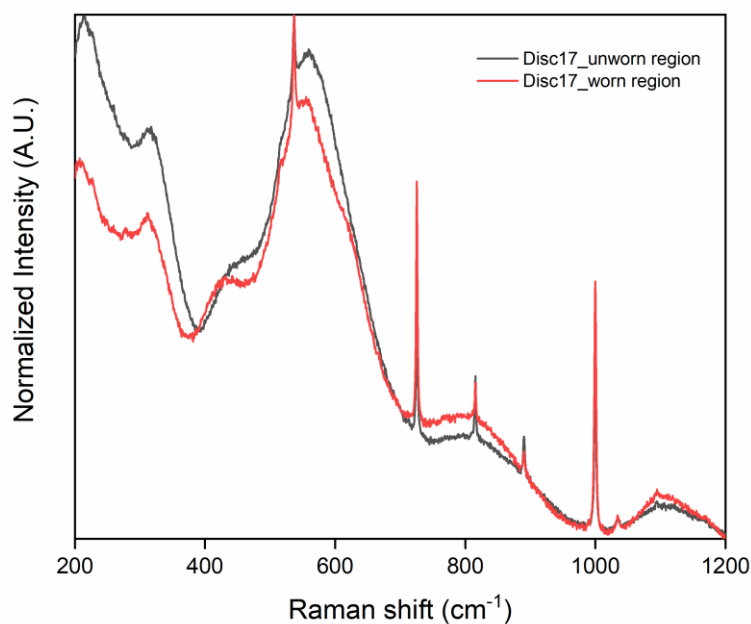


Figure 60: Raman spectroscopy for AgTiN coated disc number 17 ¹³.

When focusing on the AgTiN coated disc number 17 the results reported above has have been collected. Bypassing the main sharp peaks that are linked to the presence of o-xylene as a reference, also this kind of TiN layer has shown the same results in terms of main peaks.

¹³ The analysis has been performed twice. In red, it is possible to see the graph determined for the undamaged area, whereas the graph from the damaged zone has been colored in black. The intensity has been normalized between 0 and 1.

In fact, the main peaks were localized at the same Raman shift described by the bibliography(38).

If comparing the results obtained by the test performed in the wearing region or in the unworn one we can notice a huge shift leftward of the second-order acoustic (2A). When quantified using Microsoft Excel and the raw data given by the Raman machine, the shift has been evaluated as:

$$\text{Shift} = - 13.374 \text{ cm}^{-1}$$

Where "-" symbol is used for leftward shift and "+" sign is used for the rightwards shift. This is proof that something has changed in the damaged area affecting also the data collected by the Raman. As noticeable, this is the biggest shift between all the material studied in this test. This may be probably connected to the fact that this is the disc that had the maximum damage on its surface where a big scratch along the wearing path has been determined. In conclusion, it is useful to remember that the changes in Intensity, especially in the first two harmonics, have not been taken into account when performing a Raman analysis because the intensity is mainly affected by boundary effects and condition like air temperature and humidity, surface temperature, a small variation on the light source power or micro-movements of the machine support (39-41).

Lab disc

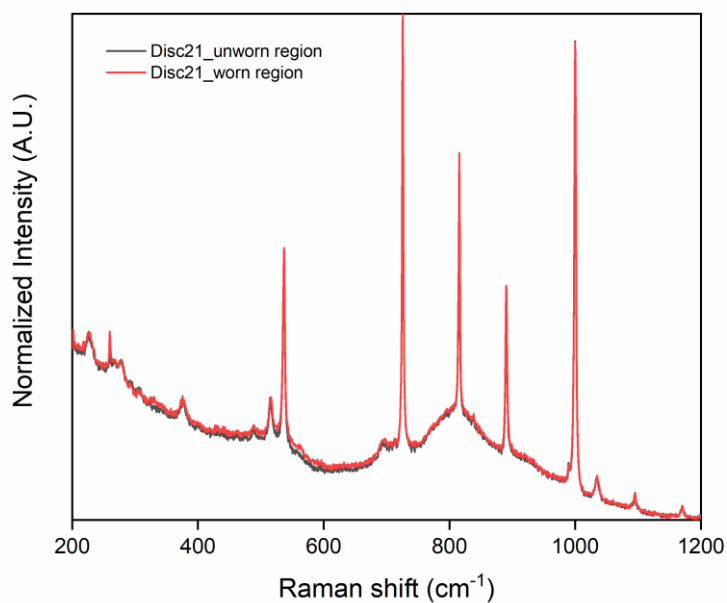


Figure 61: Raman spectroscopy for CoCr uncoated disc from the lab number 21¹⁴.

To conclude the CoCr test, it has been analyzed the bulk CoCr disc from the lab. Apart from the sharp spikes linked to the presence of o-xylene used as a reference, it is possible to notice that

¹⁴ The analysis has been performed twice. In red, it is possible to see the graph determined for the undamaged area, whereas the graph from the damaged zone has been colored in black. The intensity has been normalized between 0 and 1.

no big peaks are present because of the reduced reactivity of metallic materials to Raman spectroscopy. The resulting graph is similar to the one reported for disc 1, made of bulk CoCr.

In conclusion, when comparing the damaged zone with the untouched one no differences have been noticed. This means that no changes or material deposition have happened during the pin on disc test.

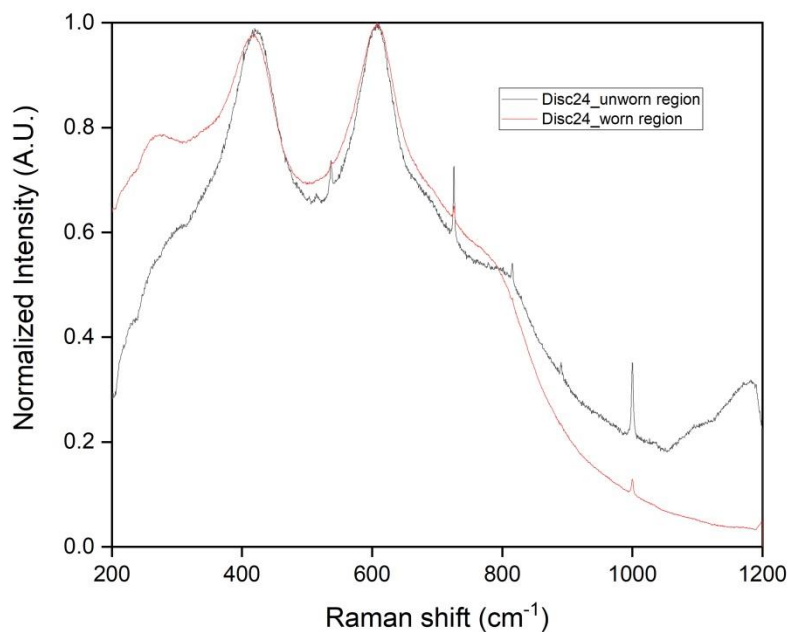
*Ti6Al4V test***Ti6Al4V disc**

Figure 62: Raman spectroscopy for Ti6Al4V uncoated disc number 24 ¹⁵.

As just seen for bulk CoCr disc, also the bulk Ti6Al4V disc number 24 seems not to be very sensible to spectroscopy. In particular, apart from the sharp spikes introduced by the o-xylene used as a reference, only two major shift has been recognized in this case.

¹⁵ The analysis has been performed twice. In red, it is possible to see the graph determined for the undamaged area, whereas the graph from the damaged zone has been colored in black. The intensity has been normalized between 0 and 1.

It is interesting to notice that no difference in the location of these peaks has been shown when comparing the results obtained for Ti6Al4V disc analyzed in its worn region or its untouched area. In particular, even if the shape of the Raman spectroscopy graphs were pretty different, the peaks are located at the same position around 400 and 630 cm^{-1} .

When focusing on the different behavior in term of intensity registered for the two conditions a wide variety of different factors has to be taken into account and it may be also the result of changes in the external condition in which the test itself has been performed.

Tech #1 disc

When focusing on the tech #1 coated disc number 28 the results reported above has have been collected. Passing over the main sharp peaks that are, as just seen, linked to the presence of o-xylene as a reference, also this kind of TiN layer has shown the same results in terms of main peaks even if in a different arrangement and with different values in term of associated intensity.

In particular, all the main peaks described in the bibliography (38) may be easily localized, but the first two, that correspond to the transverse acoustic (TA) and longitudinal acoustic (LA) have shown an intensity that was well below the one shown by the others TiN coated discs and similar to the one shown by tech #1 disc for CoCr test.

If comparing the results obtained by the test performed in the wearing region or the unworn one, no differences have been noticed and only the intensity has changed and, in particular, it has

increased for all the Raman shift except for the transverse acoustic at 235 cm^{-1} where the value for the intensity in the worn region has been smaller than in the unworn zone.

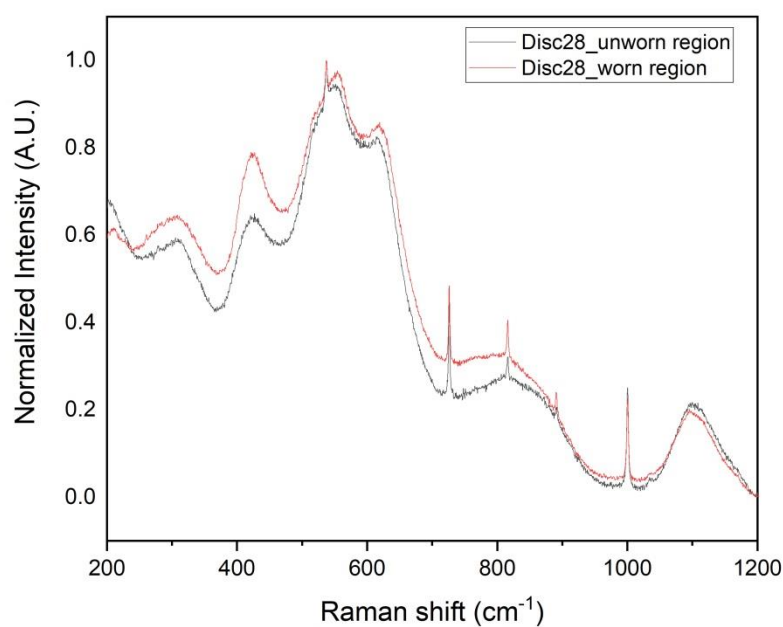


Figure 63: Raman spectroscopy for Tech #1 coated disc number 28 ¹⁶.

¹⁶ The analysis has been performed twice. In red, it is possible to see the graph determined for the undamaged area, whereas the graph from the damaged zone has been colored in black. The intensity has been normalized between 0 and 1.

Tech #2 disc

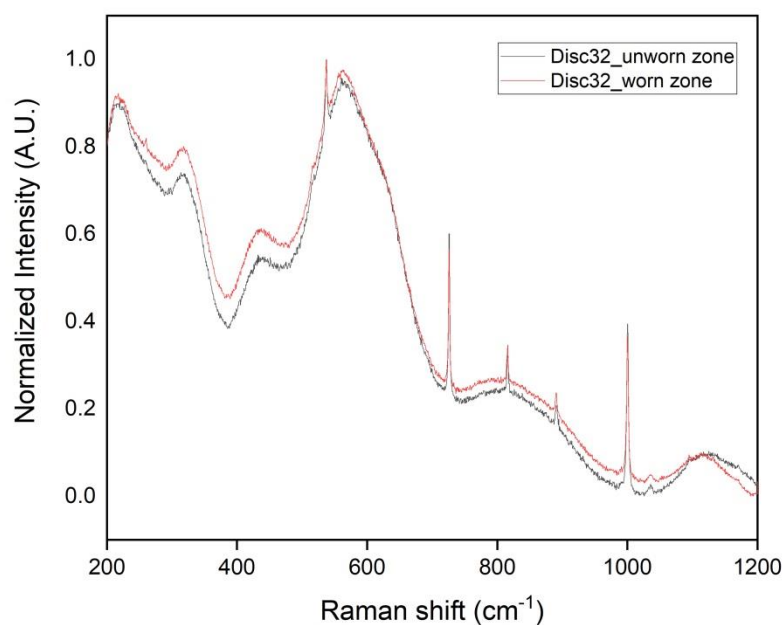


Figure 64: Raman spectroscopy for Tech #2 coated disc number 32 ¹⁷.

To complete the analysis for all the discs also the tech #2 processed disc number 32 has been analyzed. As said, the main sharp vertical spikes are linked to the presence of the o-xylene used as a reference to evaluate the exact calibration of the machine.

¹⁷ The analysis has been performed twice. In red, it is possible to see the graph determined for the undamaged area, whereas the graph from the damaged zone has been colored in black. The intensity has been normalized between 0 and 1.

When observing the results it is possible to notice the presence of all the characteristics shift of the TiN at their bibliographical² position. In particular, they have been localized at 235, 320, 440, 570, 800 and 1100 cm^{-1} . In particular, the first two have shown a different behavior with respect to the one seen for tech #1 processed disc. This difference is mainly based on different levels of intensity that is a parameter difficult to describe and explain as it is affected by a wide variety of different factors, mainly external ones.

As explained by bibliographical researches (39,40), Raman analysis results in term of intensity may be affected by a wide range of factors such as air temperature and humidity, temperature of the surface of the material, sudden changes in light source power, loss of stability of the machine support and much more. Considering this, also the difference in terms of intensity values between the measurement taken in the unworn zone and the measurement taken in the worn zone may not be considered as a sign of changes of some characteristics of the surface. In fact, all the main peaks have maintained their position and no major shifts have happened. This is a symptom that no changes in the surface of the material has occurred and also of the fact that no polymeric particles or denaturized protein coming from the testing fluid have remained embedded on the surface.

Tech #3 disc

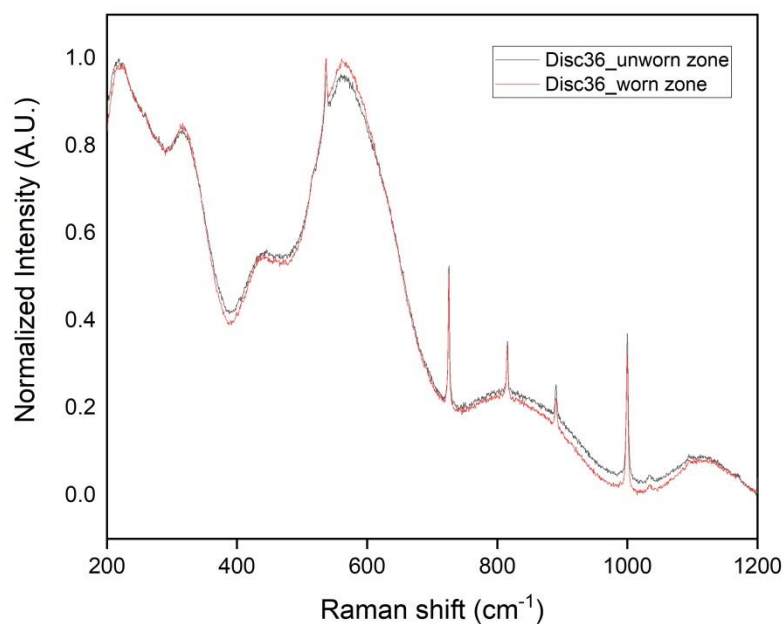


Figure 65, Raman spectroscopy for Tech #3 coated disc number 36 ¹⁸.

The same procedure followed for the previous disc has been repeated also for tech #3 disc number 36. The obtained curve has shown, in this case, a behavior that has been common to all the Raman curve defined for TiN coated biomaterials. As expected from bibliography(38), the

¹⁸ The analysis has been performed twice. In red, it is possible to see the graph determined for the undamaged area, whereas the graph from the damaged zone has been colored in black. The intensity has been normalized between 0 and 1.

presence of four principal peaks at 235, 320, 440, and 570 cm^{-1} have been verified both for the “unworn zone” measurement and the “worn zone” measurement. As said, these peaks correspond to transverse acoustic (TA), longitudinal acoustic (LA), second-order acoustic (2A), and transverse optical (TO) modes of TiN. In addition, two subsequent peaks have been observed at 800 and 1100 cm^{-1} . These peaks are not as sharp as the ones of xylene because the Raman spectroscopy is less efficient on crystalline solids with respect to fluid and the microscopic arrangement of the material deeply affects their spectroscopically measurable properties.

When comparing the two graphs, it has been observed an almost complete overlap between the two curves with no shifting of the graph.

This is proof that even if some external properties seemed to change, these may not affect the chemical characteristics of the material itself. In conclusion, it is useful to observe that no changes in Intensity have been highlighted in this particular case.

AgTiN

To conclude the analysis, a Raman spectroscopy test of the AgTiN coated Ti6Al4V disc has been performed too. As just seen, the main vertical spikes are linked to the presence of the o-xylene used as a reference to evaluate the exact calibration of the machine. The observed curve was the same shown for all the TiN coated discs, as it is representative of the fact that the surface layer of the discs is mainly made of TiN. In fact, we can notice the presence of the typical peaks

at 235, 320, 440, and 570 cm^{-1} just registered also for the other discs coated with the same material.

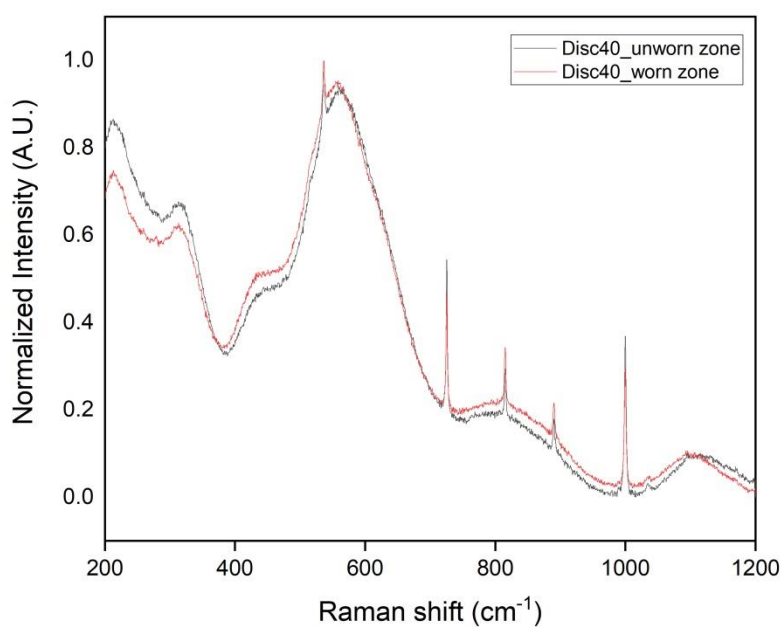


Figure 66: Raman spectroscopy for AgTiN coated disc number 40 ¹⁹.

¹⁹ The analysis has been performed twice. In red, it is possible to see the graph determined for the undamaged area, whereas the graph from the damaged zone has been colored in black. The intensity has been normalized between 0 and 1.

These peaks are not very sharp because Raman spectroscopy technique is not so effective on the metallic surface, but they are still significant, because they can help to prove the presence of other materials on the surface if the peaks are different from these.

When comparing the two graphs, no visible changes or a major shift in the graph have been highlighted, meaning that no significant changes have happened on the surface and any kind of material has remained embedded on it. In addition, it is useful to remember that the changes in Intensity are not taken into account when performing a Raman analysis because the intensity is mainly affected by boundary effects and conditions like air temperature and humidity, small variation on the light source power or micro-movements of the machine support.

5.1.3 Post-POD test evaluation of discs surface

To complete the analysis of the changes in the surface of the materials, a series of pictures have been collected using ZEISS 2000-C stereomicroscope. This operation has been performed in order to capture some qualitative representation of the surface to complete the characterization of the disc and the changes occurred because of the pin on disc test.

In order to acquire different images, light sources have been moved to find the configuration that gives the most interesting and meaningful overview of the differences between undamaged and damaged areas. This procedure has been repeated for each disc for each round in order to detect macro evidence of wear on the disc surface and, eventually, material embedded on the worn surface.

*CoCr test***CoCr disc**

Figure 67: Picture of the surface of the disc number 1.

As noticeable, no major changes have been registered on the surface of the disc. The surface appeared smooth and only some scratches have remained on it.

Tech #1 disc

Figure 68: Picture of the surface of the disc number 4.

For the disc treated with technique number 1, it has been observed an eye-visible change on the surface. In this area the disc has probably lost part of the surface coating during the POD test. When looking at the images captured with Zeiss 2000-c stereomicroscope, it is possible to see the change in color of the area that appears to be rougher.

These results confirm what seen during the Zygo analysis of the surface characteristics of the disc, where the appearance of a micro-roughness on the surface was demonstrated and quantified.

Tech #2 disc

Figure 69: Picture of the surface of the disc number 8.

When looking at the disc number 8, coated using the coating technique number, it has been observed that no major changes on the surface have taken place. However, the wearing area is well visible as shown in the image here reported and it is characterized by a darker shade that allows to distinguish it from the unworn zone. In this case, the shadow was lighter than the one observed for tech #3.

Tech #3 disc

As just observed for disc number 8, similar behavior has been observed also for disc number 12, from the tech #3 group. The surface has not been damaged by the wearing process, but a small change may be seen as a slight modification in the color of the material.

As seen for the tech #2 discs, also, in this case, it has been registered the presence of shade in the area of contact between pin and disc.



Figure 70: Picture of the surface of the disc number 12.

AgTiN disc

Figure 71: Picture of the surface of the disc number 16.

The AgTiN coated discs have shown a particular behavior in terms of their external appearance after the pin on disc test. In fact, as visible in the reported image, the interaction between the polymeric pin and the disc has caused the appearance of a relatively big and dark scratch.

In addition, as seen for tech #2 and tech #3 discs, the darker shade characterizing the wearing path is still present. With tech #1 discs, AgTiN ones have been the worst in terms of qualitatively assessed resistance to wearing test.

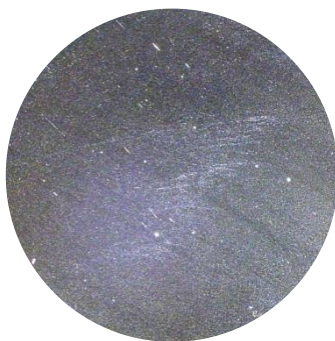
Lab disc

Figure 72: Picture of the surface of the disc number 21.

The last type of discs used to perform the pin on disc test has been the CoCr disc from the lab. These disc has shown no changes in the surface apart from some small scratches.

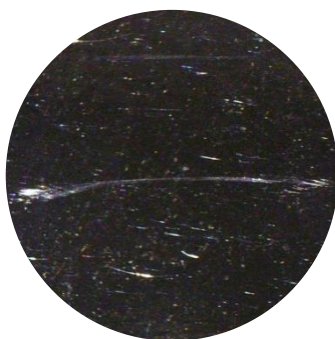
*Ti6Al4V test***Ti6Al4V disc**

Figure 73: Picture of the surface of the disc number 24.

The first type of disc that has been qualitatively observed after the second pin on disc test has been the uncoated Ti6Al4V disc. For this type of material no major changes or color modifications have been shown, but some scratches as the one shown in the center of the figure here reported have been observed.

Tech #1 disc

Figure 74: Picture of the surface of the disc number 28.

If focusing on the discs coated with tech #1, it has been observed a behavior common to the same type of discs from the CoCr test and a new characteristic. In fact, in this case both a small loss of material on the surface and a big scratch on the wearing path were observed.

This disc type has been the one showing the biggest and more visible changes on the surface between the one we have observed in the Ti6Al4V test.

Tech #2 disc

Figure 75: Picture of the surface of the disc number 32.

As far as tech #2 discs concerned, only a minor change in the surface characteristics has been shown. As visible in the picture, some areas of damage have been detected and, in general, the behavior has been worse than the one observed for the CoCr discs coated with this technique.

Tech #3 disc

For tech #3 treated discs the presence of a light scratch along the wearing path has been observed even if the overall characteristics of the surface were good and the area of damage has

been circumscribed to the wearing zone. As noticeable from the image, the damages to the disc has been really light.

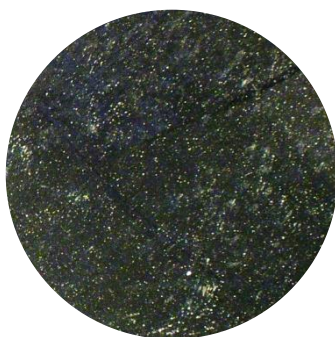


Figure 76: Picture of the surface of the disc number 36.

AgTiN disc



Figure 77: Picture of the surface of the disc number 40.

In conclusion, the last disc type that has been studied was the AgTiN coated ones. In this case, they have shown better behavior concerning the one shown for the CoCr test. In fact, the scratch along the wearing path, that is still visible, is way lighter than the one observed in the previous case. However, in this second case some little damage zones have been identified as visible in the image here reported.

5.2 Pin-on-Disc (POD) test

5.2.1 Introduction

In order to evaluate the overall amount of wear produced by the interaction of the metal surface with the UHMWPE counterpart, the Pin-on-Disc (POD) test has been chosen as the best way to assess the different performances of the materials. This section collects all the results obtained in the POD test for both CoCr based discs and Ti6Al4V based discs.

5.2.2 Test setup

To get all the materials ready for the test, it has been performed a setup session in which all the materials and settings have been prepared in order to get ready for the test.



Figure 78: Setup for the pin on disc (POD) test.

CoCr Test

The first part of the test has been dedicated to the assessment of the properties of coated and uncoated CoCr discs. As explained in the “Methods” section, a pin on disc (POD) test has been performed on all the different disc types simulating the in vivo conditions that may be experienced by the material if implanted into the Human body.

In this section, the main results obtained for each round will be presented followed by a final summary in which the main wearing rates for all the material will be calculated. In order to simplify the understanding of data, raw ones will be presented only in the appendix.

To conclude the analysis, the dependency between the roughness of the material and the wearing rate has been calculated, too, and the obtained results will be presented after the wearing rate calculation

Round 1

Being the first test to be performed, Round 1 has revealed some of the behaviors that have characterized the samples for all the tests.

Hereunder, it has been reported both the “Total weight loss” and the “Weight loss stage by stage” to calculate both the overall production of wear debris by the interaction between the pin and the specific disc, but also how this production change during the test. In particular, the overall wear production has been calculated for the total weight loss as the difference between the

initial weight of the pin and the actual one, whereas the value based on stage has been calculated as the value of the (i-1)th stage and the ith one.

All the values have been corrected for the soak pin variation that accounts for the weight changes due to hydration of the polymeric pin in the aqueous environment in order to consider only the weight variation due to the wearing process

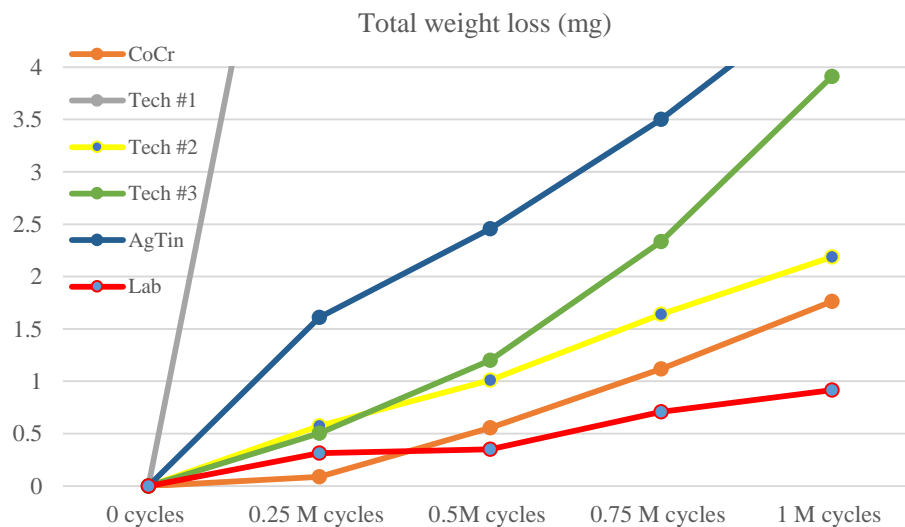


Figure 79: Total weight loss for Round 1 of CoCr test ²⁰.

²⁰ Values of weight loss have been calculated and expressed in mg every 250'000 cycles. Tech #1 is not present because it has gone rapidly out of the dynamics. Complete version of the table is present in the “Appendix” section

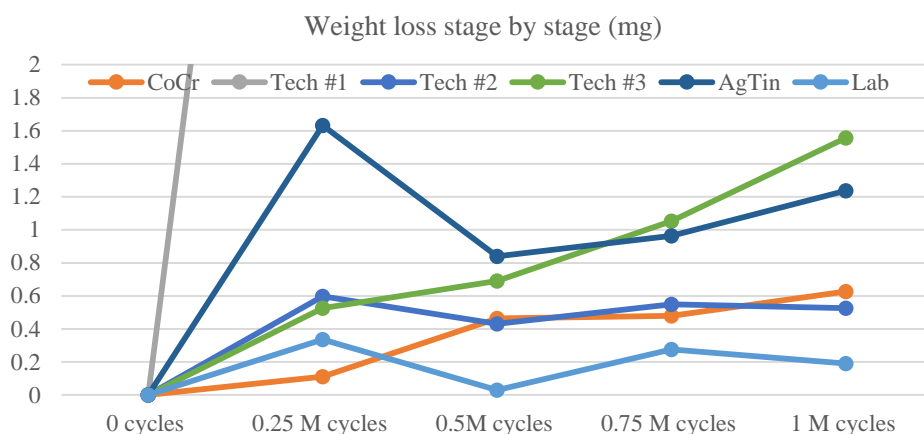


Figure 80: weight loss measured week by week for Round 1 of CoCr test ²¹.

As noticeable, Tech #1 coated disc has obtained the worst result and it is so bad that it quickly becomes not visible in these graphs, but it is still possible to observe its complete behavior at point 7.C of the appendix.

However, it is possible to observe that, in this round, CoCr, Lab and Tech #2 discs are the ones that have performed in the best way. In particular, when focusing on the CoCr and the Tech #2 disc that have been given to us by the company, it has been observed that apart from the initial

²¹ Values of weight loss have been calculated and expressed in mg every 250'000 cycles. Tech #1 is not present because it has gone rapidly out of the dynamics. Complete version of the table is present in the "Appendix" section

worse start of the Tech #2, it has performed in the same way or even better in two stages, 0.25M-0.50M and 0.75M-1M, than the CoCr itself.

Another important thing to notice is the general tendency observed in all the discs to converge in the stage by stage evaluation to a constant value. This means that the wearing rate tends to stabilize and this is a process that has been effectively demonstrated in the bibliography.

All these results find a final proof and summary in the two bar charts down reported that have been used to obtain a final assessment of the overall amount of debris that has been produced in each condition and the final weight change for each pin.

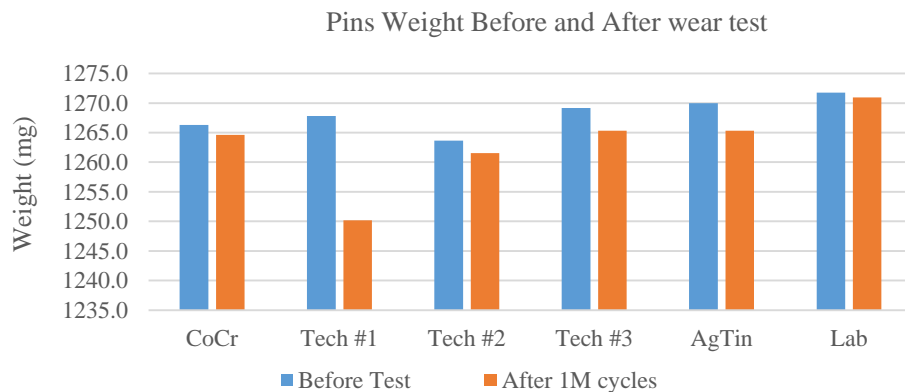


Figure 81: Pin weight “Before test” and “After 1M cycles” for Round 1, CoCr test.

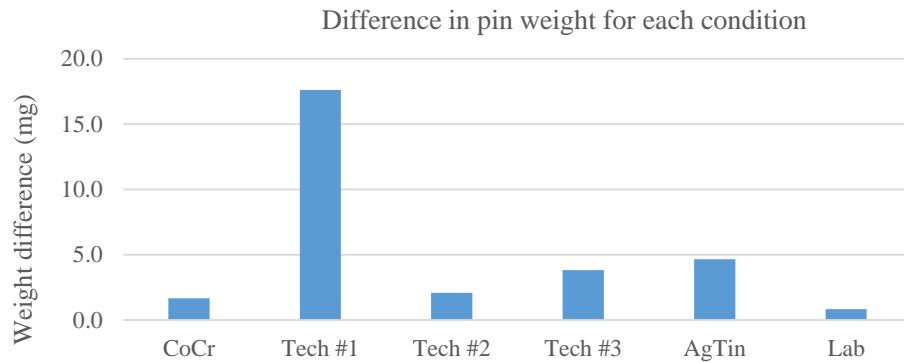


Figure 82: Final difference of weight for each pin for Round 1, CoCr test.

Round 2

When looking at the results obtained in the second round of the test, it is possible to notice that apart from the first 250'000 cycles, in which something particular has surely happened, the same material previously seen with the addition of Tech #3 processed discs have performed well and better than bulk CoCr. In particular, when looking deeper into it, it is possible to observe that CoCr from the Lab is always the material with the best performances, followed in this case by Tech #3 and Tech #2 discs that produce reach almost the same wearing rate and the bulk CoCr for which the values are slightly higher, but the final amount of debris produced is almost two times the overall production by Tech #3 disc. As just seen, also in this case AgTiN and Tech #1 are the worst with the second one that rapidly outweighs our dynamic in both graphs.

However, there are two more elements of interest in this stage. First of all, the pin moving on Tech #2 surface seems to gain weight in the first 250'000 cycles and this is probably linked to a measurement error that has taken into account also some protein still embedded in the pin. Secondly, it is interesting also to notice the abnormal weight loss for Lab disc in the first stage, while this condition rapidly comes back to the level of wearing seen in the previous experiment in the following stages. Also in this test, all the values have been corrected for the soak pin weight variation.

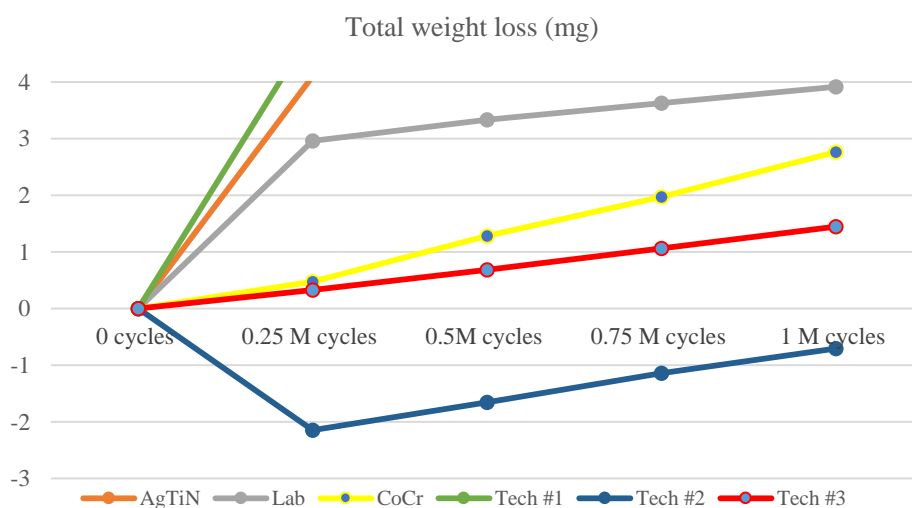


Figure 83: Total weight loss for Round 2 of CoCr test ²².

²² Values of weight loss have been calculated and expressed in mg every 250'000 cycles. Tech #1 is not present because it has gone rapidly out of the dynamics. Complete version of the table is present in the "Appendix" section

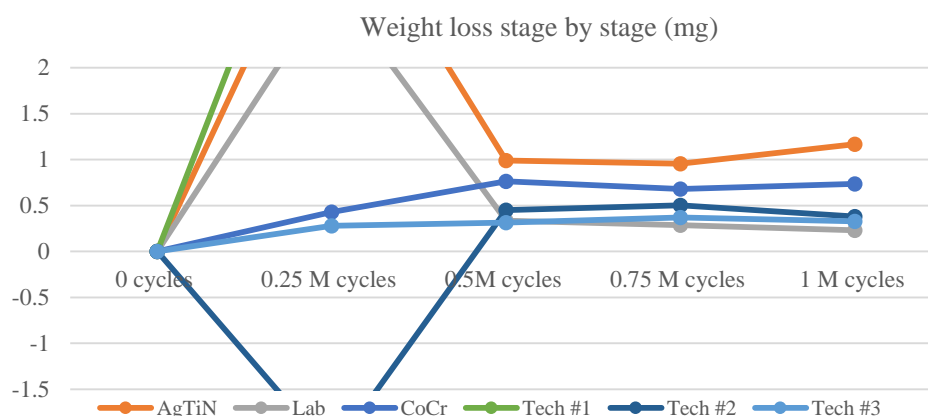


Figure 84: weight loss measured stage by stage for Round 2 of CoCr test ²³.

As just said for the first round of the test, another important thing to notice is the general tendency observed in all the discs to converge in the stage by stage evaluation to a constant value. This means that the wearing rate tends to stabilize and this behavior can be noticed as common to all the conditions except for Tech #1 for which it has continued to increase even if of a smaller value.

To summarize, the two bar charts down reported have been used to collect all the final opinions and thoughts about this round. The overall amount of debris that has been produced in each condition, with the maximum level for Tech #1 disc and the minimum for Tech#2, Tech#3

²³ Values of weight loss have been calculated and expressed in mg every 250'000 cycles. Tech #1 is not present because it has gone rapidly out of the dynamics. Complete version of the table is present in the "Appendix" section

and Lab discs, and the final weight change for each pin are a brief synthesis of the main outcomes of this part of the test.

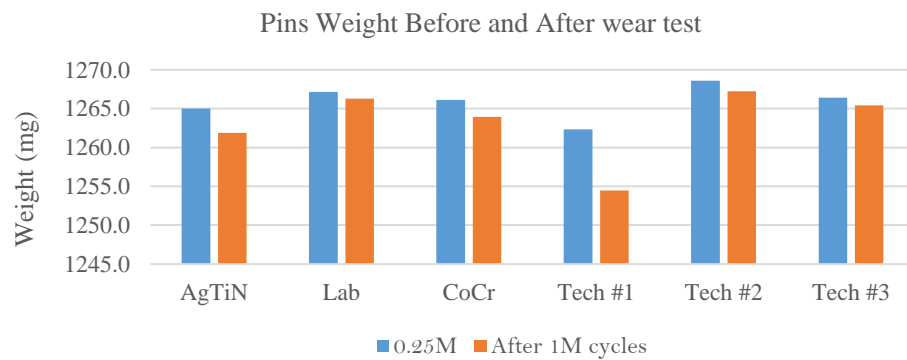


Figure 85: Pin weight at “0.25M” cycles and “After 1M cycles” for Round 2, CoCr test.

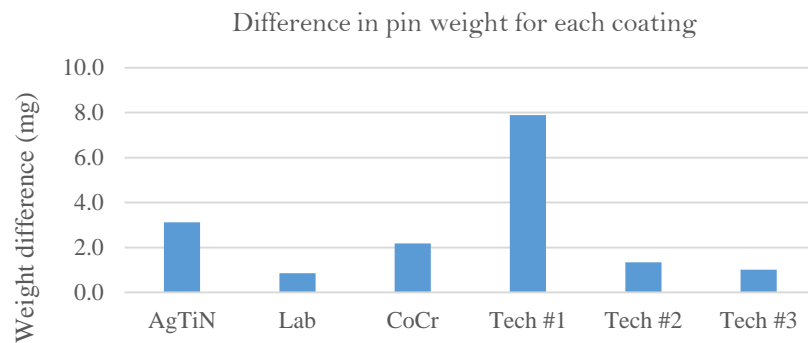


Figure 86: Final difference of weight for each pin for Round 2, CoCr test.

Round 3

To conclude the CoCr test, a third round has been processed following the settings defined into the “Methods” part. Also in this case the results have been pretty similar to the ones of the first two rounds. As just happened for round 1 and 2 also in this case Tech #2 and Tech #3 are the ones that have performed better and Tech #1 and AgTiN have been the worst.

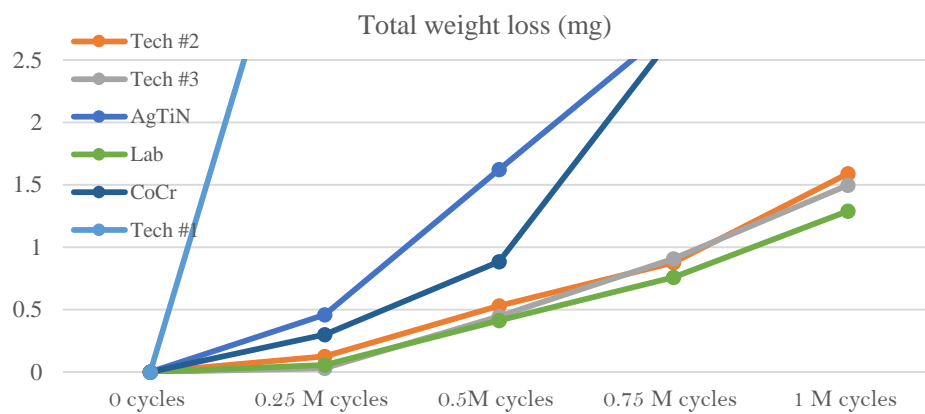


Figure 87: Total weight loss for Round 3 of CoCr test ²⁴.

²⁴ Values of weight loss have been calculated and expressed in mg every 250'000 cycles. Tech #1 is not present because it has gone rapidly out of the dynamics. Complete version of the table is present in the “Appendix” section

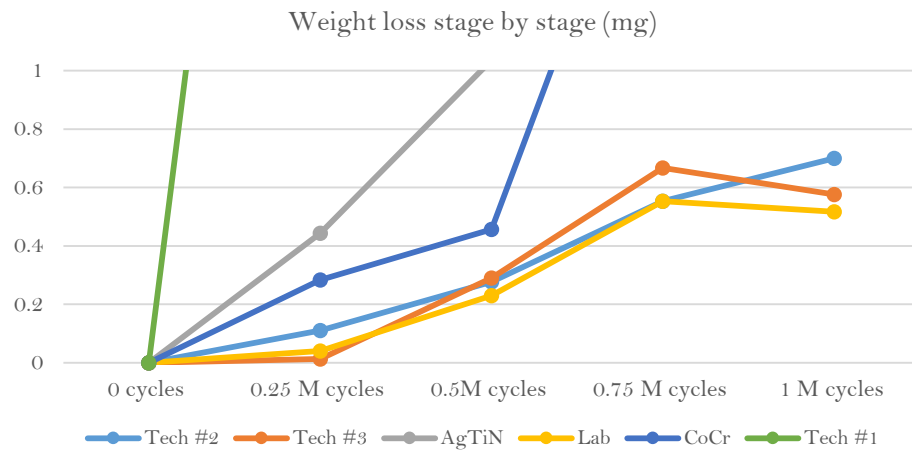


Figure 88: weight loss measured stage by stage for Round 3 of CoCr test ²⁵.

As noticeable, from the graphs that have been reported above only Tech #3 and Lab have stabilized their wearing rate, whereas Tech #2 is almost stable and the other conditions are well over. It is important to remember that all the measurements have been corrected for the weight variation due to the hydration of the sample using the soak pin.

These final two bar charts have been used to summarize all the results, by comparing the conditions before and after the pod test and by showing the overall wear debris production for all the different conditions.

²⁵ Values of weight loss have been calculated and expressed in mg every 250'000 cycles. Tech #1 is not present because it has gone rapidly out of the dynamics. Complete version of the table is present in the "Appendix" section

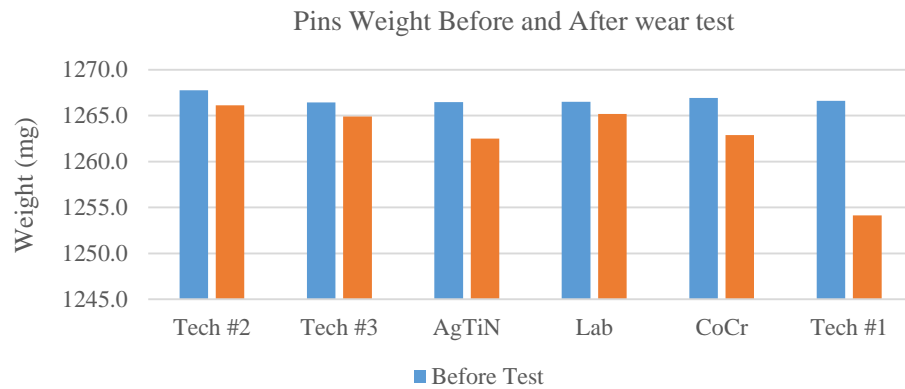


Figure 89: Pin weight “Before test” and “After 1M cycles” for Round 3, CoCr test.

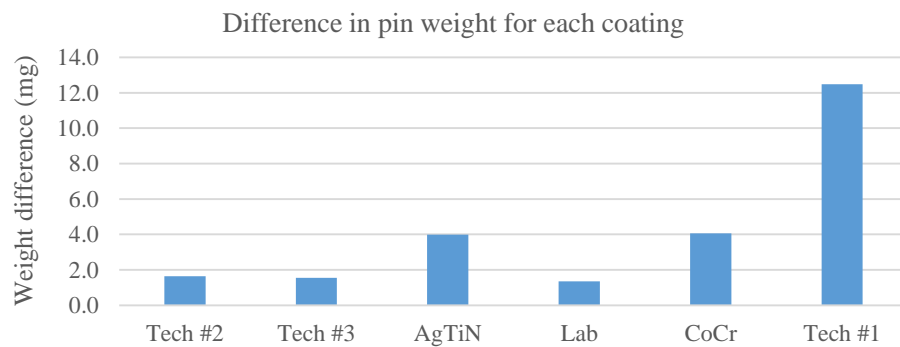


Figure 90: Final difference of weight for each pin for Round 3, CoCr test.

Wear rate calculation (mg/MLNC)

The following step of the analysis has been dedicated to the calculus of the wearing rate for each condition. The wearing rate is described as the overall amount of wear debris, expressed in mg, produced every million cycles.

This value has been calculated for each condition and the final results have been compared.

CoCr disc

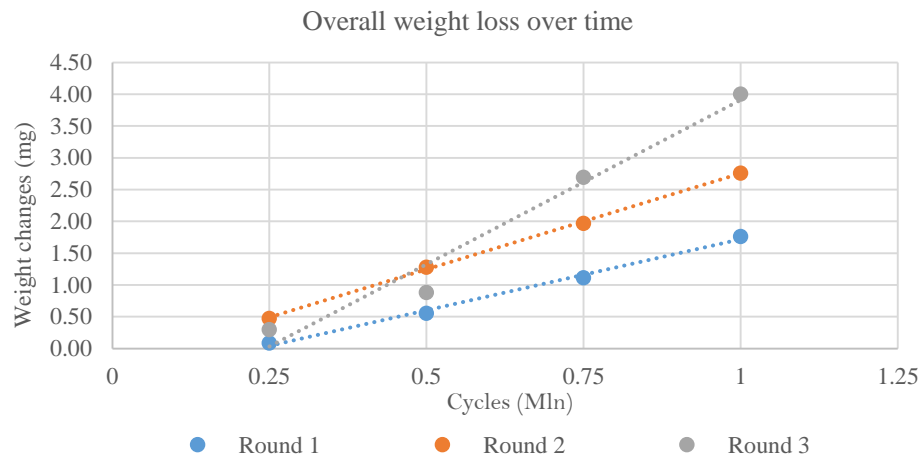



Figure 91: Interpolation curve of the debris production data from POD test on CoCr disc.

By evaluating the average slopes of the wear production curves it has been possible to determine the wearing rate (WR) that has been expressed in mg/M cycles.

For uncoated CoCr disc, this value has been determined as equal to:



$$WR = 3.4747 \text{ mg/Mcycles}$$

Tech #1 disc

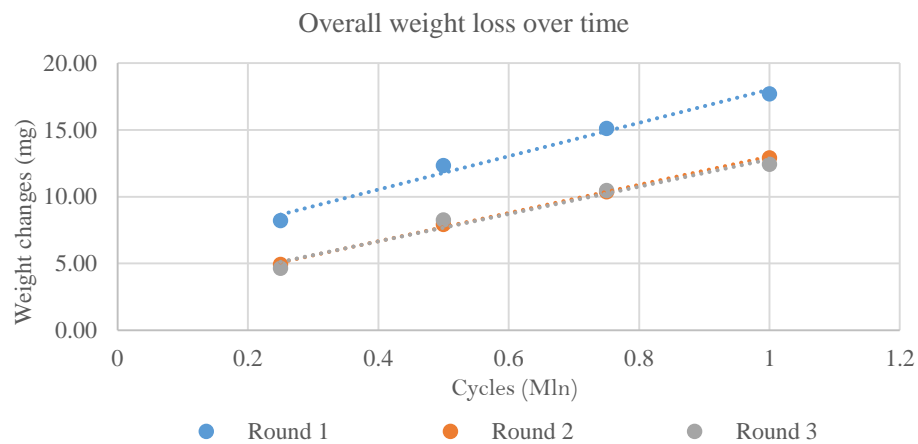



Figure 92: Interpolation curve of the debris production data from POD test on Tech #1 disc.

As just explained, the same procedure followed for the CoCr disc has been adopted also for the other discs.

In particular, for Tech #1 processed discs, it has been obtained a wear rate (WR) equal to:


$$WR = 11.1030mg/Mcycles$$

As noticeable, the value of WR for Tech #1 is bigger than the one for CoCr disc because, as seen from the results of the experiments shown in the previous paragraph the wear behavior itself of this material has been worse than the one of the uncoated CoCr. In particular wear rate has been more than three times greater than the one seen in the previous section.

Tech #2 disc

Repeating what seen for the first two conditions, the same procedure has been followed also for Tech #2 processed disc. In this particular case, it is important to notice as the negative weight loss observed in the first stage of round 2 has no relevance to determine the wearing rate of the material as the slope only of the curves is studied to calculate this parameter.

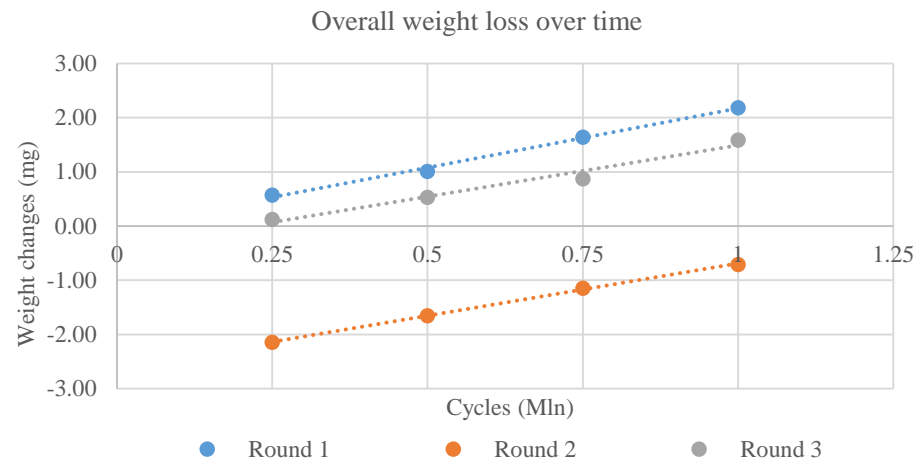


Figure 93: Interpolation curve of the debris production data from POD test on Tech #2 disc.

In particular, for Tech #2 processed discs, it has been obtained a wear rate (WR) equal to:

$$WR = 2.0049 \text{ mg/Mcycles}$$

This means that this coating technique is able to reduce by 40% the overall amount of wear debris produced every million cycles. This data is quite important because it is better than the one shown by the bulk CoCr material. The reduction of the overall amount of wear debris produced

by the interaction between the metallic interface and the polymeric insert may lead to a reduction of the cascade of “negative” events that have been explained in the introduction

Tech #3 disc

Similarly to Tech #2, even for Tech #3 it has been observed a reduction in the value of the wear rate. However, this reduction was smaller than the one observed for Tech #2 and almost equal to 20% of the debris every million cycles. Results are visible in the following graph.

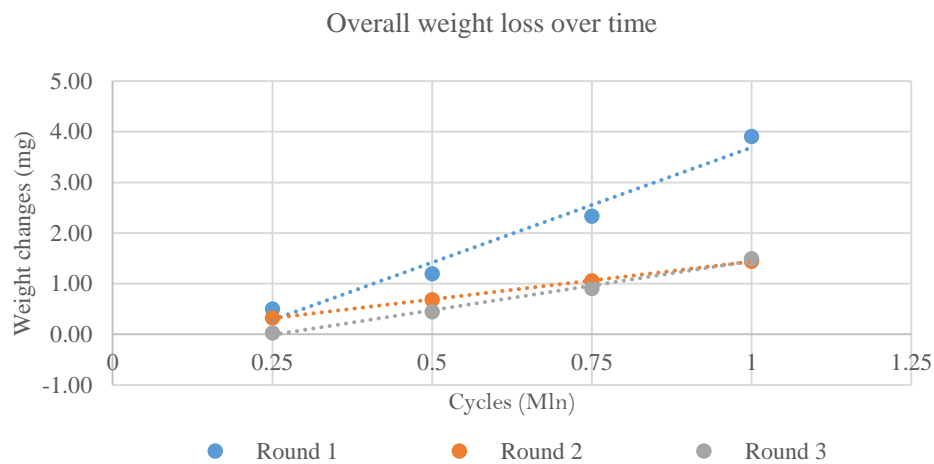
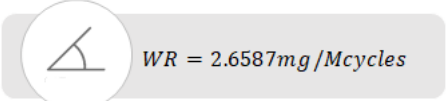


Figure 94: Interpolation curve of the debris production data from POD test on Tech #3 disc.

In this case the material has shown a higher variability of behavior especially if comparing Round 1 slope with the other two. This thing has not happened with Tech #2 material where slopes were almost equal for each round. To conclude, the WR in this case has been equal to:



$$WR = 2.6587 \text{ mg/Mcycles}$$

AgTiN disc

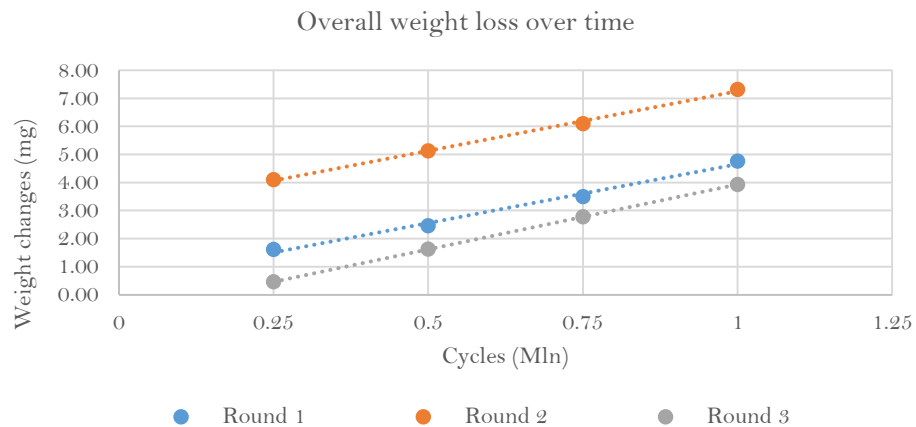
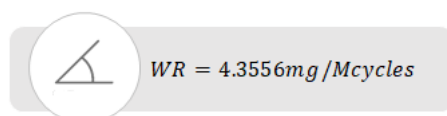


Figure 95: Interpolation curve of the debris production data from POD test on AgTiN disc.

Following the same procedure just seen for the other discs the same process has been followed to determine the wearing rate of the AgTiN disc. The behavior of the material has been almost constant in all the evaluated rounds and this is quite important for the reproducibility of the evaluations.

The calculated wearing rate (WR) was bigger than the bulk CoCr and equal to:



Lab disc

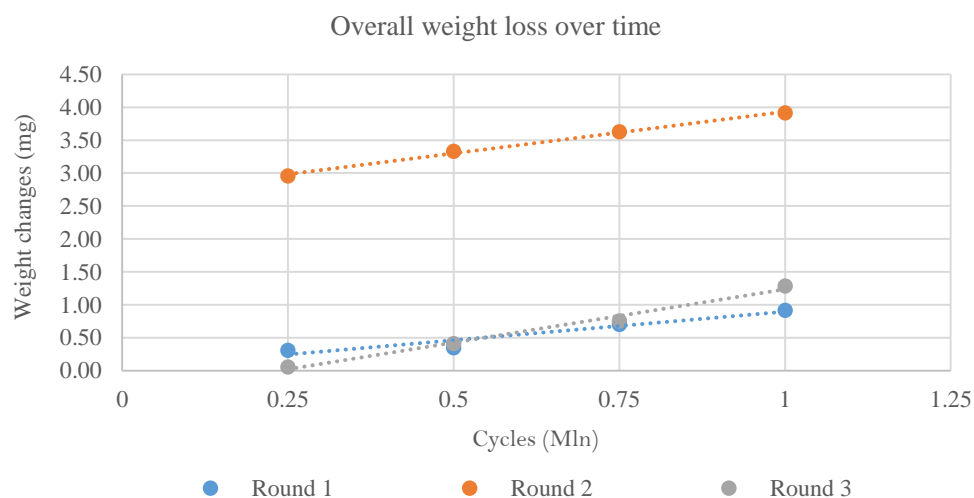
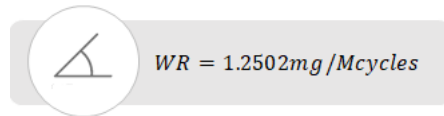


Figure 96: Interpolation curve of the debris production data from POD test on Lab disc.

To conclude the analysis for this first test, the Lab disc has been assessed, too. In this case, the results suggest that this disc is the one with the best performances.

The results have been maybe influenced by the polishing technique, the alloy characteristics and maybe also by the different supplier companies chosen for the material. This is the final result obtained for the Lab disc:



Roughness-Wearing rate dependency

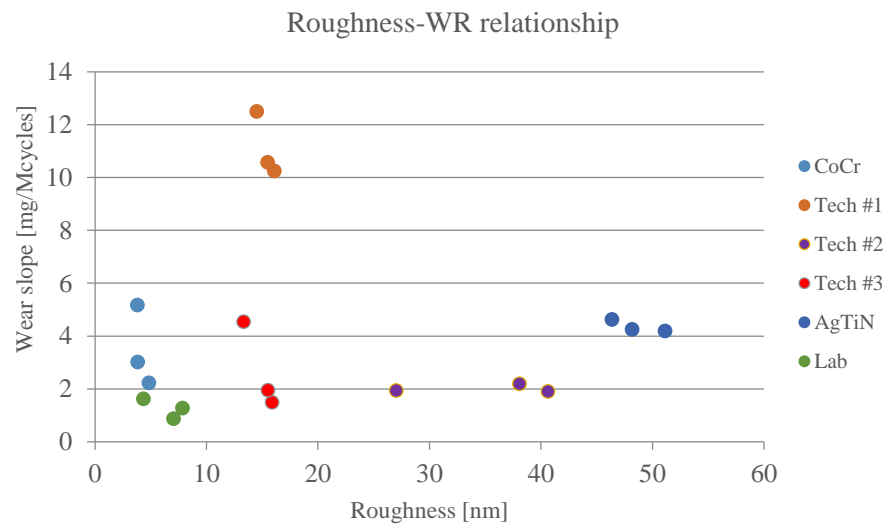


Figure 97: Roughness-Wearing rate relationship graph.

To conclude the analysis, it has also been performed a comparison between the wear rate of the different materials and their roughness. This evaluation has been processed in order to verify the independence between these two values and, as noticeable, no major correspondence between them has been found: despite its lower roughness, Tech #1 disc has shown the worst result in term of wear behavior and even between the two CoCr discs, it has performed better the less rough of the two, the CoCr from the Lab.

Ti6Al4V Test

Following the same procedure explained for the CoCr test, the same steps have been repeated also for the Ti6Al4V test, where the performances of coated/uncoated Ti alloy discs have been tested. The experiment has been performed trying to simulate the environmental, mechanical and biological experienced by the material itself when performing in vivo.

In this section, the main results obtained for each round will be presented followed by a final summary in which the main wearing rates for all the material will be calculated. In order to simplify the understanding of data, raw ones will be presented only in the appendix.

To conclude the analysis, the dependency between the roughness of the material and the wearing rate has been calculated, too, and the results have been presented after the wearing rate calculation part.

Round 1

Being the first test to be performed, Round 1 has revealed some of the behaviors that have characterized the samples for all the tests.

Hereunder, it is possible to see both the "Total weight loss" and the "Weight loss stage by stage" to calculate both the overall production of wear debris by the interaction between the pin and the specific disc, but also how this production change during the test. In particular, the overall wear production has been calculated for the total weight loss as the difference between the initial weight of the pin and the actual one, whereas the value based on stage has been calculated as the value of the $(i-1)^{\text{th}}$ stage and the i^{th} one.

All the values have been corrected for the soak pin variation that accounts for the weight changes due to hydration of the polymeric pin in the aqueous environment in order to consider only the weight variation due to the wearing process.

It is possible to notice that the best results have been obtained with Ti6Al4V bulk disc and Lab one, followed by Tech #2 and Tech #3. In particular, for Lab disc and Tech #2 it has been noticed a tendency to decrease for the overall amount of debris produced by the interaction between the pin and the disc as proceeding toward 1M cycles and in particular between 0.75M and 1M cycles.

This behavior is common also to AgTiN and similar to the one of Ti6Al4V that has reached a stable behavior for the last stage of the experiment. Tech #1 has been confirmed to be the worst type of coating and it quickly runs out of our evaluation scale.

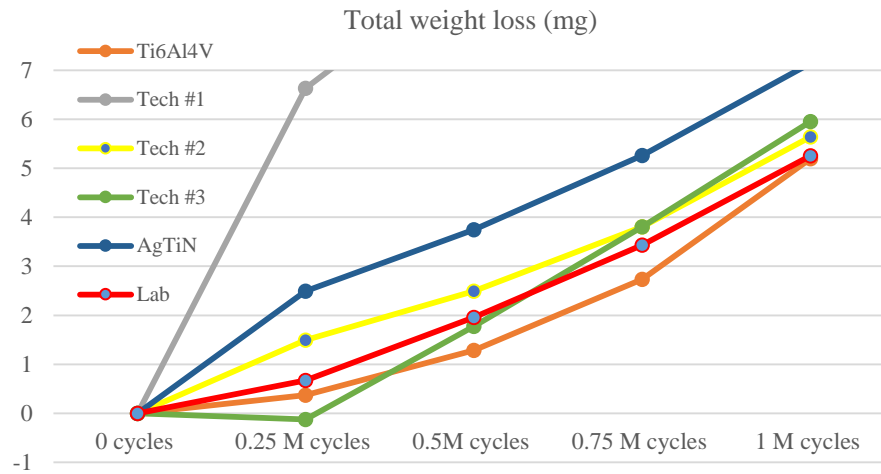


Figure 98: Total weight loss for Round 1 of Ti6Al4V test.²⁶

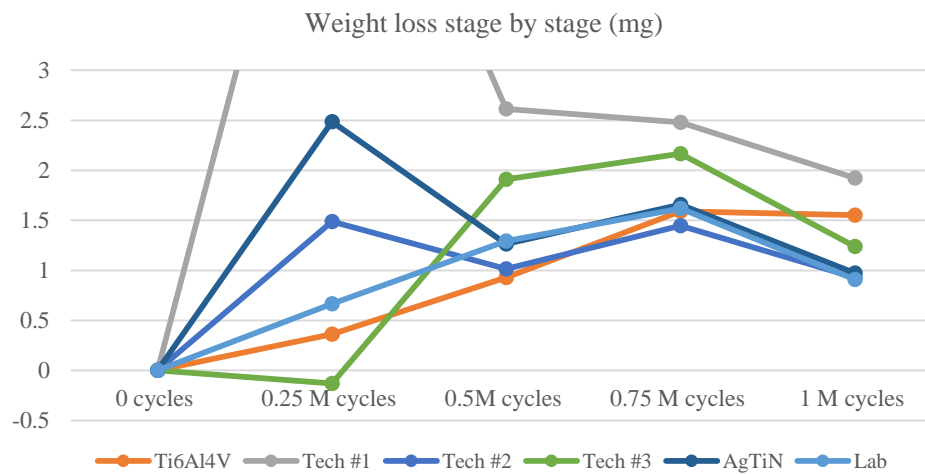


Figure 99: weight loss measured week by week for Round 1 of Ti6Al4V test²⁶.

²⁶ Values of weight loss have been calculated and expressed in mg every 250'000 cycles. Tech #1 is not present because it has gone rapidly out of the dynamics. Complete version of the table is present in the "Appendix" section.

In order to confirm and sum up all the data coming from this experiment a couple of bar charts reporting the weight difference between the initial point of the experiment and the final one and the overall amount of wear debris that has been produced for each condition has been realized.

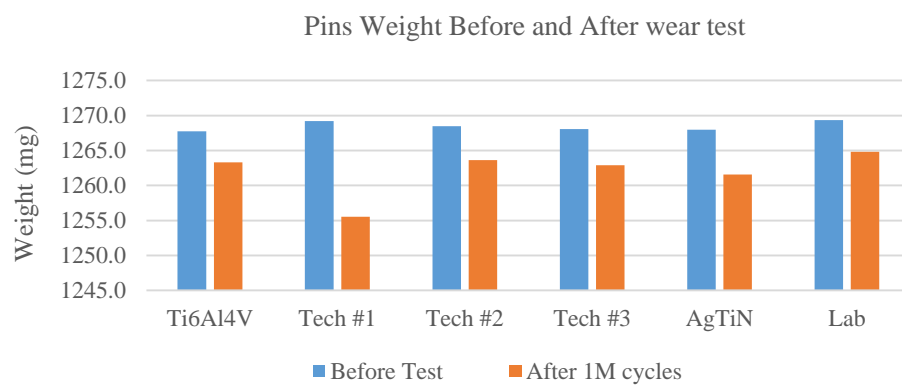


Figure 100: Pin weight “Before test” and “After 1M cycles” for Round 1, Ti6Al4V test.

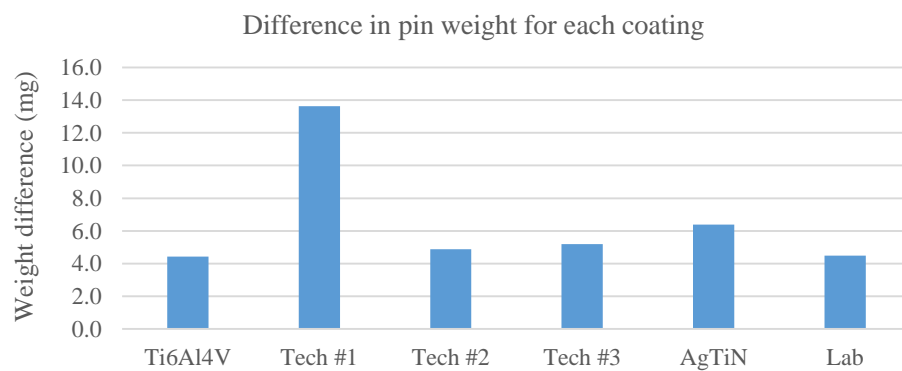


Figure 101: Final difference of weight for each pin for Round 1, Ti6Al4V test.

Round 2

If focusing on the results that have been obtained in the second round, it is possible to observe that also in this occasion, Ti6Al4V has performed, as overall production of wear debris, better than the other coating discs. In particular, Tech #2 has produced a slightly bigger amount of wear and Tech #3 has had results only a bit worse than the one of the process number two.

As just seen for CoCr test and the first round of Ti6Al4V test, AgTiN and tech #3 disc has been the worst in term of debris production by the interaction with the polymeric pin above all the tried coatings.

However, when looking at the stage by stage change in the pin weight, it is possible to observe that for mainly Tech #2 processed disc, but also for Tech #3, the obtained results showed a possible better performance of these materials on a longer run. In fact, at 1M cycles their weight loss has just been stabilized, whereas the one of bulk Ti6Al4V is still growing. This fact is important because it underlines the importance of not focusing only on absolute value, but looking also at their evolution when trying to build up a predictive model.

As just highlighted for all the previous experiments, also in this case all the measurements have been corrected for the soak pin variation that accounts for the weight changes due to hydration of the polymeric pin in the aqueous environment in order to consider only the weight variation due to the wearing process.

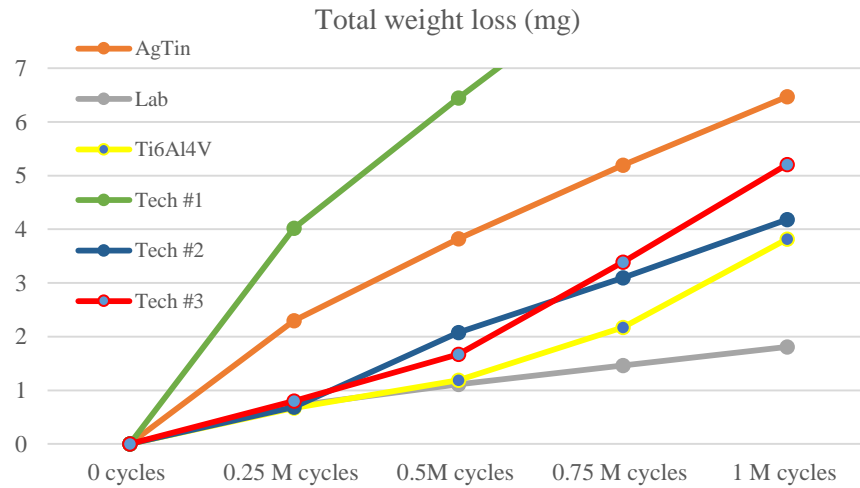


Figure 102: Total weight loss for Round 2 of Ti6Al4V test ²⁷.

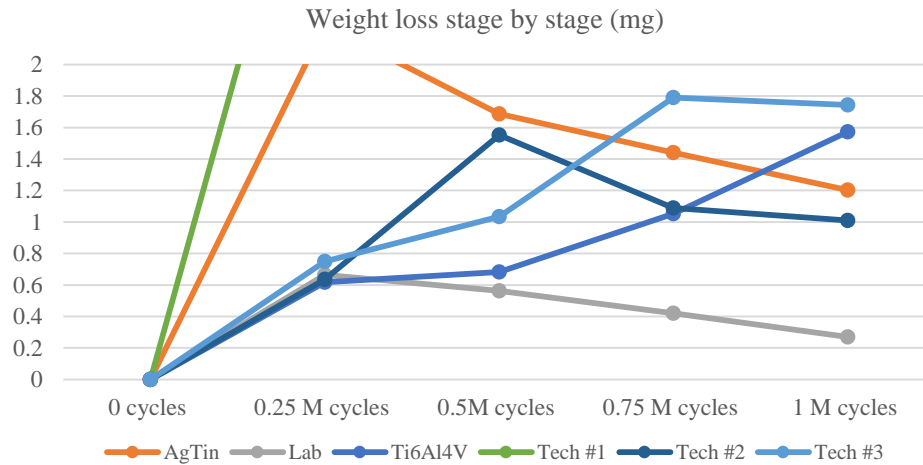


Figure 103: weight loss measured stage by stage for Round 2 of Ti6Al4V test ²⁷.

²⁷ Values of weight loss have been calculated and expressed in mg every 250'000 cycles. Tech #1 is not present because it has gone rapidly out of the dynamics. Complete version of the table is present in the "Appendix" section

As just seen for the first round of the test, another important thing to notice is the general tendency observed in all the discs to converge in the stage by stage evaluation to a constant value. This means that the wearing rate tends to stabilize and this behavior can be noticed as common to all the conditions except for Tech #1 for which it has continued to increase even if of a smaller value.

To summarize, the two bar charts down reported have been used to collect all the final opinions and thoughts about this round. The overall amount of debris that has been produced in each condition, with the maximum level for Tech #1 disc and the minimum for Ti6Al4V, Tech #2 and Tech #3, and the final weight change for each pin are a brief synthesis of the main outcomes of this part of the test.

Lab disc is made of CoCr and it has been used only to verify the reproducibility of the results of the test and its results may not be compared with the one obtained for the Ti6Al4V discs that are made of a different material.

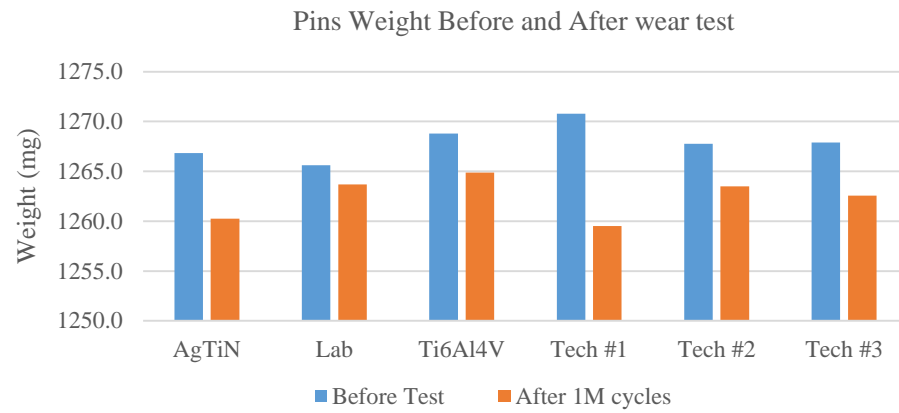


Figure 104: Pin weight at “Before test” cycles and “After 1M cycles” for Round 2, Ti6Al4V test.

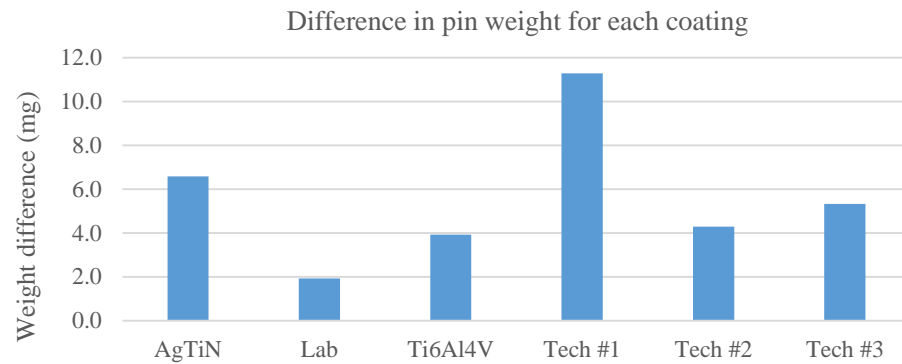


Figure 105: Final difference of weight for each pin for Round 2, Ti6Al4V test.

Round 3

To conclude the Ti alloy test, a final evaluation has been done performing a third round in the same conditions.

As shown above, in this case Tech #2 and especially Tech #3 has performed better than bulk Ti6Al4V disc. In particular, when looking at the stage by stage table, it is interesting to notice that the tendency to stabilize the wear rate common to AgTiN, Tech #2 and also Lab disc has not been followed by Ti6Al4V disc for which the production of wear debris has continuously increased nor for Tech #3 for which the growth has been smaller than the uncoated disc, but still present.

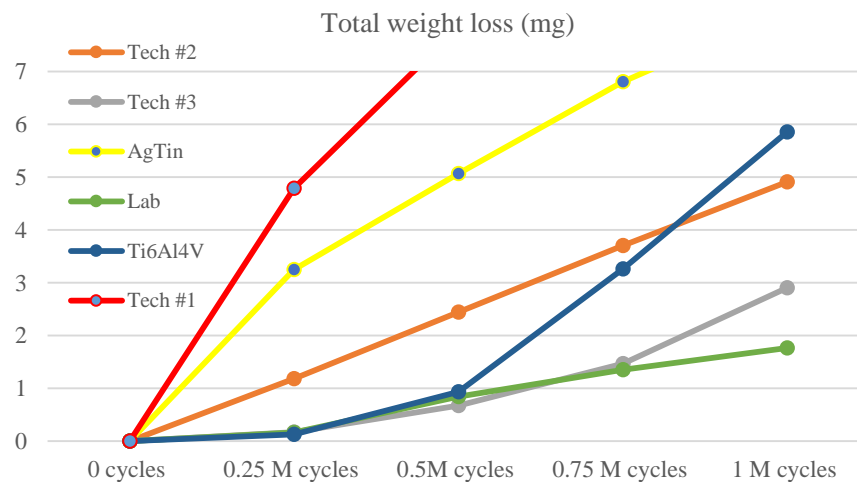


Figure 106: Total weight loss for Round 3 of Ti6Al4V test ²⁸.

²⁸ Values of weight loss have been calculated and expressed in mg every 250'000 cycles. Tech #1 is not present because it has gone rapidly out of the dynamics. Complete version of the table is present in the "Appendix" section

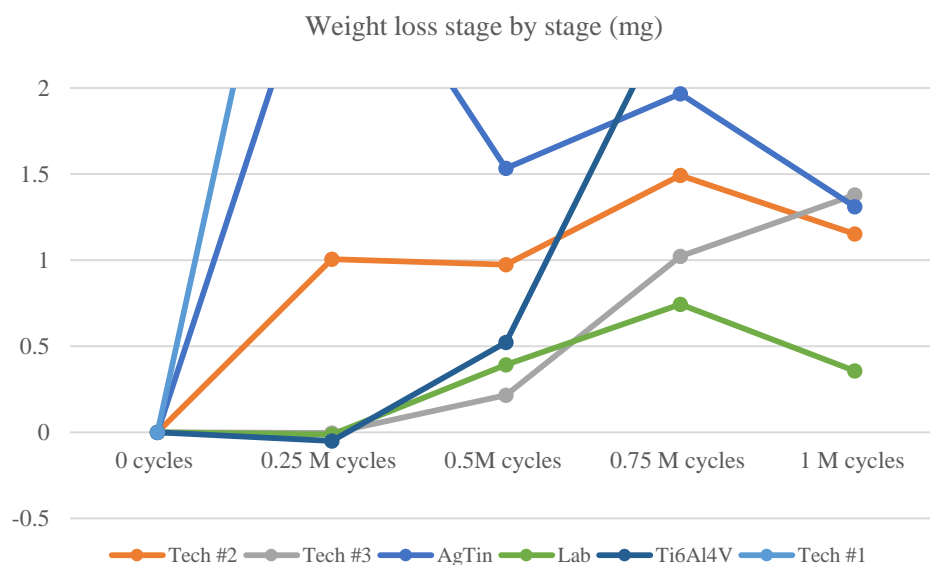


Figure 107: weight loss measured stage by stage for Round 3 of Ti6Al4V test ²⁹.

This behavior of Ti6Al4V has been common to all the performed experiments and it has to be taken into account.

The final two bar chart, that has been introduced for all the performed experiments in order to synthesize the data, are shown down here. As noticeable, the performance of Tech #2 and Tech #3 has been better than the one of the uncoated Ti6Al4V disc. Tech #1 has been revealed the worst condition also for this round.

²⁹ Values of weight loss have been calculated and expressed in mg every 250'000 cycles. Tech #1 is not present because it has gone rapidly out of the dynamics. Complete version of the table is present in the "Appendix" section

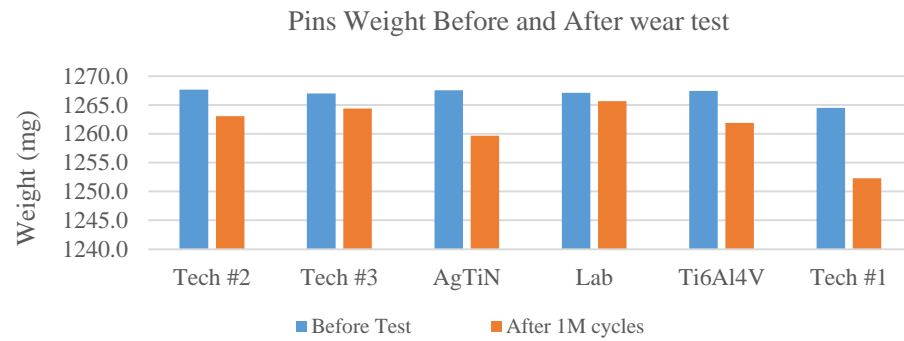


Figure 108: Pin weight “Before test” and “After 1M cycles” for Round 3, Ti6Al4V test.

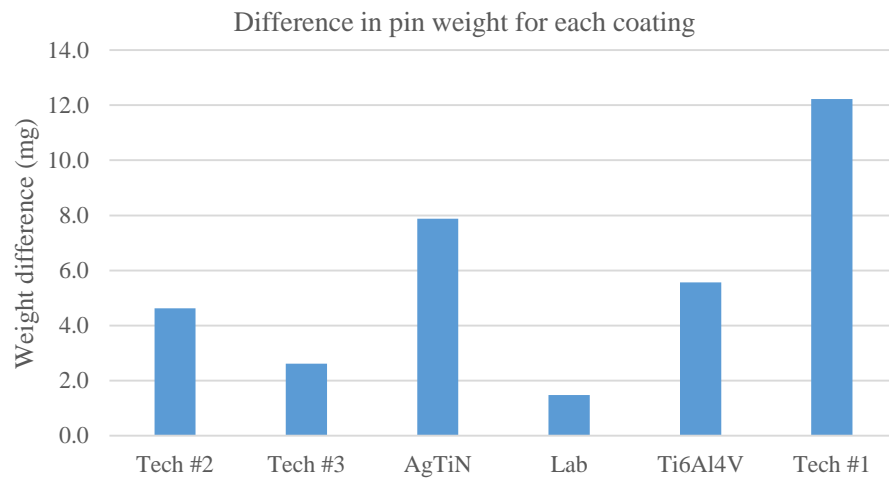


Figure 109: Final difference of weight for each pin for Round 3, Ti6Al4V test.

Wearing rate (mg/MLNC)

The following step of the analysis has been dedicated to the calculus of the wearing rate for each condition. The wearing rate is described as the overall amount of wear debris, expressed in mg, produced every million cycles.

This value has been calculated for each condition and the final results have been compared.

Ti6Al4V disc

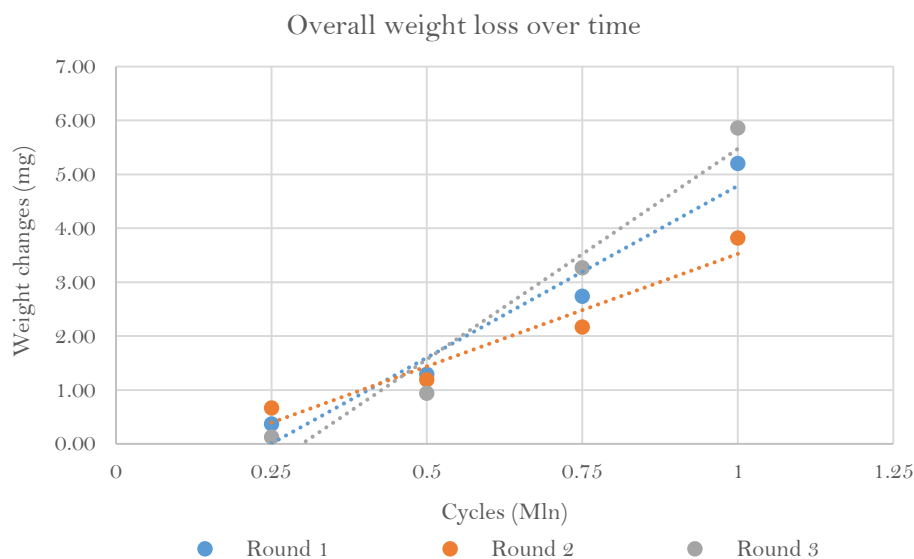
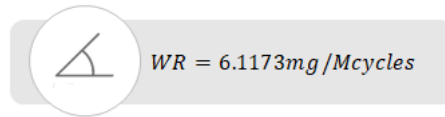


Figure 110: Interpolation curve of the debris production data from POD test on Ti6Al4V disc.

By evaluating the average slopes of the wear production curves it has been possible to determine the wearing rate (WR) that has been expressed in mg/M cycles.

For uncoated Ti6Al4V disc, this value has been determined as equal to:



This value results bigger than the one from uncoated CoCr as the Ti alloy discs had a surface roughness bigger than the one of uncoated CoCr ones. The WR has been about 1.7 times the one of uncoated CoCr from the supplier.

Tech #1 disc

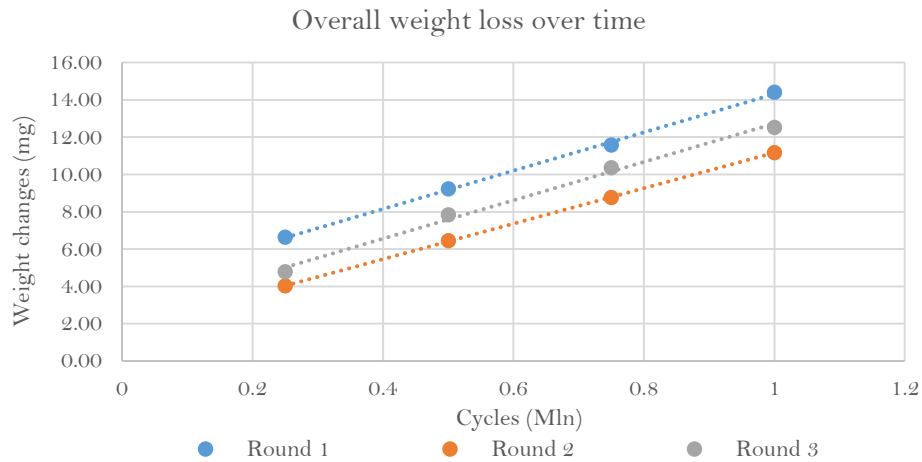



Figure 111: Interpolation curve of the debris production data from POD test on Tech #1 disc.

As just explained, the same procedure followed for all the Ti6Al4V discs to collect the WR values for all the conditions. In particular, for Tech #1 processed discs, it has been obtained a wear rate (WR) equal to:

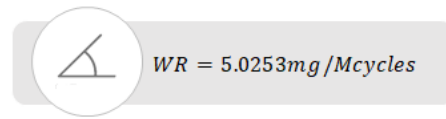


$$WR = 10.0147 \text{ mg/Mcycles}$$

As noticeable, the value of WR for Tech #1 is still bigger than the one for Ti6Al4V disc because, as seen from the results of the experiments shown in the previous paragraph the wear behavior itself of this material has been worse than the one of the uncoated Ti6Al4V. However, this wearing rate is smaller than the one observed in the CoCr test and even when compared with bulk Ti6Al4V, it is "only" 1.6 times greater than the bulk material. In any case, Tech #1 processed discs have been defined as the worst also for this test.

Tech #2 disc

Repeating what seen for the first two conditions, the same procedure has been followed also for Tech #2 processed disc. As noticeable, the behavior of the material has been almost the same during the entire length of the experiment and this is proven by the constant slope of the interpolation curves. When calculating the value of the wearing rate for Tech #2 processed discs, it has been obtained:



This value is less than the bulk Ti6Al4V disc meaning that this coating technique is able to reduce by about 20% the amount of wear debris produced every million cycles. As just said in the opening part of this work this fact has strong and durable consequences on the definition of the characteristics of the interaction between the prosthesis and the human body.

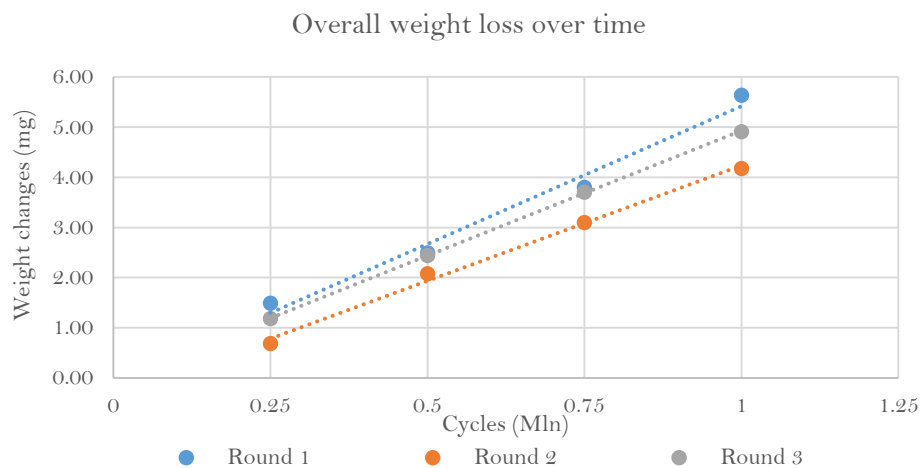


Figure 112: Interpolation curve of the debris production data from POD test on Tech #2 disc.

Tech #3 disc

Similarly to Tech #2, even for Tech #3 it has been obtained a good result in terms of wear reduction even if smaller than the one observed for Tech #2 disc. In fact, in this case, the reduction of wear debris production has been equal "only" to about 5% every million cycles. All the results have been collected in the following graph.

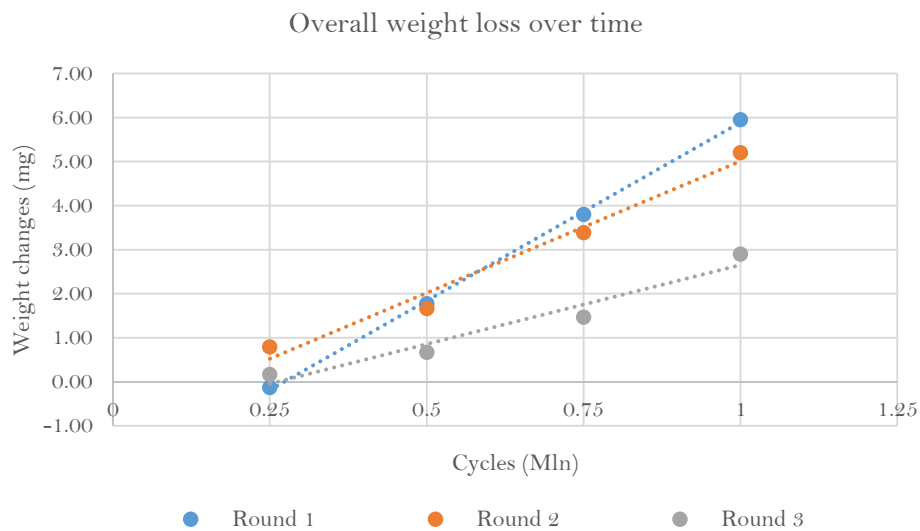



Figure 113: Interpolation curve of the debris production data from POD test on Tech #3 disc.

In this case the material has shown a higher variability of behavior especially if comparing Round 1 slope with the other two. This thing has not happened with Tech #2 material where slopes were almost equal for each round. To conclude, the WR in this case has been equal to:



$$WR = 5.8893 \text{ mg/Mcycles}$$

AgTiN disc

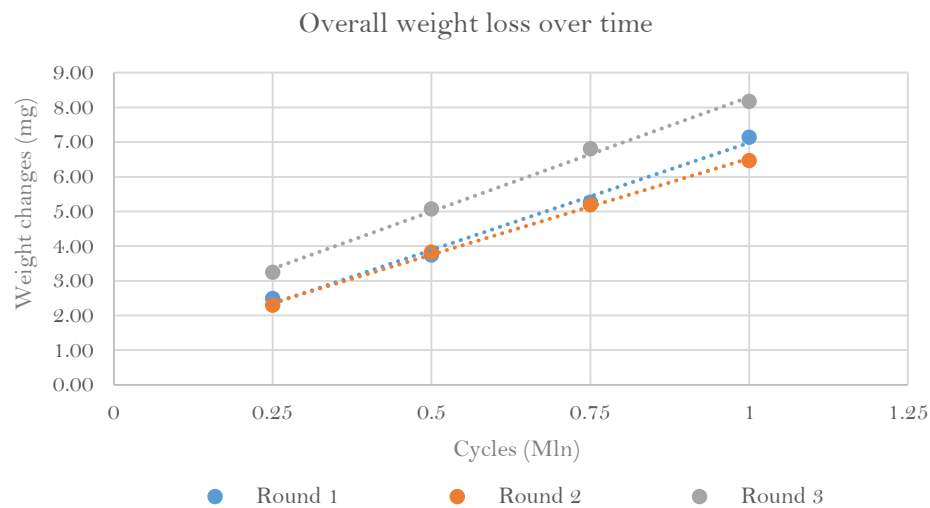



Figure 114: Interpolation curve of the debris production data from POD test on AgTiN disc.

Following the same procedure just seen for the other discs the same steps have been followed to determine the WR of the AgTiN disc that has resulted almost equal to the one of Ti6Al4V disc. In addition, the behavior of the material has been almost constant in all the evaluated rounds and this is quite important for the reproducibility of the evaluations.

The calculated wearing rate (WR) was almost the same as bulk Ti6Al4V and equal to:



$$WR = 6.1124 \text{ mg/Mcycles}$$

Roughness-Wearing rate dependency

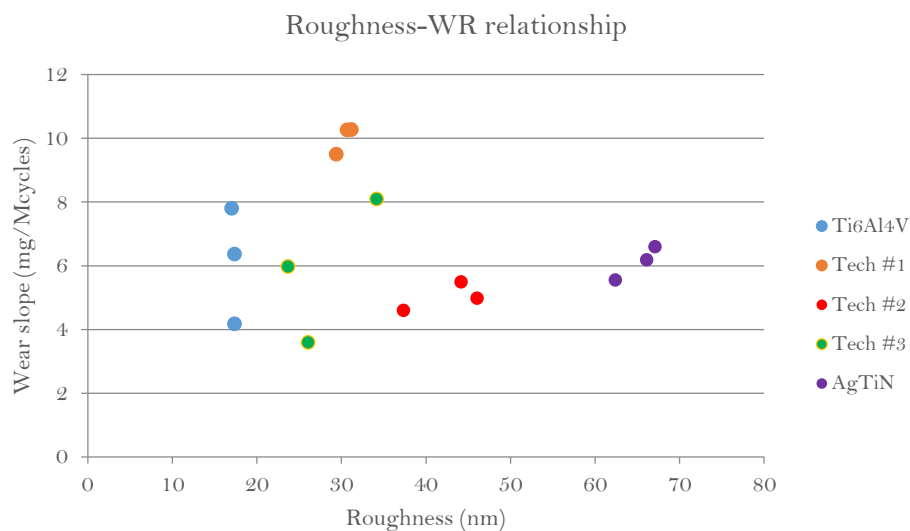


Figure 115: Roughness-wearing rate dependency.

The last step that has been performed to conclude the analysis has been the evaluation of the existence of any kind of dependency between the roughness of the discs and their WR. In order to do that, the results obtained for these two fields have been plotted together. The result is shown above.

As noticeable, for Ti6Al4V a wide variety of different behaviors have been shown for almost the same value of roughness. Tech #2 which is the case with the best performances has shown a surface roughness more than two times greater than the one of the uncoated disc. Moreover, as just seen for the CoCr test Tech #3 has shown a good wear resistance, but coupled with great variability in the behavior that led to great differences within the values of WR at a constant value for the surface roughness between 20 and 30nm.

5.3 Post-POD test pins characterization

5.3.1 Evaluation of pins surface

As done for all the discs after the pin on disc (POD) test, the surface of the pins has been qualitatively studied using the Zeiss 2000-C stereomicroscope. This process has been useful to highlight changes in the surface characteristics of the polymeric material in a cylinder with respect to the reference shape.

In order to evaluate this difference, images coming from all the different pins after the experiment will be reported for each test with also the image collected from the soak pin, used as a reference.

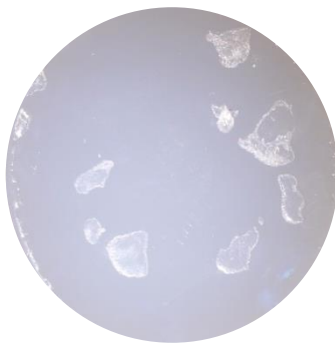
*CoCr test**CoCr disc*

Figure 116: Picture of the contact surface of the pin OE1.

For pin OE1, interacting with CoCr disc, some localized areas of damage have been observed on the surface of contact. The Zygo test has been performed to assess the characteristics of these areas of damage.

Tech #1 disc

Focusing on the OE2 pin, it has been noticed the presence of diffuse damage all around the surface with a concentrated area of damage on the center of the pin. Sharp scratches have been reported, too.

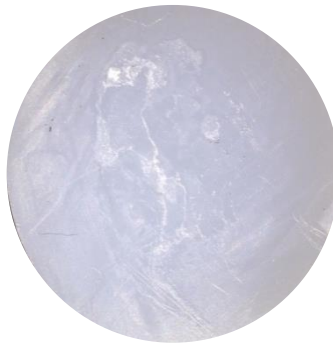


Figure 117: Picture of the contact surface of the pin OE2.

Tech #2 disc

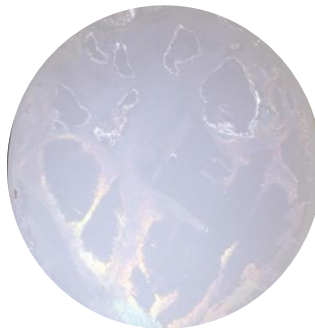


Figure 118: Picture of the contact surface of the pin OE3.

Pin OE3 has interacted with the disc coated with tech #2. As shown, the images captured with the stereomicroscope have revealed the presence of an almost flat surface on the pin with some areas of localized damage. Also in this case, Zygo analysis has been performed to characterize the damage.

Tech #3 disc

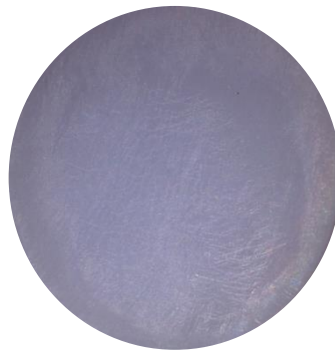


Figure 119: Picture of the contact surface of the pin OE4.

OE4 pin, interacting with tech #3 processed disc, has been characterized by the presence of a lot of sharp scratches all over the surface that generates a micro-roughness on it.

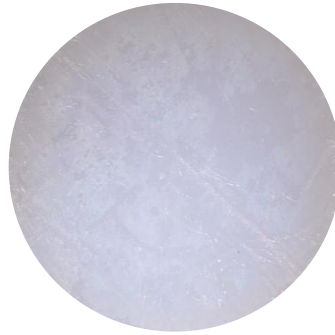
AgTiN disc

Figure 120: Picture of the contact surface of the pin OE5.

For pin OE5, interacting with AgTiN disc, an almost flat surface has been observed on the pin. Only minor damages with some linear scratches are present.

Lab disc

As seen for OE1, also for OE7 interacting with the CoCr disc from the lab the same behavior has been registered. In particular, it has been reported the presence of localized areas of damage on the surface of the pin. Also in this case, Zygo analysis has been used to characterize the surface damages.

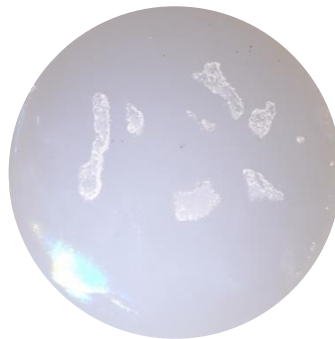


Figure 121: Picture of the contact surface of the pin OE6.

Ti6Al4V test

Ti6Al4V disc



Figure 122: Picture of the contact surface of the pin OE22.

Focusing on the pin OE22 that has been chosen as representative of all the pins interacting with bulk Ti6Al4V disc, no major changes have been observed on its surface that appears flat without any kind of scratch or big damaged area.

Tech #1 disc

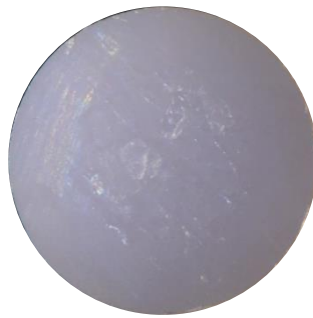


Figure 123: Picture of the contact surface of the pin OE23.

For the pin interacting with tech #1 treated disc, the presence of some localized areas of damage has been determined. In addition, some sharp scratches have been noticed on the surface of the pin itself that is the worst in terms of damage in the entire set.

As noticeable from the picture, the major damages are concentrated in the central area of the pin, whereas the scratches are localized at the boundaries.

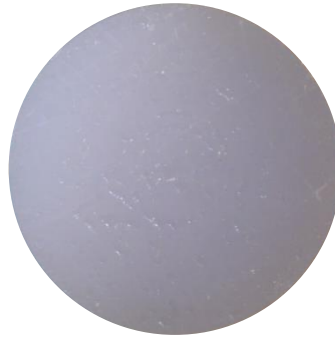
Tech #2 disc

Figure 124: Picture of the contact surface of the pin OE24.

If we focus on the pin OE24, chosen as representative of the pins that have interacted with tech #2 processed discs, it has been noticed the presence of small, localized areas of damage. These zones are arranged following the original pattern in a circular way. The Zygo analysis has been used to verify this qualitative observation and to quantify the main characteristics of this area of damage. Apart from the localized damage, the surface may be considered as flat.

Tech #3 disc

As far as the OE25 pin concern, it has been observed the presence of some localized scratches on the surface despite a general flat characteristic of the interface. Only some localized areas of damage have been determined but the changes in height of these zones are light.

Zygo analysis has been used to quantitatively describe the surface of the pin also in this case.



Figure 125: Picture of the contact surface of the pin OE25.

AgTiN disc

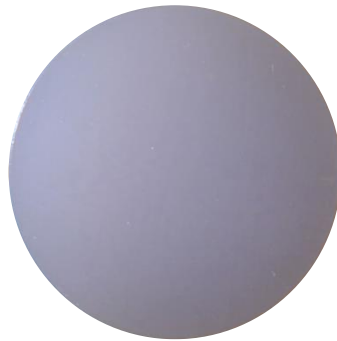


Figure 126: Picture of the contact surface of the pin OE26.

Pin number OE26 has interacted with AgTiN coated disc during the Ti6Al4V test. As shown in the image minor areas of damage have been detected and the surface appears as almost flat. However, the soak pin pattern is no more visible.

Soak pin

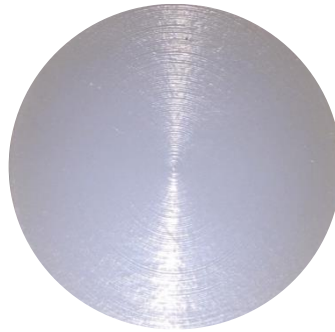


Figure 127: Picture of the contact surface of the pin OE6, used as reference.

The soak pin has been used as a reference in order to determine eventual differences in the characteristics of the pin's surface. In fact, soak pin has not been used during the test, but only as a reference to evaluate weight changes due to hydration of the polymeric samples.

As noticeable, the surface of the pin is patterned with a series of concentric circles.

5.3.2 Evaluation of pins surface using Zygo

All the quantitative surface evaluations for the after test characterization of the pins have been realized using the Zygo® Newview 6300.

These analyses have been performed to quantitatively characterize the surface properties of the pins after the test. In particular, the main focus of the work has been the quantitative description of the major changes on the surface of the interaction of the pins to assess if they were points of accumulation of material or if part of the material has been lost in that points

As seen for the stereomicroscope study, we will report and comment on the obtained results, dividing them depending on the test type.

CoCr test

CoCr disc

As noticed in the previous part, for the pin that interacts with bulk CoCr disc we had some localized areas of damage.

The analysis performed with Zygo Newview 6300 has revealed the main characteristics of these zones that are representative of an area of accumulation of material. In the surface map, it is represented the surface profile and , as visible, the areas of damage are up to 78.41 μm high.

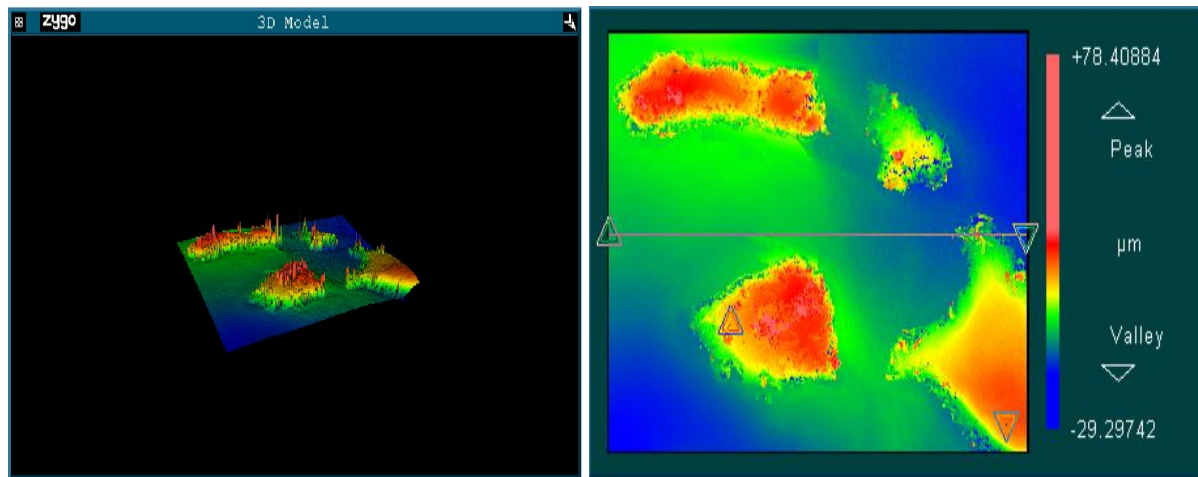


Figure 128: Picture that grouped the 3D model and the Surface map of the contact surface of the pin OE10.

Tech #1 disc

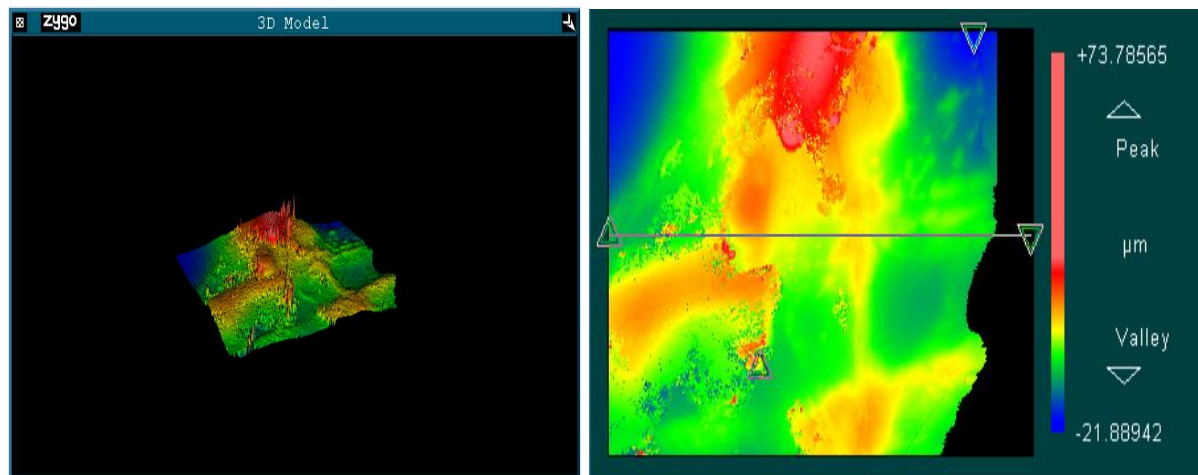


Figure 129: Picture that grouped the 3D model and the Surface map of the contact surface of the pin OE11.

Also for the pin that interacts with tech #1 processed discs, in this case OE11, the main zones of damage have been areas of accumulation of polymeric material. However, the surface appears to be not uniform and the damages seem to be randomly distributed.

Tech #2 disc

When focusing on the pin number OE12 that has interacted with Tech #2 coated disc, it is possible to notice the presence of a distributed micro-roughness on the surface of interaction between the two materials. In particular, this roughness is present at the micro-scale with a variability of the surface between $+7\text{ }\mu\text{m}$ and $-5\text{ }\mu\text{m}$.

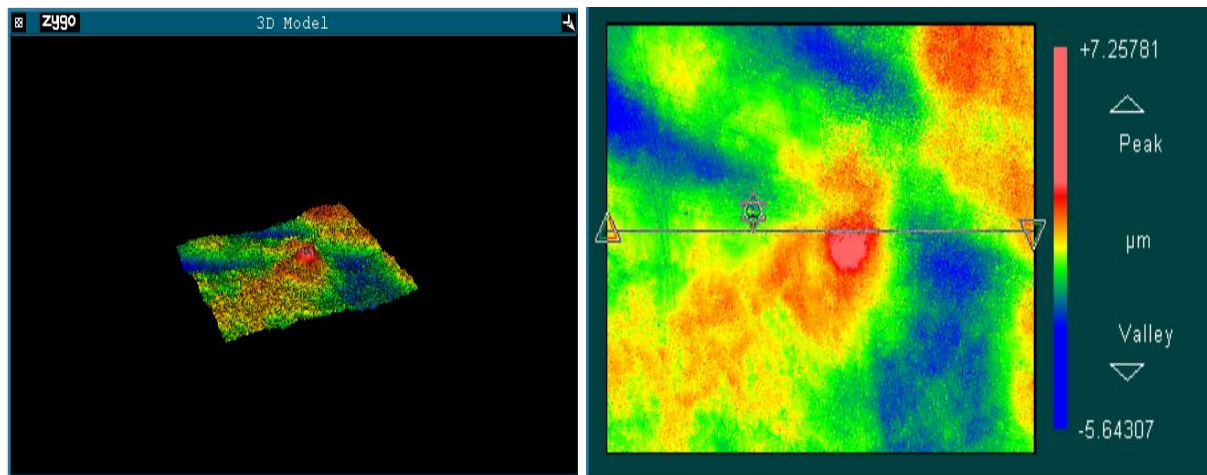


Figure 130: Picture that grouped the 3D model and the Surface map of the contact surface of the pin OE12.

Tech #3 disc

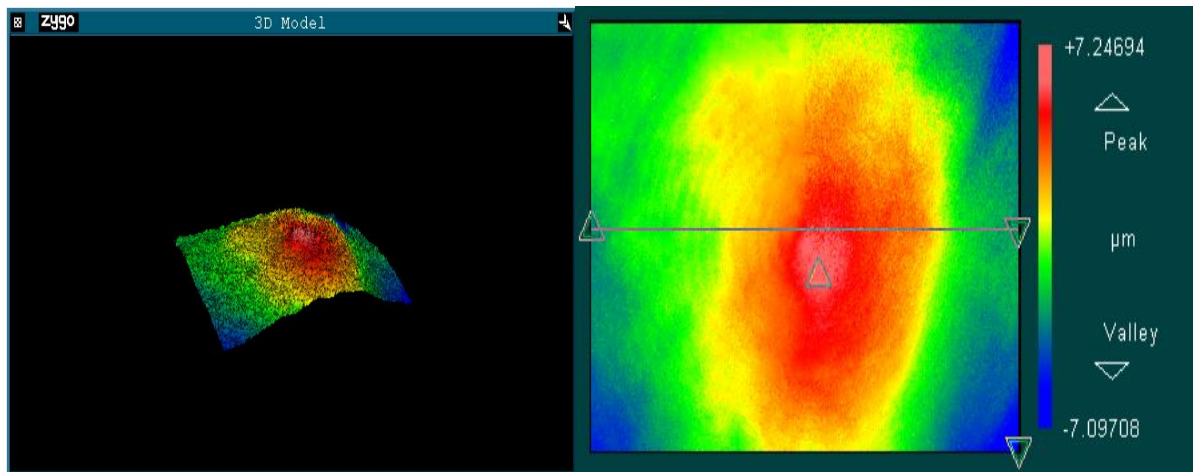


Figure 131, Picture that grouped the 3D model and the Surface map of the contact surface of the pin OE13.

Pin number OE13 has interacted with tech #3 TiN coated disc. As noticeable from the surface map, the pin has experienced only relatively minor changes and the original shape made of concentric circles. However, it is possible to notice the presence of a micro-roughness, similar to the one of the previous pin, with a variability of the surface profile between $+7\text{ }\mu\text{m}$ and $-7\text{ }\mu\text{m}$.

To conclude, it is also possible to see that the changes are quite uniform on all the surfaces.

AgTiN disc

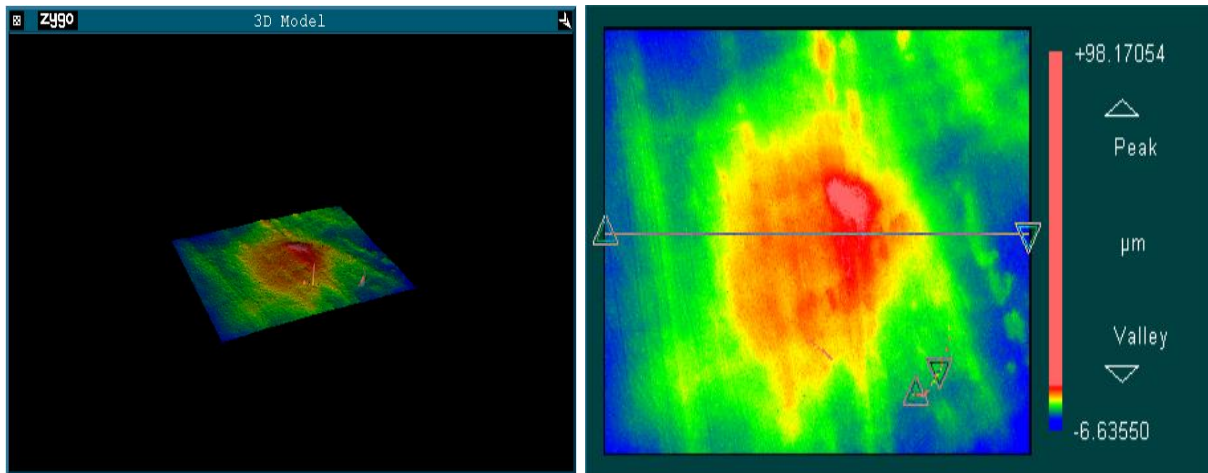


Figure 132: Picture that grouped the 3D model and the Surface map of the contact surface of the pin OE8.

As far as OE8 pin concern, the pin that interacts with AgTiN coated CoCr disc has shown a particular behavior as on it is possible to observe some linear damages. These scratches have been unique around all the pins and are present in high numbers on this pin surface.

Lab disc

Pin number OE9 has shown a behavior similar to OE13 pin. In particular, the pin interaction with CoCr disc from the lab has shown no major changes on the surface and only a micro-roughness with oscillations between $+7\text{ }\mu\text{m}$ and $-5\text{ }\mu\text{m}$.

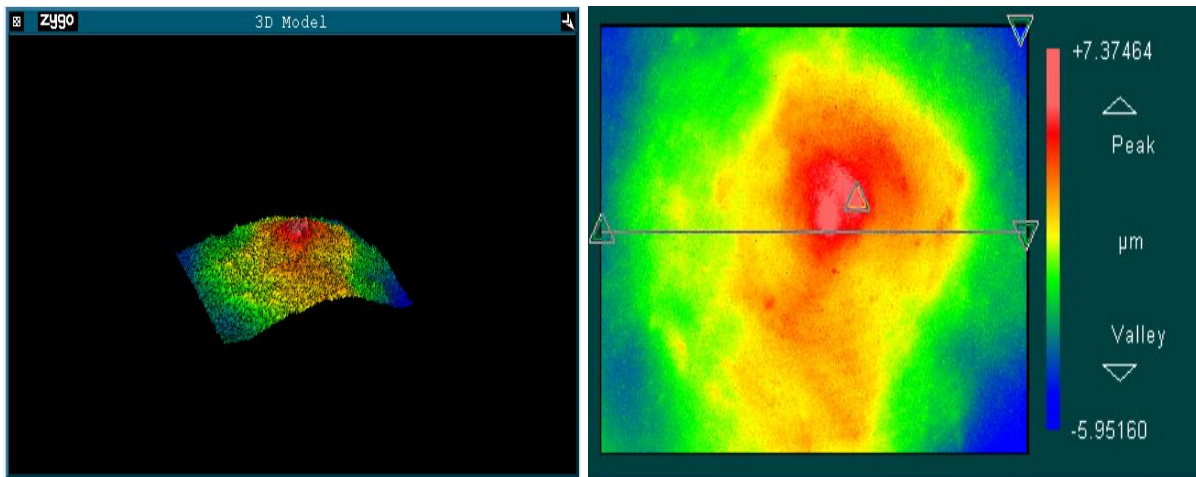


Figure 133: Picture that grouped the 3D model and the Surface map of the contact surface of the pin OE9.

Ti6Al4V test

Ti6Al4V disc

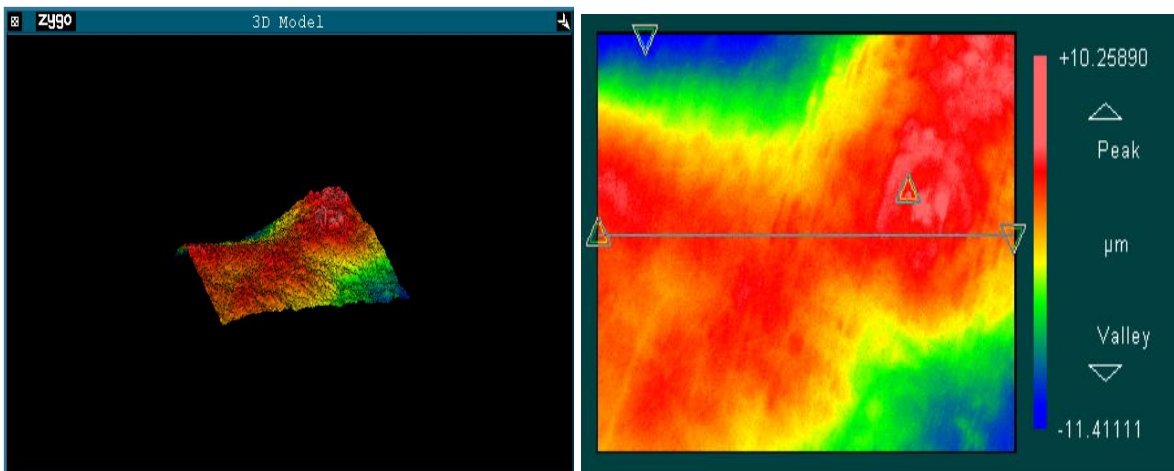


Figure 134, Picture that grouped the 3D model and the Surface map of the contact surface of the pin OE22.

The damage on the disc interacting with the bulk Ti6Al4V disc has been diffused over all the surfaces with an oscillation of the surface profile between +10 μm and -11 μm . No major pattern or common characteristics in the surface profile are recognizable

Tech #1 disc

For pin number OE23 that has interacted with tech #1 coated disc it has been noticed the presence of local damages on the surface. In particular, these damages correspond to areas of accumulation of polymeric material that creates a zone up to 100 μm higher above the mean surface level. This behavior has been characteristic of these types of disc and it has been observed also in tech #2, tech #3, AgTiN and Lab disc.

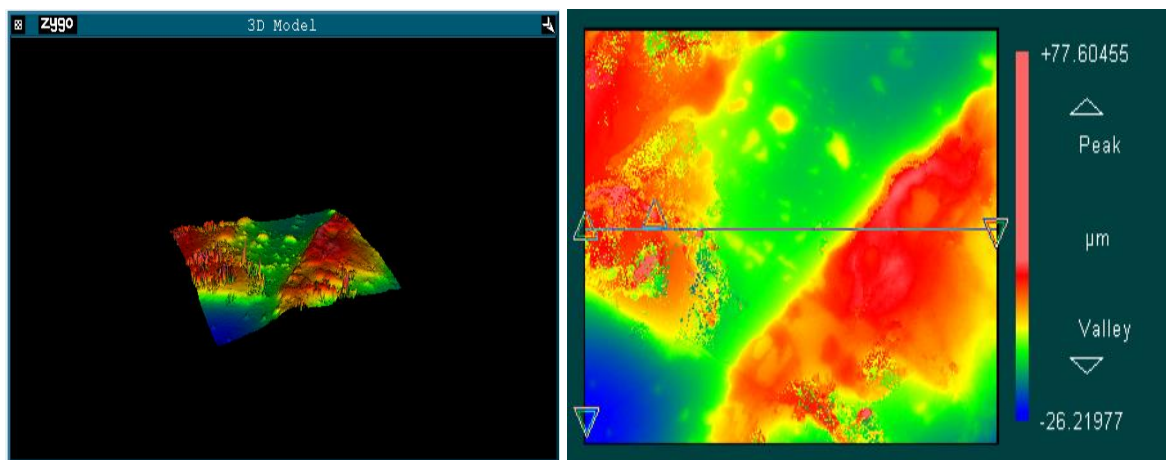


Figure 135: Picture that grouped the 3D model and the Surface map of the contact surface of the pin OE23.

Tech #2 disc

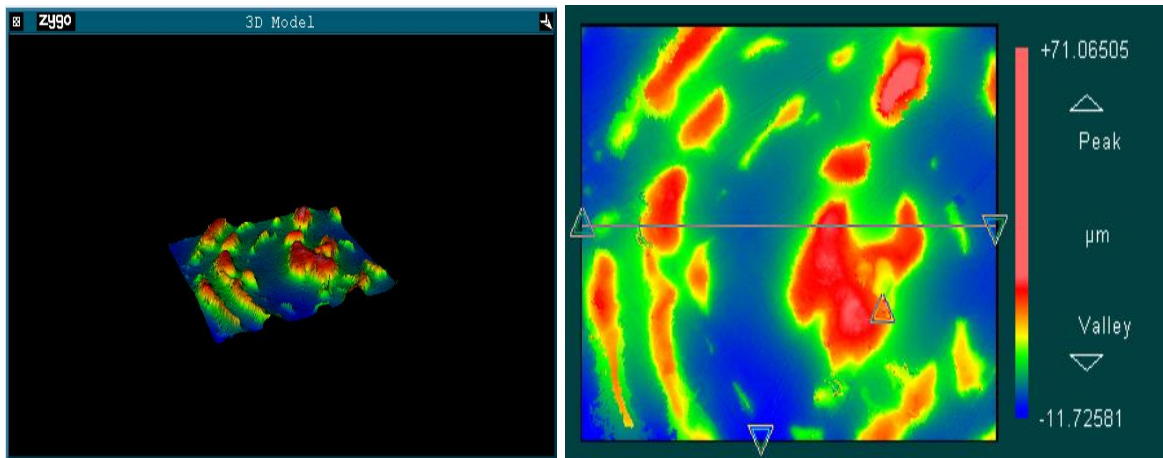


Figure 136: Picture that grouped the 3D model and the Surface map of the contact surface of the pin OE24.

As just observed for OE23 pin, the same behavior has been common also to OE24 disc interacting with Tech #2 processed disc. As visible, the damage has been concentrated to localized zones and the original pattern on the surface of the pin is still visible. In fact, all the areas of damage are organized in concentric circles similar to the soak pin surface.

Tech #3 disc

As far as pin OE25 concerned, it has been observed the presence of some localized areas of accumulation of material on the surface. The behavior shown by the pin that has interacted with tech #3 disc has been less organized than the one seen for the previous case and the original pattern has been damaged and it is not visible.

In this case the surface profile changes between $+29\text{ }\mu\text{m}$ and $-14\text{ }\mu\text{m}$ around the mean height.

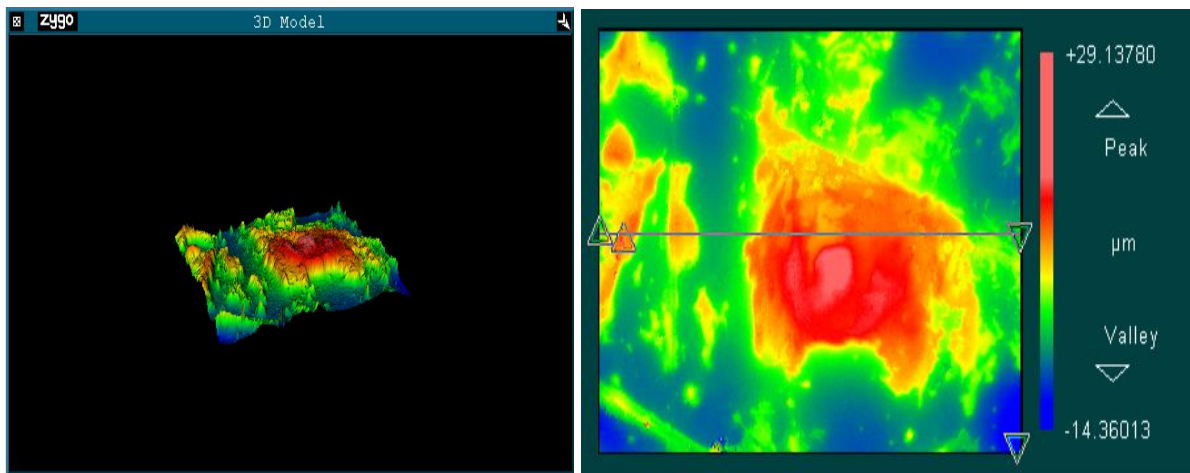


Figure 137: Picture that grouped the 3D model and the Surface map of the contact surface of the pin OE25.

AgTiN disc

When focusing on the pin OE26, that has interacted with Ag TiN disc, it has been reported the presence of some localized areas of accumulation of polymeric debris. In particular, the areas of

accumulation as no definite pattern or shape, but they seem to be randomly distributed on the surface.

However, the surface height oscillates between $+16\text{ }\mu\text{m}$ and $-16\text{ }\mu\text{m}$.

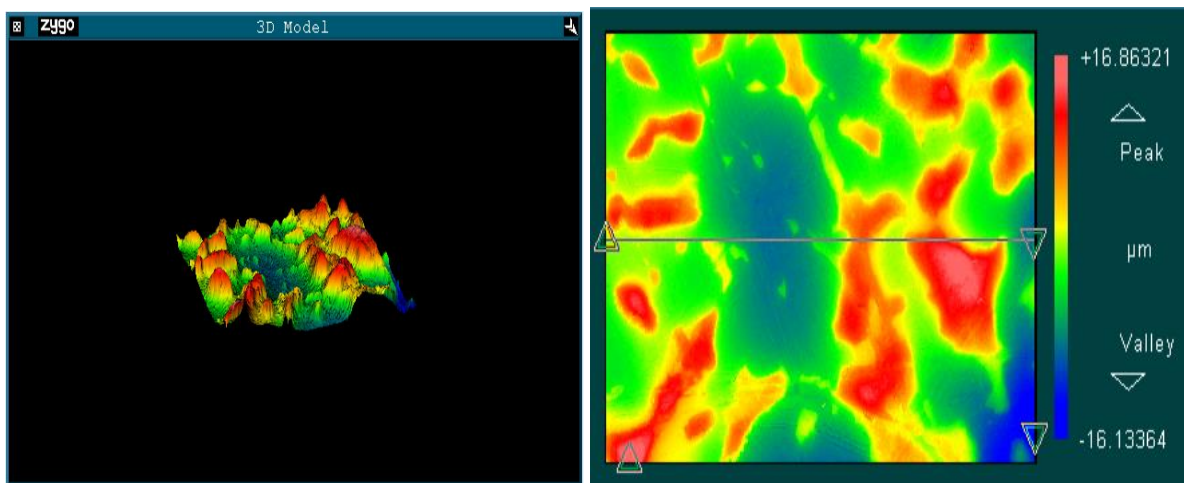


Figure 138: Picture that grouped the 3D model and the Surface map of the contact surface of the pin OE26.

Lab disc

For pin number OE27 interacting with CoCr disc from the lab, the characteristics of the pin have been preserved and the shape typical of the pin before the POD test has been maintained. In particular, only minor changes have been registered on the surface of this pin and even the data coming from the surface map are similar to the one registered for the soak pin.

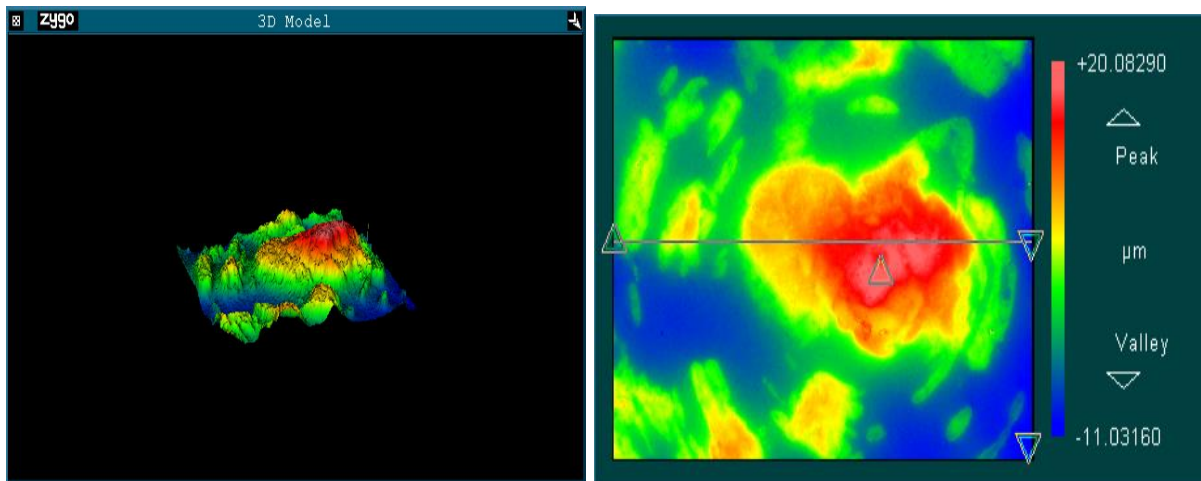


Figure 139: Picture that grouped the 3D model and the Surface map of the contact surface of the pin OE27.

Soak pin

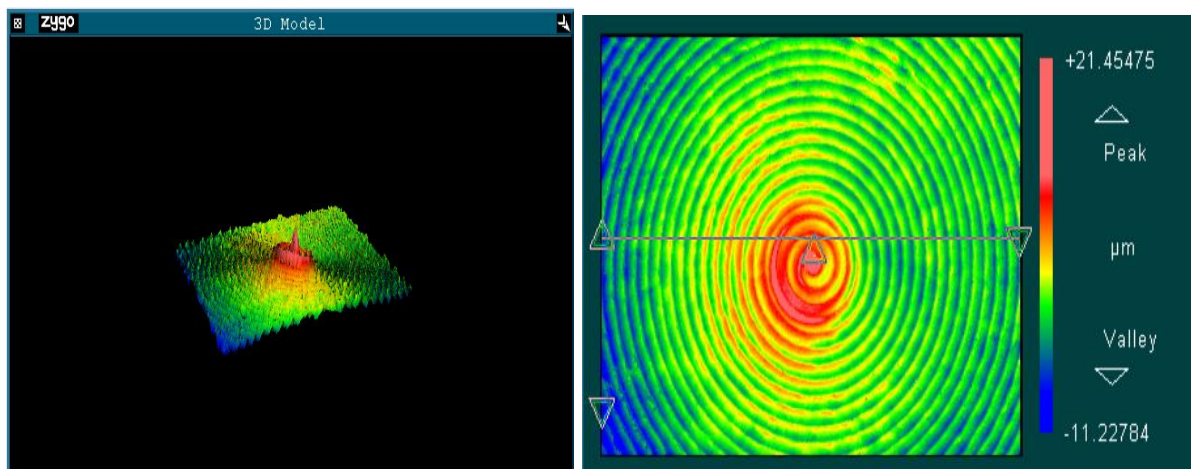


Figure 140: Picture that grouped the 3D model and the Surface map of the contact surface of the pin OE28, used as a reference.

The soak pin number OE28 has been used as a reference because it has not been used to perform the pin on the disk test, but only for the evaluation of weight changes because of hydration.

As noticeable, the surface of the pin has been patterned with some concentric circles that create a micro-roughness on the surface in the order of dozens of micrometers.

CHAPTER 6

DISCUSSION AND CONCLUSION

As specified in the Introduction to this work, the main aim of the experiment was to test the efficacy of TiN used as a coating material on different substrates while analyzing the relevance of the coating process in the determination of the final outputs. In fact, the introduction of a new coating technique may pay the way to a series of interesting developments in massive prosthesis design reducing all those "negative" effects that derive from the polymeric and metallic debris that is produced by the articulating artificial joint and released in the tissues that surround the implant site.

As explained in the introductory part, despite the enormous developments that have been registered for decades in arthroplasty, the wear production is still considered as an unsolved matter that may affect the secondary stability of the prosthesis itself.

In order to simplify the analysis of the obtained results, a summary table containing all the main outcomes of the experiments has been realized and it is shown on the next page.

As noticeable, TiN coating may represent a good solution to reduce the overall amount of wear that is produced due to the relative movement between the metallic component and the polymeric part.

TABLE XXIII: FINAL SUMMARY TABLE CONTAINING ALL THE RESULTS OBTAINED DURING THE EXPERIMENT.

Sample	Substrate	Avg WR (mg/Mcycles)	Std (mg/Mcycle)	WR Variation	Roughness variation (nm)	Raman shift (cm^{-1})	Pins	Discs
Ref	CoCr	3.475	1.519	/	0.547	/	Localized damage on the surface	/
Ref	Ti6Al4V	6.117	1.830	/	7.948	/	Nearly flat surface	/
Tech #1	CoCr	11.103	1.219	+219.5%	2.584	-8.422	Sharp scratches on the surface	Big area of damage
Tech #1	Ti6Al4V	10.015	0.442	+63.7%	4.002	/	Sharp scratches on the surface	Big area of damage
Tech #2	CoCr	2.005	0.160	-42.3%	-7.273	/	Small damages	Slight damage
Tech #2	Ti6Al4V	5.025	0.449	-17.9%	1.248	/	Well-visible damaged zones	Slight damage
Tech #3	CoCr	2.659	1.646	-23.5%	-2.304	-4.943	Sharp scratches	Slight damage
Tech #3	Ti6Al4V	5.889	2.254	-3.7%	4.573	/	Almost flat	Slight damage
AgTiN	CoCr	4.356	0.234	+25.4%	13.603	-13.374	Small scratches	Eye-visible scratch
AgTiN	Ti6Al4V	6.112	0.527	-0.1%	-1.3076	/	Small scratches	Slight damage
Ref LAB	CoCr	1.250	0.376	/	0.904	/	Localized damage on the surface	/

However, this reduction is strongly dependent on the procedure that has been followed to deposit the TiN layer on the substrate and on the substrate characteristics themselves and this is the explanation of why the obtained results have been so different depending on these two characteristics.

Anyway, before introducing any kind of comment, it is important to remember that this has been only a preliminary test and at least 5 runs for samples set have to be performed to obtain more complete results.

The first interesting thing to notice is that the best results have been obtained during the CoCr test and, in particular with Tech #2 and Tech #3 processed disc for which it has been observed, respectively, a reduction of 40% and 20% of the produced wear after every million cycles. In particular, the encouraging results obtained by Tech #2 disc gain even more relevance when considering that the standard deviation is very low, with a value around 0.160 mg/Mcycles, meaning that the behavior of the material has been almost constant during the entire experiment, but considering also the fact that the damage on the surface of the pin and on the disc itself has been minimum. Last consideration has been proven to the fact that also the Raman spectroscopy of the surface has not shown any relevant shift.

On the other hand, even if the behavior of Tech #2 processed disc has been better than the one shown by the uncoated CoCr disk, it is important to consider the high variability in the behavior observed in the calculated WR of the material and proven by the high value of the standard deviation registered for this particular condition and equal to 1.646 mg/Mcycles. Damages on pins and discs have been considered as minor side effects.

A completely separate consideration is needed when talking about Raman shifts. These phenomena that has been registered for Tech #1, Tech #2 and AgTiN, with values that seem to be

proportional to the level of damage caused on the surface of the disc by the pin on disc (POD) test, might be explained considering two different processes that may have occurred on the surface layers of this discs.

Firstly, it may be caused by a change in the chemical arrangement of the crystalline structure of the first layers on the surface due to the external stresses induced by the pin on disc experiment.

Secondly, it may be due to the fact that when damaging the first layers of the surface of the discs the process led to the exposition of deeper levels that eventually may have a different chemical structure or, with higher probability, may have residual stresses, derived from the deposition technique that has been used to deposit the TiN layer on the substrate, that are different from the ones experienced by the upper levels. Thus, when performing the Raman spectroscopy analysis the characteristics of a different layer of TiN, with different residual stresses are studied and this is why the higher the damage on the surface, for Tech #1 for instance, the higher the determined Raman shift. However, these shifts were quite small and it is hard to make conclusions about them.

Another important thing to consider about CoCr test is the verified independence between the roughness of the disc and the wearing rate that has been proven and shown in fig. 97.

To conclude this part, it has been also noticed that Lab disc has performed better than the CoCr disc coming from the company. This behavior may be linked with different properties

characterizing the two discs as they come from a different lot and this means that different polishing techniques may have been used, the alloy may have a different composition or the two materials may also be different due to the different supplier. Further analysis may be performed to prove these hypotheses.

The results obtained for the Ti6Al4V test have proven the fact that Tech #2 and Tech #3 are the TiN deposition techniques that guarantee the best performances. Despite that, the advantage in terms of debris production has been smaller in this case with only a 5% reduction for Tech #3 and a bit less than 18% for Tech #2.

However, the same results in term of results variability have been shown also for the Ti6Al4V test, with reduced variability for Tech #2 processed disc, std equals to 0.499 mg/Mcycles, and a big variability observed for disc Tech #3 disc for which a standard deviation of 2.254mg/Mcycles has been calculated.

AgTiN and Tech #1 have been the worst also in this case, meaning that doping TiN with silver particles for antibacterial purposed may deeply affect the properties of the material and that Tech #2 is not able to guarantee sufficiently good properties to the TiN coating.

Also in this test the independence between surface roughness and wear rate (WR) has been verified and when considering the external properties of the discs no major changes have been observed, proven also by the absence of a shift in the Raman spectroscopy performed in the damaged and undamaged areas.

To summarize, TiN has revealed to be a good coating material, when deposited using Tech #2, guaranteeing a reduction of the wear debris produced of about 20-40% depending on the material constituting the substrate. This coating may guarantee improved lasting performances with high repeatability.

A possible explanation of the observed behaviors could be hypothesized when looking at the surface morphology of the different materials, which might be observed from the SEM images captured after the end of the polishing procedure and obtained by the discs supplier.

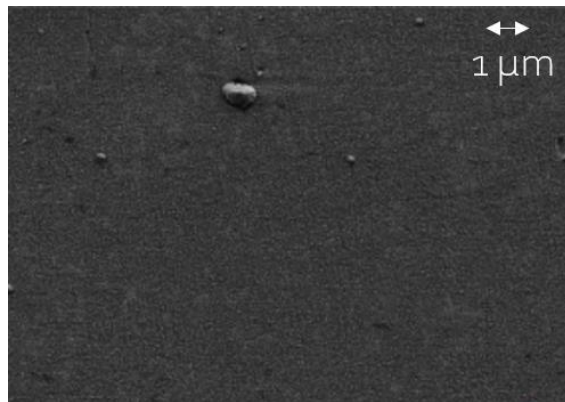


Figure 141: SEM image from Tech #1 coated disc surface.

When looking at the surface of Tech #1 coated discs it has been observed the presence of some sharp asperities on the flat surface layer. It might be supposed that, during the POD test,

these particles have detached from the surface of the material and have been released inside the testing chamber.

This theory will explain both the sharp scratches that have been found on the surface of the polyethylene pin, but also the decrease of surface defects and the increase of surface roughness that have been observed on the disc.

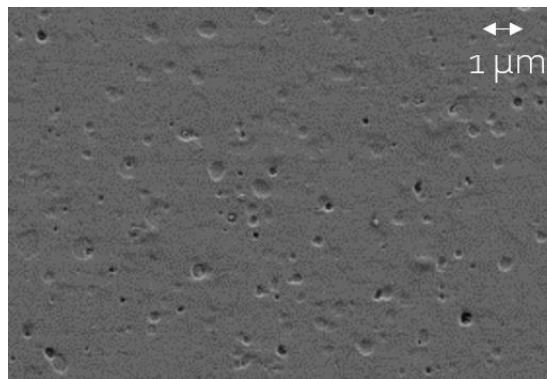


Figure 142: SEM image from Tech #2 coated disc surface.

On the other hand, when looking at the surface morphology of Tech #2 discs it has been observed a higher presence of defects that appear to be depression. This may be the reason why this material has demonstrated the best behavior when articulating against the polyethylene counterpart.

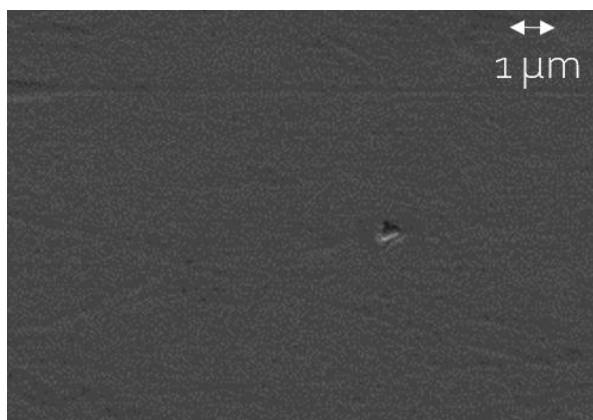


Figure 143: SEM image from Tech #3 coated disc surface.

When looking at Tech #3 coated discs, this processing technique has been demonstrated to create highly flat TiN layers with only minor defects that appear to be all holes after the polishing procedure. These surface characteristics are promising and this is one of the main reasons why it might be advisable to perform more tests on this material in order to complete its characterization and give a conclusive judgment about this deposition technique.

Hereunder, it has been reported also the surface morphology of the discs coated with AgTiN. As noticeable, this material presents bigger defects than all the other conditions that have been observed, but they are mainly holes and this is a possible explanation of why this material has performed halfway between Tech #1 and the other two deposition techniques.

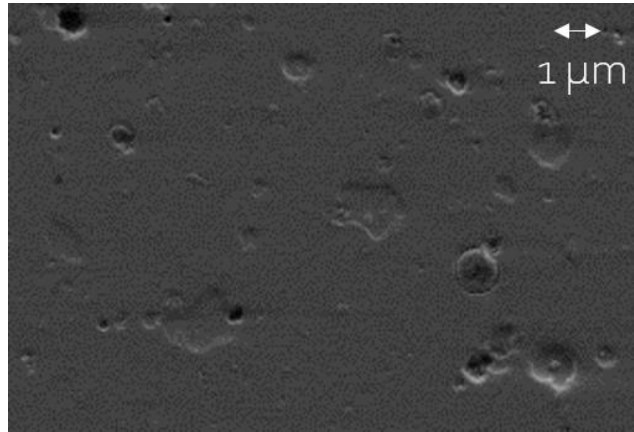


Figure 144: SEM image from Tech #1 coated disc surface.

In order to complete the work some final statistical analysis have been performed. As shown below, the first analyzed aspect has been the dependency between the measured Wear Rate and the two variable parametres: the *substrate* and the *coating technique*.

It has been performed an ANOVA two-factors test with replication choosing 0.05 as significance level.

For both parametres it has been assessed the statistical relevance of the term in the determination of the evaluated final Wear Rate. In other words, it has been statistically assessed the dependency of the obtained results from these two parameters.

In addition, it has been observed that also the interaction tem has an important role in the definition of the final behavior of the sample. In fact for some coating techniques they have been obtained better results having CoCr as substrate, for others having Ti6Al4V as substrate.

TABLE XXIV: ANOVA TWO-FACTORS WITH REPLICATIONS TEST.

ANOVA Two-Factors with replications (alpha = 0.05)						
Source of variation	SS (Sum of squares)	Df (Degrees of freedom)	MS (Mean of squares)	F	P-value	F crit
Substrate	27.4296	1	27.4296	17.4891	0.000459669	4.3512
Coating	188.6859	4	47.1715	30.0765	3.31631E-08	2.8661
Interaction	18.7889	4	4.6972	2.9950	0.043438242	2.8661
Within	31.36766	20	1.5684			
Total	266.2721	29				

Moreover, it has been performed a post hoc analysis adjusted for multiple comparison. As noticeable from the results that have been reported down below, all the different coatings have been compared two by two and grouped by substrate.

TABLE XXV: POST HOC ANALYSES ADJUSTED FOR MULTIPLE COMPARISON.

Substrate	Coating(1) - Coating(2)		Difference	adj. <i>p</i>	95%CI []	
CoCr	Uncoated	Tech #1	-7.6283	<0.0001	-11.0985	-4.1581
		Tech #2	1.4698	0.868	-2.0004	4.94
		Tech #3	0.816	0.9965	-2.6542	4.2862
		AgTiN	-0.8807	0.994	-4.3509	2.5895
	Tech #1	Tech #2	9.0981	<0.0001	5.6279	12.5683
		Tech #3	8.4443	<0.0001	4.9741	11.9145
		AgTiN	6.7477	<0.0001	3.2775	10.2179
	Tech #2	Tech #3	-0.6538	0.9994	-4.124	2.8164
		AgTiN	-2.3504	0.3651	-5.8206	1.1198
	Tech #3	AgTiN	-1.6967	0.7539	-5.1669	1.7735
Ti6Al4V	Uncoated	Tech #1	-3.8977	0.0008	-7.3679	-0.4275
		Tech #2	1.0917	0.9747	-2.3785	4.5619
		Tech #3	0.228	1	-3.2422	3.6982
		AgTiN	0.004433	1	-3.4658	3.4746
	Tech #1	Tech #2	4.9893	0.0021	1.5191	8.4595
		Tech #3	4.1257	0.0129	0.6555	7.5959
		AgTiN	3.9021	0.0206	0.4319	7.3723
	Tech #2	Tech #3	-0.8637	0.9948	-4.3339	2.6065
		AgTiN	-1.0872	0.9753	-4.5574	2.383
	Tech #3	AgTiN	-0.2236	1	-3.6938	3.2466

In yellow, they have been reported the statistically significant results. In particular, the only conclusion that may be derived from this test is that Tech #1 has performed worse than all the other conditions and may be excluded from future studies. For all the other conditions, more analysis will be necessary in order to obtain statistically relevant conclusions.

However, it may not be forgotten some of the difficulties that have been found during the execution of this experiment. First of all, it has been observed a case of negative loss of weight for one pin (Tech #2, Round 2, CoCr test) probably linked to an error during the cleaning procedure that has caused some protein to remain embedded in the disc. Fortunately, this error has not affected the results that have been verified to be coherent with the other measurements as explained in chapter 5. In addition, the extremely variable behavior of Tech #3 processed disc in both the experiments make it really difficult to give a final opinion about this material. Extremely good performances have been followed by bad ones and it has not been understood why this may have happened. All the data collected about Tech #3 has not explained this behavior. In conclusion, the POD testing machine has had some issues with the pin motion control after the end of the first test. The sensor has been substituted, the machine has been calibrated and this problem seems not to consider as relevant for the analysis.

In order to conclude a complete analysis of the material, some further steps may be performed.

As observed in the introduction, one of the main advantages of using TiN as a coating material of CoCr disc may be the reduction of the metal ions released in the implant site that may cause

higher inflammation in the implant site, tends to be accumulated in target organs as liver and kidneys and may cause, especially for CoCr, severe allergies in the patient. To proof this "shield" effect the testing fluid that has been collected after each round of the test may be studied looking for the difference of concentration of metal ions between the reference case, bulk CoCr or bulk Ti6Al4V, and the coated disc.

Another interesting property to study may be the increased resistance to third body wear that is usually caused by bone cement particles that accidentally end in the joint area during the implantation of the prosthesis. In order to verify gained resistance due to the use of TiN as coating, the experiments that have been performed may be repeated adding some bone cement to the testing chamber. By analyzing the difference in the behavior of coated and uncoated discs it will be possible to understand the real efficacy of these coating techniques.

If all these tests will confirm the good results obtained by Tech #2 disc in the POD test and the costs/benefits ratio will be high enough this process technique associated with a TiN layer deposited on the surface of prosthesis like hip or knee prosthesis may represent a further innovative step oriented toward a reduction of the side effects associated to this kind of implants like high inflammation, loss of secondary stability and subsequent revision of the implant, third body wear and even allergies.

A lot of studies have still to be done, but the road seems encouraging.

CHAPTER 7

APPENDICES

This section is dedicated to all the raw data from which the outcomes introduced in the “Result” chapter has been calculated.

The following contents have been reported:

- A. Integral version of Roughness measurements table for CoCr test;
- B. Integral version of Roughness measurements table for Ti6Al4V test;
- C. Raw data from Round 1, CoCr test;
- D. Raw data from Round 2, CoCr test;
- E. Raw data from Round 3, CoCr test;
- F. Raw data from Round 1, Ti6Al4V test;
- G. Raw data from Round 2, Ti6Al4V test;
- H. Raw data from Round 3, Ti6Al4V test.
- I. Permissions to reprint copyright materials.

Appendix A

A. INTEGRAL VERSION OF ROUGHNESS MEASUREMENT TABLE FOR CoCr TEST

TABLE XXVI: INTEGRAL VERSION OF ROUGHNESS MEASUREMENT TABLE, CoCr TEST

Surface roughness - Ra [nm]												
Test #1												
	#1 (CoCr)		#5 (tech #1)		#9 (tech #2)		#13 (tech #3)		#17 (AgTiN)		#21 (LAB)	
1	6.000	5.206	14.197	20.164	41.530	25.700	12.574	10.326	46.794	67.299	9.296	7.237
2	4.351	4.442	13.738	17.498	40.017	26.514	13.813	12.757	45.876	49.523	5.957	6.656
3	4.043	4.937	16.530	24.087	48.513	36.390	12.408	11.643	36.822	54.849	7.146	8.690
4	4.726	4.190	17.070	21.059	30.301	22.602	14.239	11.683	44.457	80.296	6.332	5.140
5	5.059	4.482	11.017	11.342	29.967	30.296	13.675	12.995	66.869	44.990	6.532	5.829
Avg	4.836	4.651	14.510	18.830	38.066	28.300	13.342	11.881	48.164	59.391	7.053	6.710
Std	0.7551	0.4106	2.4253	4.8018	7.9189	5.2879	0.8062	1.0633	11.1733	14.3610	1.3259	1.3640
Test #2												
	#2 (CoCr)		#6 (tech #1)		#10 (tech #2)		#14 (tech #3)		#18 (AgTiN)		#22 (LAB)	
1	4.082	3.735	16.274	22.575	26.827	21.837	14.714	12.651	47.966	60.197	8.067	11.753
2	3.783	4.240	16.845	19.492	30.659	26.970	16.452	14.434	50.997	57.992	9.006	6.486
3	3.771	4.651	10.024	18.750	25.202	20.832	16.207	12.900	60.612	64.918	8.472	7.010
4	3.665	4.758	20.032	12.510	26.242	27.941	15.029	13.336	62.673	49.243	6.681	12.099
5	3.905	4.846	14.212	17.040	26.143	21.905	17.076	14.930	33.469	45.185	6.950	7.721
Avg	3.841	4.446	15.477	18.073	27.015	23.897	15.896	13.650	51.143	55.507	7.835	9.014
Std	0.159	0.460	3.694	3.700	2.119	3.294	0.993	0.989	11.674	8.101	0.993	2.697
Test #3												
	#3 (CoCr)		#7 (tech #1)		#11 (tech #2)		#15 (tech #3)		#19 (AgTiN)		#23 (LAB)	
1	3.624	7.228	22.197	16.635	35.829	25.225	14.939	12.488	41.854	82.191	4.371	7.207
2	3.997	4.112	9.844	22.397	31.833	35.949	15.408	16.353	35.519	90.220	3.966	5.445
3	3.669	5.356	21.670	16.692	34.481	32.766	14.034	6.671	45.658	98.460	4.899	7.002
4	3.905	4.129	11.754	18.427	39.526	31.254	19.012	13.805	64.303	38.548	4.460	6.013
5	3.821	4.295	14.961	10.451	61.526	33.323	14.180	12.227	44.550	48.554	3.964	5.375
Avg	3.803	5.024	16.085	16.920	40.639	31.703	15.515	12.309	46.377	71.595	4.332	6.208
Std	0.157	1.335	5.646	4.308	12.001	3.998	2.034	3.550	10.765	26.476	0.390	0.858

Appendix B

B. INTEGRAL VERSION OF ROUGHNESS MEASUREMENT TABLE FOR Ti6Al4V TEST

TABLE XXVII: INTEGRAL VERSION OF ROUGHNESS MEASUREMENT TABLE,
Ti6Al4V TEST

Surface roughness - Ra [nm]										
Test #1										
	#24 (CoCr)		#28 (S3p)		#32 (Arc)		#36 (KILA)		#40 (Ag)	
1	14.832	16.100	34.756	24.418	43.498	32.280	30.705	52.581	63.241	66.211
2	13.974	20.211	28.400	56.423	40.746	35.804	36.169	23.511	65.112	55.961
3	17.714	14.965	26.045	38.921	47.974	51.918	30.171	44.950	75.879	78.834
4	20.969	27.510	31.690	28.827	47.152	40.130	33.582	28.828	74.151	55.962
5	19.219	17.674	32.355	44.657	41.373	73.345	40.144	40.611	52.090	68.196
Avg	17.342	19.292	30.649	38.649	44.149	46.695	34.154	38.096	66.095	65.033
Std	2.935	4.998	3.432	12.758	3.292	16.636	4.124	11.850	9.564	9.571
Test #2										
	#25 (CoCr)		#29 (S3p)		#33 (Arc)		#37 (KILA)		#41 (Ag)	
1	22.266	17.299	29.956	28.392	35.826	46.450	25.920	18.032	53.376	59.874
2	12.617	33.760	26.639	43.170	35.944	31.446	19.939	22.574	66.479	49.271
3	14.606	21.153	31.401	38.469	34.137	29.415	22.510	26.807	55.685	82.347
4	19.154	15.961	30.412	38.414	43.693	30.723	23.998	22.740	62.208	55.845
5	18.122	18.056	28.553	38.395	36.978	32.715	25.970	44.232	74.263	84.893
Avg	17.353	21.246	29.392	37.368	37.316	34.150	23.667	26.877	62.402	66.446
Std	3.806	7.251	1.849	5.422	3.708	6.979	2.536	10.187	8.425	16.153
Test #3										
	#26 (CoCr)		#30 (S3p)		#34 (Arc)		#38 (KILA)		#42 (Ag)	
1	15.003	29.000	27.758	28.000	43.095	79.000	25.217	27.000	73.418	36.000
2	24.265	28.000	20.844	18.000	42.554	54.000	26.904	31.000	72.321	55.000
3	15.447	37.000	45.034	26.000	47.669	44.000	26.759	35.000	71.815	87.000
4	15.896	13.000	34.822	43.000	55.200	36.000	26.188	34.000	60.271	48.000
5	14.390	68.000	27.393	21.000	41.664	39.000	25.088	36.000	57.699	75.000
Avg	17.000	35.000	31.170	27.200	46.036	50.400	26.031	32.600	67.105	60.200
Std	4.099	20.384	9.193	9.680	5.624	17.387	0.847	3.647	7.490	20.608

Appendix C

C. RAW DATA FROM ROUND 1, CoCr TEST

TABLE XXVIII: AVERAGE WEIGHT AND STANDARD DEVIATION OF THE WEIGHT EVALUATED FOR EACH STAGE OF THE TEST.

Before the testing			After testing (0.25M)			After testing (0.5M)			After testing (0.75M)			After testing (1M)		
Pin	Mean	SD	Pin	Mean	SD	Pin	Mean	SD	Pin	Mean	SD	Pin	Mean	SD
1	1266.28	0.03	1	1266.17	0.02	1	1265.71	0.02	1	1265.23	0.00	1	1264.60	0.03
2	1267.79	0.02	2	1259.55	0.02	2	1255.43	0.02	2	1252.73	0.02	2	1250.17	0.02
3	1263.62	0.02	3	1263.03	0.01	3	1262.60	0.02	3	1262.05	0.02	3	1261.52	0.01
4	1269.15	0.03	4	1268.62	0.00	4	1267.93	0.00	4	1266.88	0.01	4	1265.32	0.00
5	1270.00	0.03	5	1268.37	0.03	5	1267.53	0.01	5	1266.56	0.01	5	1265.33	0.01
6	1271.78	0.01	6	1271.44	0.02	6	1271.41	0.02	6	1271.14	0.01	6	1270.95	0.01

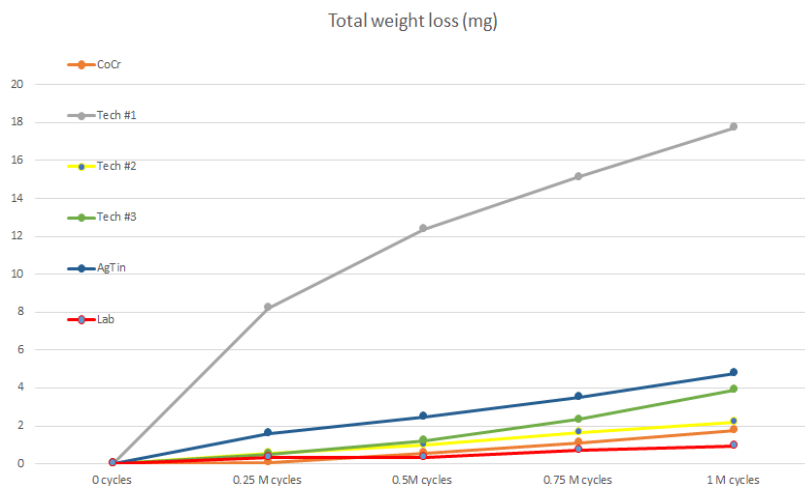


Figure 145: Complete version of the "Total weight loss" graph.

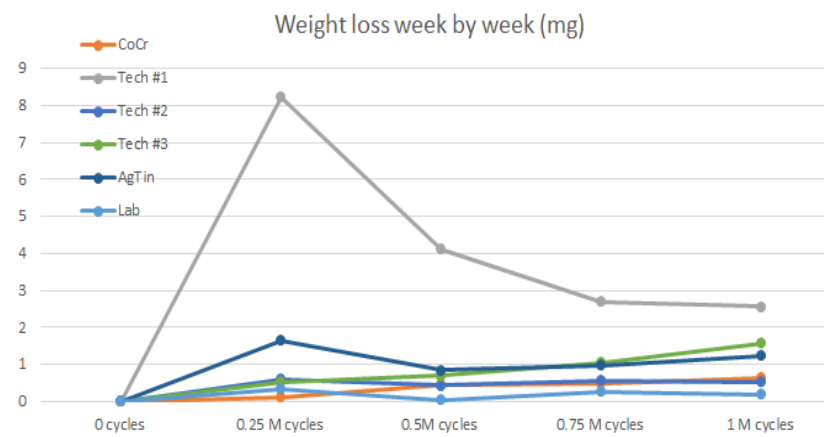


Figure 146: Complete version of the "Weight loss week by week" graph.

TABLE XXIX: AVERAGE WEIGHT AND STANDARD DEVIATION OF THE WEIGHT EVALUATED FOR THE SOAK PIN.

Before the testing			After testing (0.25M)			After testing (0.5M)			After testing (0.75M)			After testing (1M)		
Pin	Mean	SD	Pin	Mean	SD	Pin	Mean	SD	Pin	Mean	SD	Pin	Mean	SD
7	1271.86	0.02	7	1271.84	0.02	7	1271.84	0.02	7	1271.92	0.02	7	1271.94	0.02

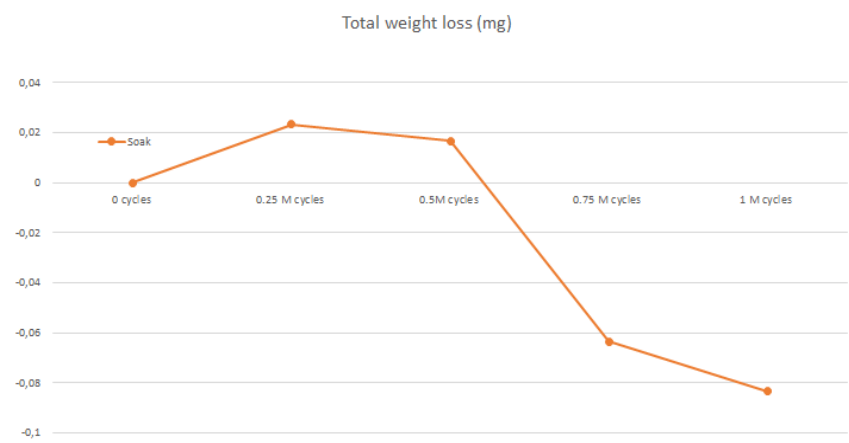
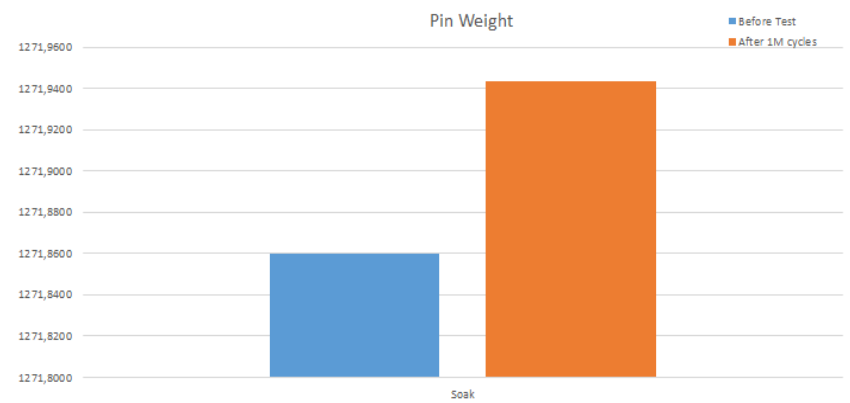


Figure 147, Soak pin weight variation.



148, Soak pin weight “before” and “after” the pin on disc test.

Appendix D

D. RAW DATA FROM ROUND 2, CoCr TEST

TABLE XXX: AVERAGE WEIGHT AND STANDARD DEVIATION OF THE WEIGHT EVALUATED FOR EACH STAGE OF THE TEST.

Before the testing			After testing (0.25M)			After testing (0.5M)			After testing (0.75M)			After testing (1M)		
Pin	Mean	SD	Pin	Mean	SD	Pin	Mean	SD	Pin	Mean	SD	Pin	Mean	SD
1	1269.05	0.03	1	1265.00	0.01	1	1264.01	0.00	1	1263.05	0.01	1	1261.89	0.04
2	1270.07	0.01	2	1267.16	0.03	2	1266.82	0.01	2	1266.54	0.02	2	1266.31	0.02
3	1266.54	0.04	3	1266.11	0.02	3	1265.35	0.01	3	1264.67	0.02	3	1263.93	0.01
4	1267.22	0.02	4	1262.34	0.03	4	1259.38	0.01	4	1256.94	0.03	4	1254.45	0.02
5	1266.41	0.01	5	1268.60	0.02	5	1268.15	0.01	5	1267.65	0.01	5	1267.27	0.02
6	1266.71	0.01	6	1266.43	0.01	6	1266.12	0.01	6	1265.75	0.01	6	1265.42	0.02

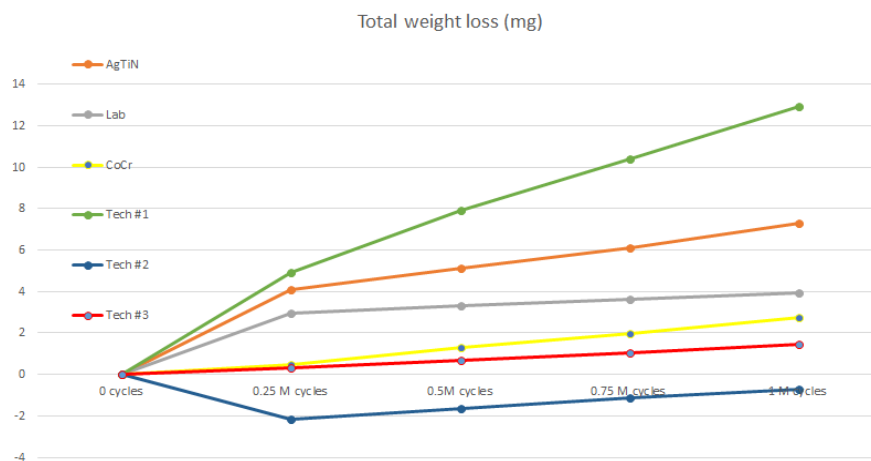


Figure 149, Complete version of the "Total weight loss" graph.

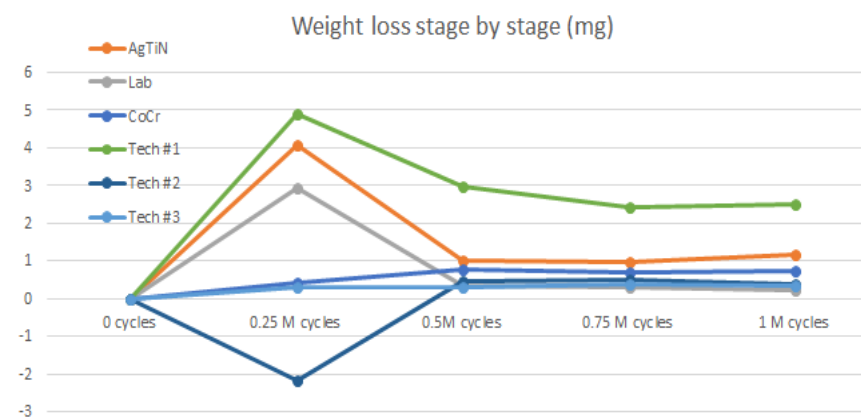


Figure 150, Complete version of the "Weight loss week by week" graph.

TABLE XXXI: AVERAGE WEIGHT AND STANDARD DEVIATION OF THE WEIGHT EVALUATED FOR THE SOAK PIN.

Before the testing			After testing (0.25M)			After testing (0.5M)			After testing (0.75M)			After testing (1M)		
Pin	Mean	SD	Pin	Mean	SD	Pin	Mean	SD	Pin	Mean	SD	Pin	Mean	SD
14	1266.43	0.01	14	1266.48	0.01	14	1266.52	0.02	14	1266.53	0.01	14	1266.59	0.01

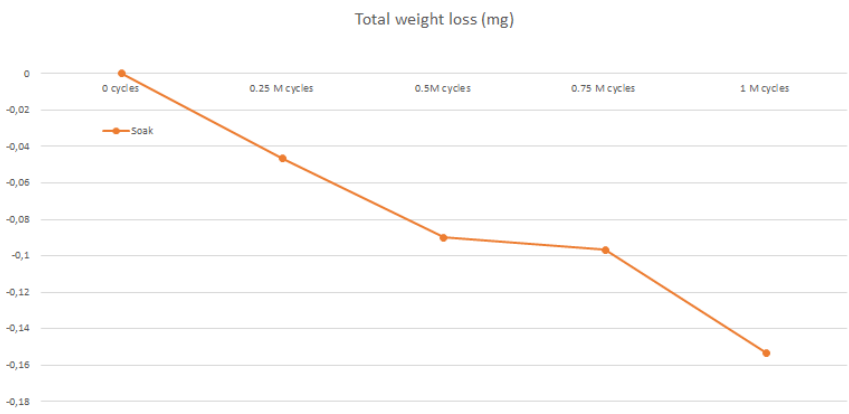


Figure 151, Soak pin weight variation.

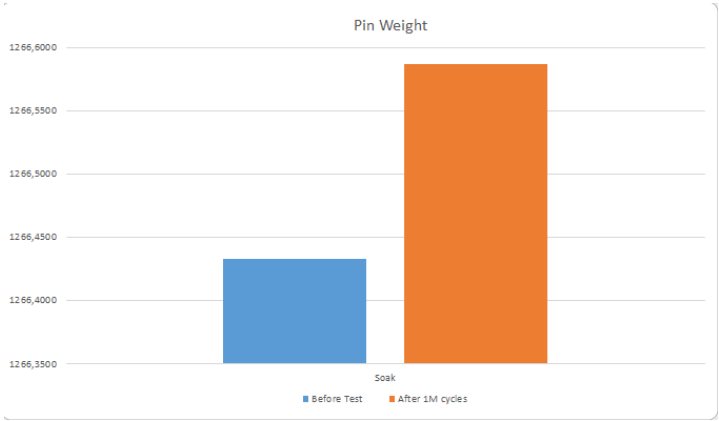


Figure 152, Soak pin weight “before” and “after” the pin on disc test.

Appendix E

E. RAW DATA FROM ROUND 3, CoCr TEST

TABLE XXXII: AVERAGE WEIGHT AND STANDARD DEVIATION OF THE WEIGHT EVALUATED FOR EACH STAGE OF THE TEST.

Before the testing			After testing (0.25M)			After testing (0.5M)			After testing (0.75M)			After testing (1M)		
Pin	Mean	SD	Pin	Mean	SD	Pin	Mean	SD	Pin	Mean	SD	Pin	Mean	SD
15	1267.77	0.03	15	1267.66	0.01	15	1267.38	0.01	15	1266.83	0.02	15	7.5100	10.5925
16	1266.44	0.02	16	1266.43	0.01	16	1266.14	0.00	16	1265.47	0.04	16	8.0176	11.2889
17	1266.48	0.02	17	1266.04	0.02	17	1265.00	0.01	17	1263.65	0.01	17	8.5029	12.0167
18	1266.52	0.00	18	1266.48	0.01	18	1266.25	0.02	18	1265.70	0.01	18	9.0029	12.7238
19	1266.93	0.01	19	1266.65	0.01	19	1266.19	0.02	19	1264.17	0.01	19	9.5050	13.4280
20	1266.63	0.03	20	1262.00	0.02	20	1258.50	0.02	20	1256.09	0.01	20	10.0029	14.1381

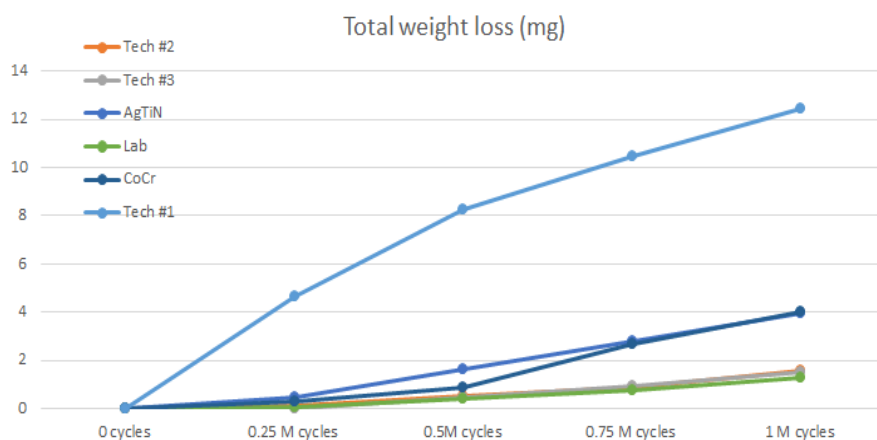


Figure 153, Complete version of the "Total weight loss" graph.

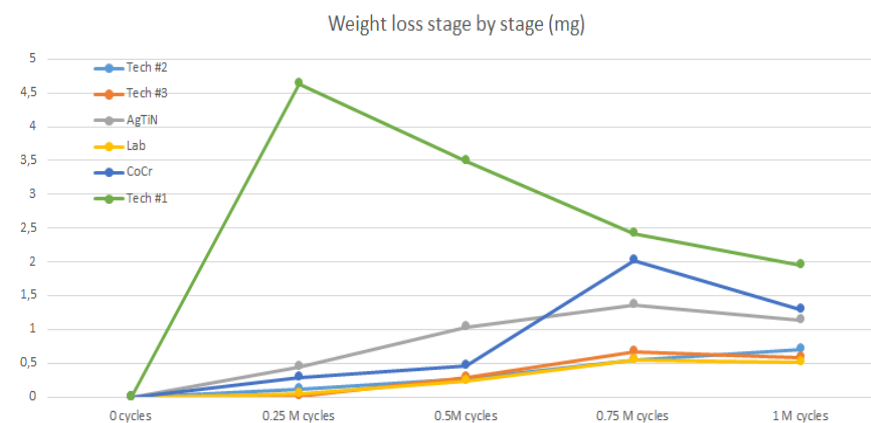


Figure 154, Complete version of the "Weight loss week by week" graph.

TABLE XXXIII: AVERAGE WEIGHT AND STANDARD DEVIATION OF THE WEIGHT EVALUATED FOR THE SOAK PIN.

Before the testing			After testing (0.25M)			After testing (0.5M)			After testing (0.75M)			After testing (1M)		
Pin	Mean	SD	Pin	Mean	SD	Pin	Mean	SD	Pin	Mean	SD	Pin	Mean	SD
21	1265.16	0.01	21	1265.18	0.01	21	1265.30	0.02	21	1265.10	0.01	21	1265.11	0.00

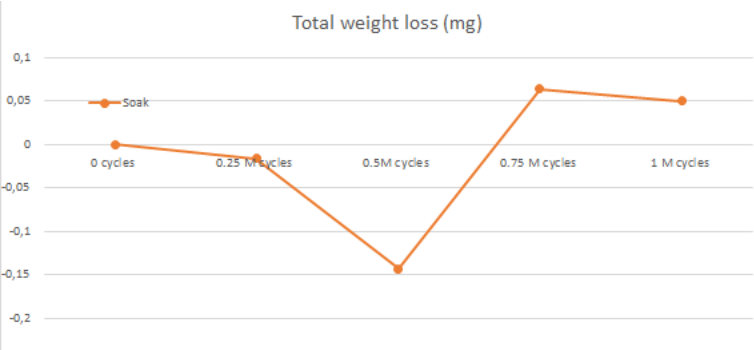


Figure 155, Soak pin weight variation.

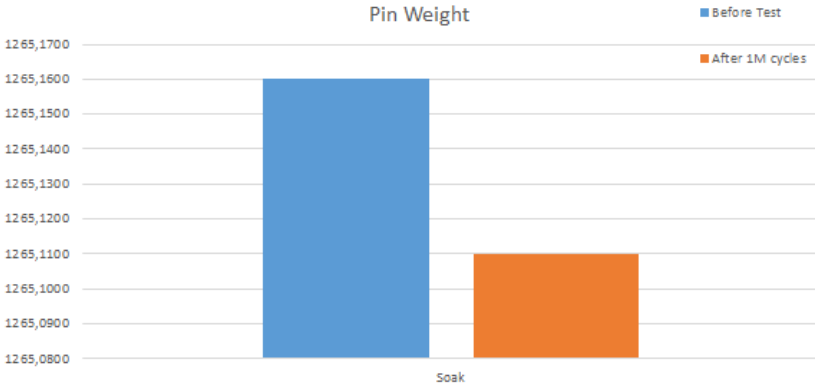


Figure 156, Soak pin weight “before” and “after” the pin on disc test.

Appendix F

F. RAW DATA FROM ROUND 1, Ti6Al4VTEST

TABLE XXXIV: AVERAGE WEIGHT AND STANDARD DEVIATION OF THE WEIGHT EVALUATED FOR EACH STAGE OF THE TEST.

Before the testing			After testing (0.25M)			After testing (0.5M)			After testing (0.75M)			After testing (1M)		
Pin	Mean	SD	Pin	Mean	SD	Pin	Mean	SD	Pin	Mean	SD	Pin	Mean	SD
1	1267.74	0.02	1	1267.38	0.02	1	1266.45	0.02	1	1264.86	0.02	1	1263.31	0.01
2	1269.19	0.02	2	1262.57	0.01	2	1259.95	0.01	2	1257.47	0.02	2	1255.55	0.00
3	1268.48	0.02	3	1266.99	0.02	3	1265.98	0.01	3	1264.53	0.01	3	1263.60	0.01
4	1268.07	0.02	4	1268.20	0.03	4	1266.29	0.01	4	1264.12	0.01	4	1262.88	0.01
5	1267.97	0.02	5	1265.48	0.02	5	1264.22	0.01	5	1262.56	0.02	5	1261.59	0.01
6	1269.32	0.01	6	1268.66	0.02	6	1267.36	0.02	6	1265.74	0.01	6	1264.83	0.02

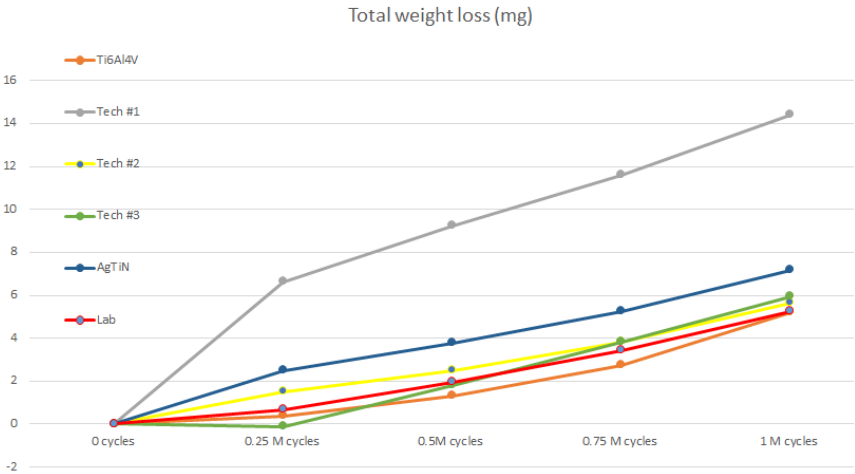


Figure 157, Complete version of the "Total weight loss" graph.

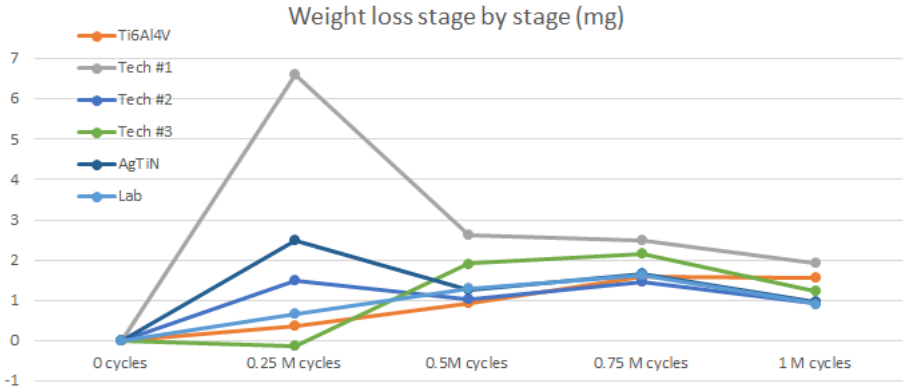


Figure 158, Complete version of the "Weight loss stage by stage" graph.

TABLE XXXV: AVERAGE WEIGHT AND STANDARD DEVIATION OF THE WEIGHT EVALUATED FOR THE SOAK PIN.

Before the testing			After testing (0.25M)			After testing (0.5M)			After testing (0.75M)			After testing (1M)		
Pin	Mean	SD	Pin	Mean	SD	Pin	Mean	SD	Pin	Mean	SD	Pin	Mean	SD
28	1267.35	0.01	28	1267.35	0.01	28	1267.34	0.01	28	1267.20	0.01	28	1268.11	0.01

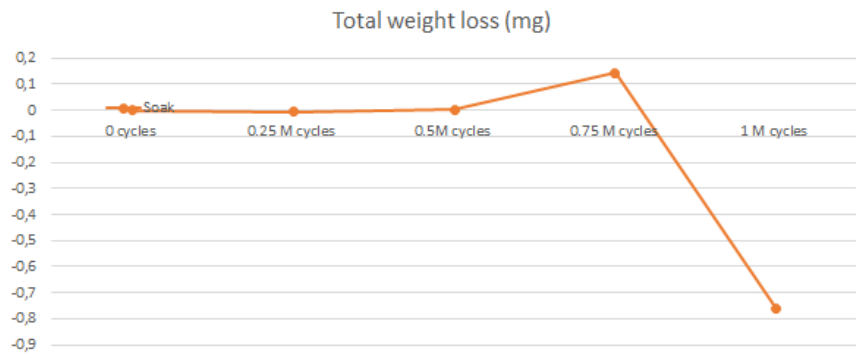


Figure 159, Soak pin weight variation.

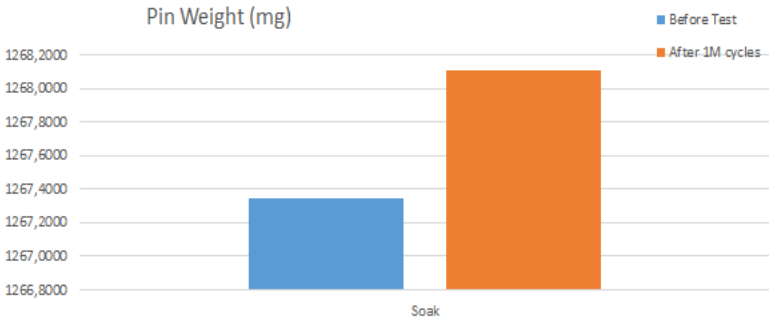


Figure 160, Soak pin weight “before” and “after” the pin on disc test.

Appendix G

G. RAW DATA FROM ROUND 2, Ti6Al4VTEST

TABLE XXXVI: AVERAGE WEIGHT AND STANDARD DEVIATION OF THE WEIGHT EVALUATED FOR EACH STAGE OF THE TEST.

Before the testing			After testing (0.25M)			After testing (0.5M)			After testing (0.75M)			After testing (1M)		
Pin	Mean	SD	Pin	Mean	SD	Pin	Mean	SD	Pin	Mean	SD	Pin	Mean	SD
1	1267.74	0.02	1	1267.38	0.02	1	1266.45	0.02	1	1264.86	0.02	1	1263.31	0.01
2	1269.19	0.02	2	1262.57	0.01	2	1259.95	0.01	2	1257.47	0.02	2	1255.55	0.00
3	1268.48	0.02	3	1266.99	0.02	3	1265.98	0.01	3	1264.53	0.01	3	1263.60	0.01
4	1268.07	0.02	4	1268.20	0.03	4	1266.29	0.01	4	1264.12	0.01	4	1262.88	0.01
5	1267.97	0.02	5	1265.48	0.02	5	1264.22	0.01	5	1262.56	0.02	5	1261.59	0.01
6	1269.32	0.01	6	1268.66	0.02	6	1267.36	0.02	6	1265.74	0.01	6	1264.83	0.02

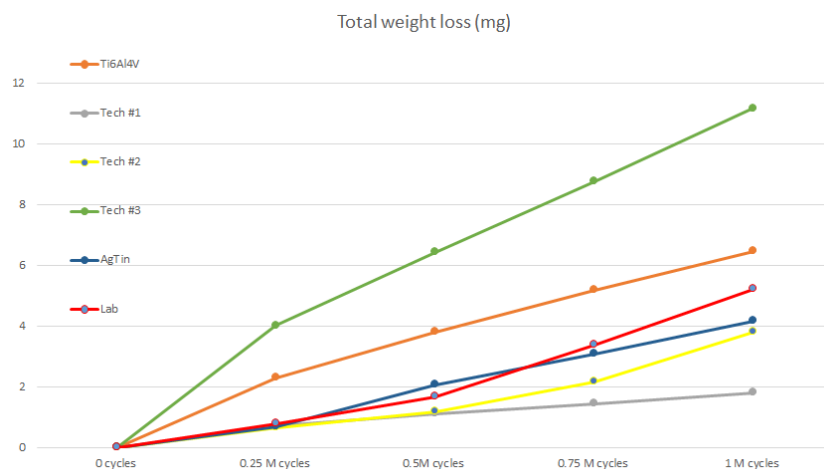


Figure 161, Complete version of the "Total weight loss" graph.

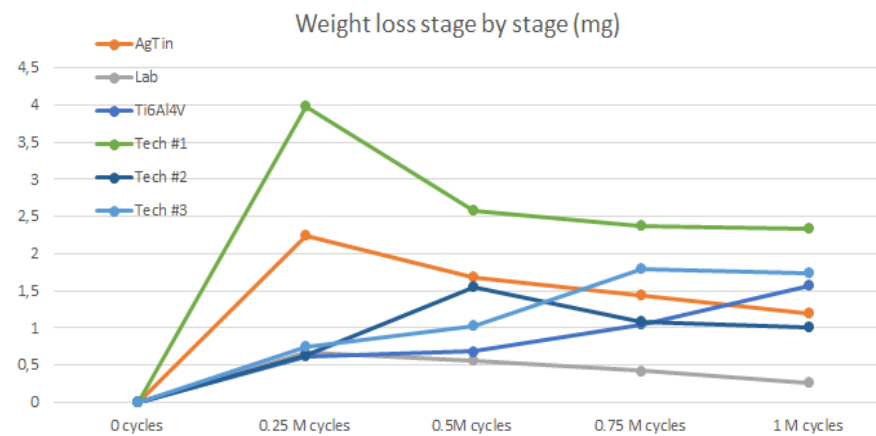


Figure 162, Complete version of the "Weight loss stage by stage" graph.

TABLE XXXVII: AVERAGE WEIGHT AND STANDARD DEVIATION OF THE WEIGHT EVALUATED FOR THE SOAK PIN.

Before the testing			After testing (0.25M)			After testing (0.5M)			After testing (0.75M)			After testing (1M)		
Pin	Mean	SD	Pin	Mean	SD	Pin	Mean	SD	Pin	Mean	SD	Pin	Mean	SD
35	1268.11	0.01	35	1268.16	0.03	35	1268.00	0.01	35	1267.93	0.04	35	1268.00	0.01

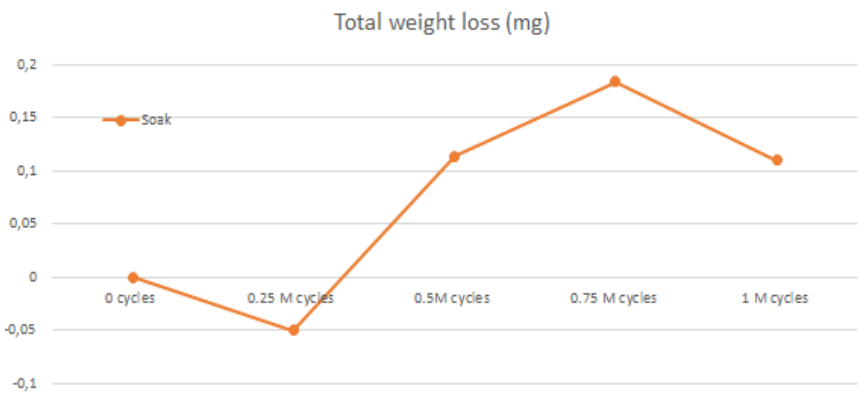


Figure 163, Soak pin weight variation.

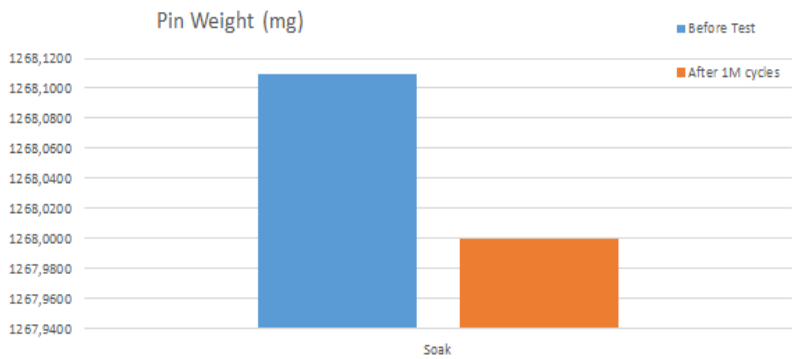


Figure 164, Soak pin weight “before” and “after” the pin on disc test.

Appendix H

H. RAW DATA FROM ROUND 3, Ti6Al4VTEST

TABLE XXXVIII: AVERAGE WEIGHT AND STANDARD DEVIATION OF THE WEIGHT EVALUATED FOR EACH STAGE OF THE TEST.

Before the testing			After testing (0.25M)			After testing (0.5M)			After testing (0.75M)			After testing (1M)		
Pin	Mean	SD	Pin	Mean	SD	Pin	Mean	SD	Pin	Mean	SD	Pin	Mean	SD
36	1267.70	0.03	36	1266.69	0.02	36	1265.72	0.01	36	1264.23	0.02	36	1263.07	0.01
37	1267.00	0.01	37	1267.00	0.02	37	1266.79	0.02	37	1265.76	0.01	37	1264.38	0.03
38	1267.56	0.01	38	1264.49	0.02	38	1262.95	0.02	38	1260.99	0.01	38	1259.68	0.04
39	1267.14	0.01	39	1267.15	0.01	39	1266.76	0.02	39	1266.02	0.03	39	1265.66	0.00
40	1267.47	0.01	40	1267.52	0.01	40	1267.00	0.01	40	1264.44	0.02	40	1261.90	0.03
41	1264.52	0.02	41	1259.91	0.00	41	1257.15	0.01	41	1254.40	0.02	41	1252.30	0.01

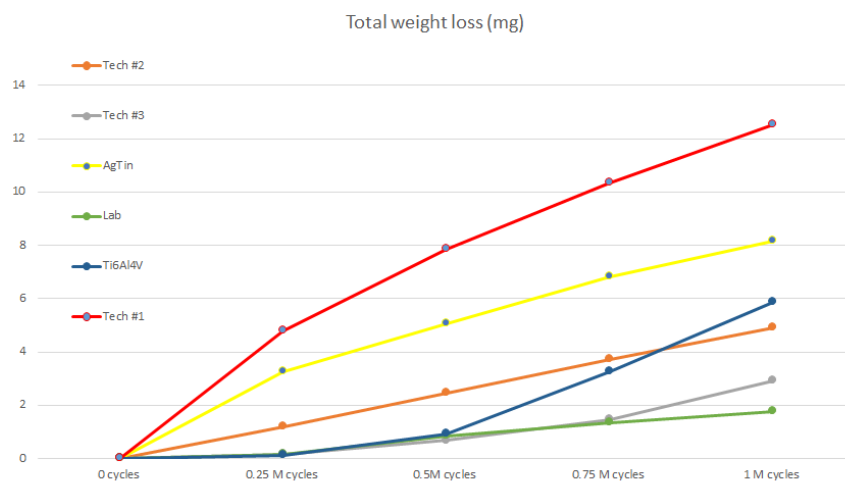


Figure 165, Complete version of the "Total weight loss" graph.

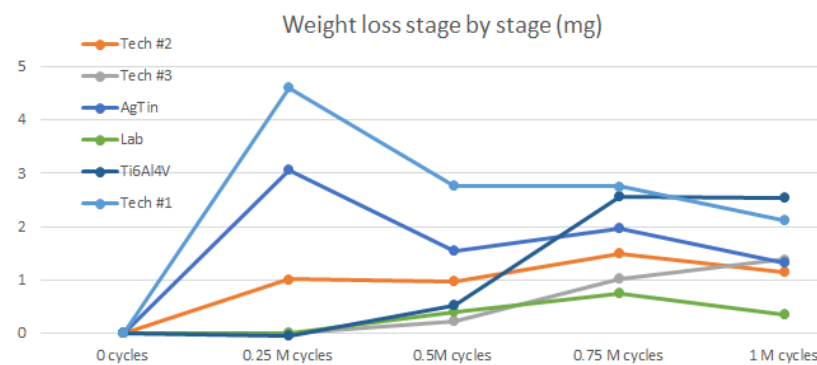


Figure 166, Complete version of the "Weight loss stage by stage" graph.

TABLE XXXIX: AVERAGE WEIGHT AND STANDARD DEVIATION OF THE WEIGHT EVALUATED FOR THE SOAK PIN.

Before the testing			After testing (0.25M)			After testing (0.5M)			After testing (0.75M)			After testing (1M)		
Pin	Mean	SD	Pin	Mean	SD	Pin	Mean	SD	Pin	Mean	SD	Pin	Mean	SD
42	1266.13	0.02	42	1266.31	0.01	42	1266.59	0.01	42	1266.36	0.01	42	1266.42	0.02

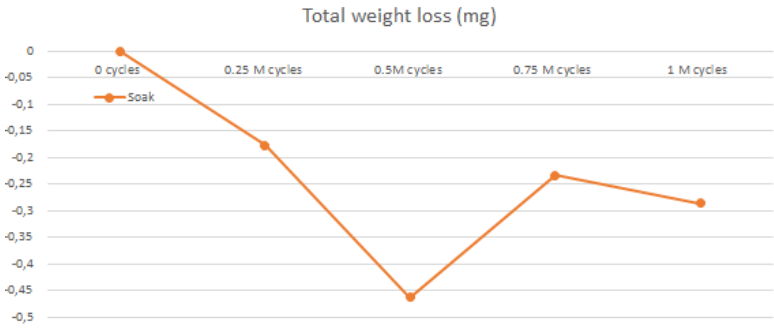


Figure 167, Soak pin weight variation.

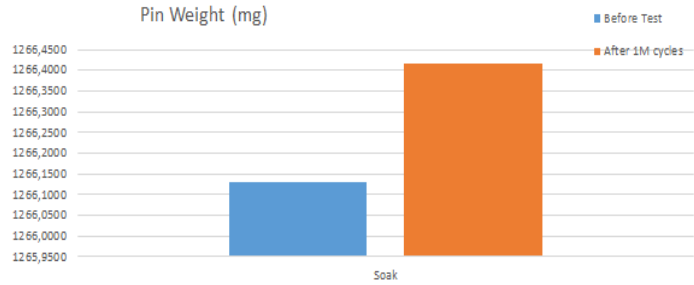


Figure 168, Soak pin weight “before” and “after” the pin on disc test.

Appendix I

I. PERMISSIONS TO REPRINT COPYRIGHT MATERIALS

SPRINGER NATURE LICENSE
TERMS AND CONDITIONS

Feb 17, 2020

This Agreement between Filippo Cinotti ("You") and Springer Nature ("Springer Nature") consists of your license details and the terms and conditions provided by Springer Nature and Copyright Clearance Center.

License Number	4767190165371
License date	Feb 13, 2020
Licensed Content Publisher	Springer Nature
Licensed Content Publication	International Orthopaedics
Licensed Content Title	Total hip arthroplasties: What are the reasons for revision?
Licensed Content Author	Stef D. Ulrich, Thorsten M. Seyler, Derek Bennett et al
Licensed Content Date	Jan 1, 2007
Licensed Content Volume	32
Licensed Content Issue	5
Type of Use	Thesis/Dissertation
Requestor type	academic/university or research institute
Format	print and electronic
Portion	figures/tables/illustrations
Number of figures/tables/illustrations	1
Will you be translating?	no
Circulation/distribution	1 - 29
Author of this Springer Nature content	no
Title	Wear Behavior Of Titanium Nitride Coated Biomaterials
Institution name	University of Illinois at Chicago
Expected presentation date	May 2020
Portions	Figure 1
Requestor Location	Filippo Cinotti 360W Illinois street CHICAGO, IL 60654 United States Attn: Filippo Cinotti
Customer VAT ID	ITCNTFPP96S25G713K
Billing Type	Invoice
Billing Address	Filippo Cinotti 360W Illinois street CHICAGO, IL 60654 United States Attn: Filippo Cinotti
Total	0.00 USD

Figure 169: Permission to reprint Figure 1 from (4)

SPRINGER NATURE LICENSE
TERMS AND CONDITIONS

Feb 17, 2020

This Agreement between Filippo Cinotti ("You") and Springer Nature ("Springer Nature") consists of your license details and the terms and conditions provided by Springer Nature and Copyright Clearance Center.

License Number	4767190274291
License date	Feb 13, 2020
Licensed Content Publisher	Springer Nature
Licensed Content Publication	HSS Journal ®
Licensed Content Title	The Central Role of Wear Debris in Periprosthetic Osteolysis
Licensed Content Author	P. Edward Purdue, Panagiotis Koulouvaris, Bryan J. Nestor et al
Licensed Content Date	Jan 1, 2006
Licensed Content Volume	2
Licensed Content Issue	2
Type of Use	Thesis/Dissertation
Requestor type	academic/university or research institute
Format	print and electronic
Portion	figures/tables/illustrations
Number of figures/tables/illustrations	1
Will you be translating?	no
Circulation/distribution	1 - 29
Author of this Springer Nature content	no
Title	Wear Behavior Of Titanium Nitride Coated Biomaterials
Institution name	University of Illinois at Chicago
Expected presentation date	May 2020
Portions	Figure 2
Requestor Location	Filippo Cinotti 360W Illinois street CHICAGO, IL 60654 United States Attn: Filippo Cinotti
Customer VAT ID	ITCNTFPP96S25G713K
Total	0.00 USD

Figure 170: Permission to reprint Figure 2 from (11)

ELSEVIER LICENSE
TERMS AND CONDITIONS

Feb 17, 2020

This Agreement between Filippo Cinotti ("You") and Elsevier ("Elsevier") consists of your license details and the terms and conditions provided by Elsevier and Copyright Clearance Center.

License Number	4767181051917
License date	Feb 13, 2020
Licensed Content Publisher	Elsevier
Licensed Content Publication	Nanomedicine: Nanotechnology, Biology and Medicine
Licensed Content Title	Systemic and local toxicity of metal debris released from hip prostheses: A review of experimental approaches
Licensed Content Author	Divya Rani Bijukumar, Abhijith Segu, J�lio C.M. Souza, XueJun Li, Mark Barba, Louis G. Mercun, Joshua J. Jacobs, Mathew Thoppil Mathew
Licensed Content Date	Apr 1, 2018
Licensed Content Volume	14
Licensed Content Issue	3
Licensed Content Pages	13
Start Page	951
End Page	963
Type of Use	reuse in a thesis/dissertation
Portion	figures/tables/illustrations
Number of figures/tables/illustrations	2
Format	both print and electronic
Are you the author of this Elsevier article?	No
Will you be translating?	No
Title	Wear Behavior Of Titanium Nitride Coated Biomaterials
Institution name	University of Illinois at Chicago
Expected presentation date	May 2020
Portions	Figure 3
Requestor Location	Filippo Cinotti 360W Illinois street CHICAGO, IL 60654 United States Attn: Filippo Cinotti
Publisher Tax ID	98-0397604
Customer VAT ID	ITCNTFFPP96S25G713K
Total	0.00 USD

Figure 171: Permission to reprint Figure 3 from (13)

13th February 2020

AMTI Force and Motion

I am writing to request permission to use the following material from your publication in my thesis.

Fig. from:

AMTI Ortho-POD

<https://www.pinterest.it/pin/82542605641404695/#>

This material will appear as originally published. Unless you request otherwise, I will use the conventional style of the Graduate College of the University of Illinois at Chicago as acknowledgment.

A copy of this letter is included for your records. Thank you for your kind consideration of this request.

Sincerely,

Filippo Cinotti

Via col di lana 3
21052 Busto Arsizio
VA
Italy

The above request is approved.

Approved by:


Cindy Samra

Date: Feb 18, 2020

Figure 172: Permission to reprint Figure 14

11th March 2020

WZWOpticAG

I am writing to request permission to use the following material from your publication in my thesis.

Fig.

ZYGO NEWVIEW 6300

from:

["https://www.superpolishing.com/"](https://www.superpolishing.com/)

This material will appear as originally published. Unless you request otherwise, I will use the conventional style of the Graduate College of the University of Illinois at Chicago as acknowledgment.

A copy of this letter is included for your records. Thank you for your kind consideration of this request.

Sincerely,

Filippo Cinotti

Via col di lana 3
21052 Busto Arsizio
VA
Italy

The above request is approved.

Approved by:

David Varrie
DAVID VARRIE

Date:



11 March 2020

WE HEREBY APPROVE THE USE OF THE
ATTACH PICTURE FROM THE WZWOPTICAG
WEBSITE.

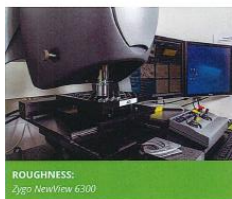


Figure 173: Permission to reprint Figure 15

13th February 2020

HORIBA Scientific

I am writing to request permission to use the following material from your publication in my thesis.

Fig. from:

LabRAM HR Evolution

<https://www.horiba.com/it/scientific/products/raman-spectroscopy/raman-spectrometers/raman-microscopes/hr-evolution/labram-hr-evolution-17309/>

This material will appear as originally published. Unless you request otherwise, I will use the conventional style of the Graduate College of the University of Illinois at Chicago as acknowledgment.

A copy of this letter is included for your records. Thank you for your kind consideration of this request.

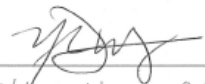
Sincerely,

Filippo Cinotti

Via col di lana 3
21052 Busto Arsizio
VA
Italy

The above request is approved.

Approved by:


Nolan Wong, Sales Engineer,
HORIBA Scientific

Date:

2/26/2020.

Figure 174: Permission to reprint Figure 16

13th February 2020

Labconco

I am writing to request permission to use the following material from your publication in my thesis.

Fig. from:

LABCONCO Xpert Weigh

<https://www.labconco.com/product/xpert-weigh-boxes/13/search/106/-/-/24/0>

This material will appear as originally published. Unless you request otherwise, I will use the conventional style of the Graduate College of the University of Illinois at Chicago as acknowledgment.

A copy of this letter is included for your records. Thank you for your kind consideration of this request.

Sincerely,

Filippo Cinotti

Via col di lana 3
21052 Busto Arsizio
VA
Italy

The above request is approved.

Approved by: Scott Anthony Patterson Date: 02/17/2020

Figure 175: Permission to reprint Figure 17

9th February 2020

E. Rinnert

I am writing to request permission to use the following material from your publication in my thesis.

Fig. 3 from:

Moreau J, Rinnert E.

Fast identification and quantification of BTEX coupling by Raman spectrometry and chemometrics.

Royal Society of Chemistry;

2015.

This material will appear as originally published. Unless you request otherwise, I will use the conventional style of the Graduate College of the University of Illinois at Chicago as acknowledgment.

A copy of this letter is included for your records. Thank you for your kind consideration of this request.

Sincerely,

Filippo Cinotti

Via col di lana 3
21052 Busto Arsizio
VA
Italy

The above request is approved.

Approved by: Dr. Emmanuel Rinnert Date: 02/13/2020



Figure 176: Permission to reprint Figure 56 from (37)

CITED LITERATURE

1. Knight, S., Aujla, R., Biswas, S.: *Total Hip Arthroplasty - over 100 years of operative history*. Orthopedic reviews (Pavia); 3:2–4, 2011.
2. Kremers ,H., Larson, D., Crowson, C., Kremers W., Washington, R., Steiner, C., et al. *Prevalence of Total Hip and Knee Replacement in the United States*. The journal of bone and joint surgery; 1386–97, 2015.
3. Bitar, D. and Parvizi, J. *Biological response to prosthetic debris*. World Journal of Orthopedics; 6(2):172–89, 2015.
4. Ulrich, S., Seyler, T., Bennett, D. *Total hip arthroplasties : What are the reasons for revision ?*. International Orthopaedics, 2007.
5. Lum, Z., Shieh, A., Dorr, L., Shieh, A., Dorr, L. *Why total knees fail-A modern perspective review*. World Journal of Orthopedics ;9(4):60–4, 2018.
6. Journal, A., Kt, S., Me, L., Mt, M. *Failure Causes in Total Hip Replacements : A Review*.Austin journal of Orthopedics & Rheumatology; 5(1):1–7, 2018.
7. Wawrzynski, J., Gil. J, Goodman, A., Waryasz, G., *Hypersensitivity to Orthopedic Implants : A Review of the Literature*. Rheumatology and Therapy; 4(1):45–56, 2017.
8. Lewis, P. and Goharian, A. *Implant Failure - An overview*, Sciencedirect, 2018.
9. Onuoha, K., Omotola, O., Bulus, B., Alo, M. and Onuoha, C. *Orthopaedic Implant Failure*. Lupine publisher, 2019.
10. Abu-amer, Y., Darwech, I., Clohisy, J. *Aseptic loosening of total joint replacements : mechanisms underlying osteolysis and potential therapies*. Arthritis research & Therapy; 7:1–7, 2007.

CITED LITERATURE (continued)

11. Purdue, P., Koulouvaris, P., Nestor, B., Sculco, T. *The Central Role of Wear Debris in Periprosthetic Osteolysis*. HSS journal; 102–13, 2006.
12. Bi, Y., Seabold, J., Kaar, S., Ragab, A., Goldberg, V., Anderson, J., et al. *Adherent Endotoxin on Orthopedic Wear Particles Stimulates Cytokine Production and Osteoclast Differentiation*. Journal of Bone and Mineral Research, 2009.
13. Bijukumar, D., Segu, A., Souza, J., Li, X., Barba, M., Mercuri, L., et al. *Systemic and local toxicity of metal debris released from hip prostheses : A review of experimental approaches*. Nanomedicine Nanotechnology ;14(3):951–63, 2018.
14. Chang, B., Brown, P., Sieber, A., Valdevit, A., Tateno, K., Kostuik, J. *Evaluation of the biological response of wear debris*. The spine journal; 4:239–44, 2004.
15. Hallab, N. and Jacobs, J. *Biomaterials Science: An Introduction to Materials in Medicine. Orthopedic Biomaterials Design. Third Edition.*, 2009.
16. Akil, S., Newman, J., Shah, N., Ahmed, N., Deshmukh, A., Maheshwari, A. *Metal hypersensitivity in total hip and knee arthroplasty : Current concepts*. Journal of Clinical Orthopaedics and Trauma; 9(1):3–6, 2018.
17. Bao, W., He, Y., Fan, Y., Liao, Y. *Metal allergy in total-joint arthroplasty*. Medicine, 2018.
18. Processing, M., Fotovvati, B., Namdari, N., Dehghanghadikolaei, A. *On Coating Techniques for Surface Protection : A Review*. Journal of manufacturing and material processing, 2019.
19. Zhang, S. *TiN coating of tool steels : a review*. Journal of material processing technology ;39:165–77, 1993.
20. Gaudet, P., *Application F*, Data P. United States Patent.;56(56):54–5, 1968.

CITED LITERATURE (continued)

21. *TiN (Titanium Nitride)*, <https://www.tincoat.net/coatings-offered/tin-titanium-nitride/>, 2019. [Online, accessed 02/07/2020].
22. *BryCoat Titanium Nitride (TiN) Coatings*, <https://www.brycoat.com/surface-engineering/brycoat-pvd-coating-solutions/brycoat-titanium-nitride-tin-coatings/>. [Online, accessed 02/07/2020].
23. *Titanium Nitride (TiN)*, <https://www.wallworkht.co.uk/content/tin/>, 2020. [Online, accessed 02/07/2020].
24. *Titanium Nitride (TiN) Advanced Coating Technology*, <https://www.coringroup.com/solutions/titanium-nitride-tin/>, 2020. [Online, accessed 02/07/2020].
25. Scarano, A., Piattelli, M., Vrespa, G., Caputi, S., Piattelli, A. *Bacterial adhesion on titanium nitride-coated and uncoated implants: an in vivo human study*. Journal of Oral Implantology, 2003.
26. Wang, X., Bai, S., Li, F., Li, D., Zhang, J. *Effect of plasma nitriding and titanium nitride coating on the corrosion resistance of titanium*. Journal of Prosthetic Dentistry; 116(3):450–6, 2016.
27. Hove, R., Sierevelt, I., Royen, B., Nolte, P. *Titanium-Nitride Coating of Orthopaedic Implants : A Review of the Literature*. Hindawi, 2015.
28. Hajduga, M., Bobinski, R. *TiN , ZrN and DLC nanocoatings - a comparison of the effects on animals , in- vivo study*. Materials Science & Engineering C, 2019.
29. Amini, F., Bahador, A., Kiaee, B., Kiaee, G. *The effect of the titanium nitride coating on bacterial adhesion on orthodontic stainless steel wires: in vivo study*. Bioscience Biotechnology Research Communcation; 10(1):28–33, 2017.

CITED LITERATURE (continued)

30. Hove, R., Brohet, R., Royen, B., Nolte, P. *No clinical benefit of titanium nitride coating in cementless mobile-bearing total knee arthroplasty.* Knee Surgery, Sport Traumatol Arthroscopy ;23(6):1833–40, 2015.
31. Raimondi, M., Pietrabissa, R. *The in-vivo wear performance of prosthetic femoral heads with titanium nitride coating.* Biomaterials ;21:907–13, 2000.
32. *AMTI Ortho-POD: Description and Specifications*, https://amti.biz/select_product_PDFs/Simulator_machines/Ortho-POD_brochure.pdf. [Online, accessed 02/08/2020].
33. *Zygo NewView 6300*, <http://www.bu.edu/photronics/files/2013/04/Zygo-New-View-6300.pdf>. [Online, accessed 02/08/2020].
34. *LabRam HR Evolution* <https://kaplanscientific.nl/horiba-scientific-raman-microscopes/>. [Online, accessed 02/08/2020].
35. *XPert Weigh Box* <https://www.labconco.com/product/xpert-weigh-boxes-4/480>. [Online, accessed 02/08/2020].
36. *CARL ZEISS: STEMI 2000* <https://microscopy-news.com/products/stereo-microscopes/carl-zeiss-stemi-2000/>. [Online, accessed 02/08/2020].
37. Moreau, J., Rinnert, E. *Fast identification and quantification of BTEX coupling by Raman spectrometry and chemometrics.* Royal Society of Chemistry, 2015.
38. Cheng, Y., Tay, B., Lau, S., Kupfer, H., Richter, F. *Substrate bias dependence of Raman spectra for TiN films deposited by filtered cathodic vacuum arc Substrate bias dependence of Raman spectra for TiN films deposited by filtered cathodic vacuum arc.* Journal of Applied Physics;1845(2002):1–6, 2013.
39. Bryant, T., Bowie, D., Peter, G. *Factors Affecting the Performance of Bench – Top Raman Spectrometers. Part II.*Applied spectroscopy,

CITED LITERATURE (continued)

40. Rea, D. *Study of the Experimental Factors Affecting Raman Band Intensities in Liquids.* Journal of the optical society of america;49(1955):90–101, 1959.
41. Bryant, T., Bowie, D., Peter, G. *Factors Affecting the Performance of Bench – Top Raman Spectrometers.* Part I. Applied spectroscopy,

VITA

NAME: Filippo Cinotti.

EDUCATION:

Master of science in Biomedical Engineering, Present, Politecnico di Milano, Milano, Italy.

Master of science in Bioengineering, May 2020, University of Illinois at Chicago, Chicago, USA.

Bachelor's degree in Ingegneria Biomedica, Jul 2018, Politecnico di Milano, Milano, Italy.

LANGUAGE SKILLS:

Italian Native speaker.

English Full working proficiency.

A.Y. 2019/20 Six months of study abroad in Chicago, Illinois.

A.Y.s 2018/20 Lessons and exam in English.

PROFESSIONAL EXPERIENCES

Spring 2020 Graduate researcher at Wearable Neuroprosthesis Laboratory, IRCCS "S. Maria Nascente", Milano, Italy.

Fall 2019 Graduate researcher at Orthopedic Surgery Laboratory, Rush University, Chicago Illinois, USA.

SCHOLARSHIP

Summer 2015 Best Freshman scholarship winner, Politecnico di Milano.

